

Matteo Carlesso

# Lecture Notes on Quantum Algorithms in Open Quantum Systems

Department of Physics, University of Trieste

Version 1.0 – June 2024

# Preface

These lecture notes aim to provide a clear and comprehensive introduction to using open quantum system theory for quantum algorithms. They are based on various sources, including research papers and textbooks, which can be found in literature. While I have focused on clarity and consistency, there is always space for improvement. I will work on expanding these notes and welcome your constructive feedback and comments. Feel free to send them to [matteo.carlesso@units.it](mailto:matteo.carlesso@units.it).

In the *Suggested Bibliography* reported below, the reader can find the list of references I considered to prepare these notes. Some of these are unpublished (please contact me directly for more info). I apologise in advance to all the numerous authors whose contributions I did not cite. The field is vast and the intent of these notes is not to serve as a comprehensive review article. I have certainly not done justice to the literature.

These notes will be used as a basis for some courses that I held at the Department of Physics of the University of Trieste. Specifically, these are

- 357SM - *Quantum Algorithms in Open Quantum Systems (Spring 2024)*
- 987DF - *Quantum Computing Algorithms (Autumn 2024)*

## Acknowledgments

For the preparation of these lecture notes, I am in great debt with several people. Among these Angelo Bassi, Francesco Cesa, Giulio Crognaletti, Giovanni di Bartolomeo, Sandro Donadi and Michele Vischi for inputs, discussion and support.

I also acknowledge the financial support from the National Quantum Science and Technology Institute through the PNRR MUR project PE0000023-NQSTI, the University of Trieste and the Italian National Institute for Nuclear Physics (INFN).

©Matteo Carlesso<sup>1,2</sup>, June 2024, Trieste

<sup>1</sup>Department of Physics, University of Trieste, Strada Costiera 11, 34151 Trieste, Italy

<sup>2</sup>Istituto Nazionale di Fisica Nucleare, Trieste Section, Via Valerio 2, 34127 Trieste, Italy

# Suggested Bibliography

## Open Quantum Systems

Although not explicitly discussed in these notes, a part of the above mentioned courses regards the theory of open quantum systems. For this part of the courses, I suggest the following literature.

- Angelo Bassi. Lecture Notes on Advanced Quantum Mechanics. Unpublished.
- Heinz-Peter Breuer, Francesco Petruccione. The theory of open quantum systems. Oxford, 2022.
- Mahn-Soo Choi. A Quantum Computation Workbook. Springer, 2022.
- Roberto Floreanini. Lecture Notes on Quantum Information. Unpublished.
- Daniel A. Lidar. Lecture Notes on Theory of Open Quantum Systems. arXiv preprint arXiv:1902.00967.
- Ahsan Nazir. Lecture notes on open quantum systems. <https://www.yumpu.com/en/document/view/8219582/lecture-notes-on-open-quantum-systems-workspace>.
- Stefano Olivares. Lecture Notes on Quantum Computing. University of Milano, 2020.

## Quantum Computation

- Giuliano Benenti, Giulio Casati, Davide Rossini, and Giuliano Strini. Principles of quantum computation and information: a comprehensive textbook. World Scientific, 2019.
- Mahn-Soo Choi. A Quantum Computation Workbook. Springer, 2022.
- Christoph Dittel. Lecture Notes on Quantum information theory. arXiv preprint arXiv:2311.12442.
- Ronald de Wolf. Lecture Notes on Quantum Computing. arXiv preprint arXiv:1907.09415.
- Aram W Harrow, Avinatan Hassidim, and Seth Lloyd. Quantum algorithm for linear systems of equations. Physical Review Letters **103**, 150502, (2009).
- Anton Frisk Kockum, Ariadna Soro, Laura García-Álvarez, Pontus Vikstål, Tom Douce, Göran Johansson, and Giulia Ferrini. Lecture Notes on Quantum Computing. arXiv preprint arXiv:2311.08445.
- Lin Lin. Lecture notes on quantum algorithms for scientific computation. arXiv preprint arXiv:2201.08309.
- M. A. Nielsen and I. L. Chuang Quantum Computation and Quantum Information. Cambridge University Press 2010.
- Stefano Olivares. Lecture Notes on Quantum Computing. University of Milano, 2020.
- Oswaldo Zapata. A Short Introduction to Quantum Computing for Physicists. arXiv preprint arXiv:2306.09388.

## Quantum Error Correction

- Giuliano Benenti, Giulio Casati, Davide Rossini, and Giuliano Strini. Principles of quantum computation and information: a comprehensive textbook. World Scientific, 2019.
- Mahn-Soo Choi. A Quantum Computation Workbook. Springer, 2022.
- Andrew N. Cleland. An introduction to the surface code. *SciPost Phys. Lect. Notes* 49 (2022).
- Ronald de Wolf. Lecture Notes on Quantum Computing. arXiv preprint arXiv:1907.09415.
- Sandro Donadi. Lecture Notes on Quantum Algorithms in Open Quantum Systems. Unpublished.
- Ekert, A and Hosgood, T and Kay, A and Macchiavello, C. Introduction to Quantum Information Science. <https://qubit.guide>.
- Austin G. Fowler, Matteo Mariantoni, John M. Martinis, and Andrew N. Cleland. Surface codes: Towards practical large-scale quantum computation. *Phys. Rev. A*, 86:032324, 2012.
- Steven M. Girvin. Introduction to quantum error correction and fault tolerance. *SciPost Phys. Lect. Notes* 70 (2023).
- Stefano Olivares. Lecture Notes on Quantum Computing. University of Milano, 2020.
- Andrew M. Steane. A Tutorial on Quantum Error Correction. IOS Press 2006.
- Oswaldo Zapata. A Short Introduction to Quantum Computing for Physicists. arXiv preprint arXiv:2306.09388.

## Dynamical Decoupling and Quantum Error Mitigation

- Zhenyu Cai, Ryan Babbush, Simon C. Benjamin, Suguru Endo, William J. Huggins, Ying Li, Jarrod R. McClean, and Thomas E. O'Brien. Quantum error mitigation. *Review Modern Physics* **95**, 045005 (2023).
- Sandro Donadi. Lecture Notes on Quantum Algorithms in Open Quantum Systems. Unpublished.
- Tudor Giurgica-Tiron, Yousef Hindy, Ryan LaRose, Andrea Mari, and William J. Zeng. Digital zero noise extrapolation for quantum error mitigation. In 2020 IEEE International Conference on Quantum Computing and Engineering (QCE). IEEE, 2020.

# Contents

<b>1</b>	<b>Circuit model for quantum computation</b>	1
1.1	Qubit gates . . . . .	1
1.1.1	Hadamard test . . . . .	4
1.2	No-cloning theorem . . . . .	5
1.3	Dense coding . . . . .	5
1.4	Quantum teleportation . . . . .	6
1.5	Quantum Phase estimation . . . . .	7
1.5.1	Single-qubit quantum phase estimation . . . . .	8
1.5.2	Kitaev's method for single-qubit quantum phase estimation . . . . .	8
1.5.3	$n$ -qubit quantum phase estimation . . . . .	9
1.6	Harrow-Hassidim-Lloyd algorithm . . . . .	11
<b>2</b>	<b>Variational Quantum Algorithms</b> . . . . .	15
2.1	The Ising model . . . . .	15
2.2	Mapping combinatorial optimisation problems into the Ising model . . . . .	16
2.3	Adiabatic Theorem . . . . .	17
2.4	Quantum Annealing . . . . .	19
2.5	Quantum Approximate Optimisation Algorithm (QAOA) . . . . .	20
2.6	Variational Quantum Eigensolver (VQE) . . . . .	22
<b>3</b>	<b>Noisy Intermediate-Scale Quantum (NISQ) computation</b> . . . . .	24
3.1	Miscalibrated gates . . . . .	25
3.2	Projection noise and sampling error . . . . .	26
3.3	Measurement error . . . . .	28
3.3.1	Environmental noise . . . . .	30
3.3.2	Global noise action . . . . .	31
<b>4</b>	<b>Quantum Error Correction</b> . . . . .	33
4.1	Quantum Error Correction . . . . .	33
4.1.1	Classical error correction . . . . .	33
4.1.2	Quantum information context . . . . .	35
4.1.3	The 3-qubit bit-flip code . . . . .	35
4.1.4	The 3-qubit phase-flip code . . . . .	37
4.1.5	The 9-qubit Shor code . . . . .	38
4.1.6	On the redundancy and threshold . . . . .	41
4.1.7	More layers of encoding or only more qubits . . . . .	44
4.2	Stabiliser formalism . . . . .	47
4.2.1	Inverting quantum channels . . . . .	48

4.2.2	Correctable errors .....	51
4.2.3	Stabilisers .....	53
4.2.4	Normalisers and Centralisers .....	55
4.2.5	Stabiliser code .....	56
4.3	Surface code .....	56
4.3.1	Detecting errors .....	60
4.4	Fault-tolerant computation .....	62
4.4.1	Steane code or 7-qubit code .....	64
<b>5</b>	<b>Dynamical Decoupling and Quantum Error Mitigation</b> .....	70
5.1	Dynamical Decoupling .....	70
5.2	Quantum Error Mitigation .....	79
5.2.1	Zero noise extrapolation .....	80
5.2.2	Probabilistic error cancellation .....	83
<b>A</b>	<b>Solutions of the exercises</b> .....	88
A.1	Solution to Exercise 1.1 .....	88
A.2	Solution to Exercise 1.2 .....	88
A.3	Solution to Exercise 1.3 .....	89
A.4	Solution to Exercise 1.4 .....	90



# Chapter 1

## Circuit model for quantum computation

In quantum computation, the basic ingredients are qubits and gates. The composition of different gates acting on a series of qubits is what we called an algorithm. Here we introduce quantum gates and some algorithms.

### 1.1 Qubit gates

The single qubit algebra can be described in terms of the identity  $\hat{\mathbb{1}}$  and Pauli  $\hat{\sigma}_x$ ,  $\hat{\sigma}_y$  and  $\hat{\sigma}_z$  operators. All single qubit gates are a linear composition of these. In particular, they can be visualised as rotations of the state  $|\psi\rangle$  on the Bloch sphere. The three elementary rotations by an angle  $\theta$  around the Cartesian axes are defined as  $\hat{R}^j(\theta) = e^{-i\theta\hat{\sigma}_j/2}$  for  $j = x, y, z$ . In particular, in the computational basis, which is the one mainly used in quantum computation, one has

$$\begin{aligned} R^x(\theta) &= \begin{pmatrix} \cos(\theta/2) & -i\sin(\theta/2) \\ -i\sin(\theta/2) & \cos(\theta/2) \end{pmatrix}, \\ R^y(\theta) &= \begin{pmatrix} \cos(\theta/2) & -\sin(\theta/2) \\ \sin(\theta/2) & \cos(\theta/2) \end{pmatrix}, \\ R^z(\theta) &= \begin{pmatrix} \exp(-i\theta/2) & 0 \\ 0 & \exp(i\theta/2) \end{pmatrix}. \end{aligned} \quad (1.1)$$

Then, the rotation of an angle  $\theta$  around the unit axis  $\mathbf{n}$  is given by

$$\hat{R}^{\mathbf{n}}(\theta) = e^{-i\theta\mathbf{n}\cdot\hat{\boldsymbol{\sigma}}/2} = \cos(\theta/2)\hat{\mathbb{1}} - i\sin(\theta/2)\mathbf{n}\cdot\hat{\boldsymbol{\sigma}}. \quad (1.2)$$

Beside the rotations, there are six important single-qubit gates that are standard. These are  $X$ ,  $Y$ ,  $Z$  and

$$H = \frac{1}{\sqrt{2}} \begin{pmatrix} 1 & 1 \\ 1 & -1 \end{pmatrix}, \quad S = \begin{pmatrix} 1 & 0 \\ 0 & i \end{pmatrix}, \quad T = \begin{pmatrix} 1 & 0 \\ 0 & e^{i\pi/4} \end{pmatrix}. \quad (1.3)$$

In particular,  $X$ ,  $Y$  and  $Z$  are respectively the Pauli operators  $\hat{\sigma}_x$ ,  $\hat{\sigma}_y$  and  $\hat{\sigma}_z$  represented in the computational basis, and  $H$  is known as the Hadamard gate.

Eventually, the state of the qubit is measured. In particular, this is always the measurement of  $\hat{\sigma}_z$  and one always obtains one of the two discrete outcomes: “0” or “1”. Given the generic state  $|\psi\rangle = \alpha|0\rangle + \beta|1\rangle$ , with  $\alpha$  and  $\beta$  being complex and  $|\alpha|^2 + |\beta|^2 = 1$ , then one has a probability  $p_0 = |\alpha|^2$  to have the outcome “0” and  $p_1 = |\beta|^2$  to have the outcome “1”.

**Example 1.1**

The gate  $X$  flips states. Indeed,

$$X \begin{pmatrix} \alpha \\ \beta \end{pmatrix} = \begin{pmatrix} 0 & 1 \\ 1 & 0 \end{pmatrix} \begin{pmatrix} \alpha \\ \beta \end{pmatrix} = \begin{pmatrix} \beta \\ \alpha \end{pmatrix}. \quad (1.4)$$

**Example 1.2**

The Hadamard gate  $H$  generates uniform superpositions. In particular, one has

$$\begin{aligned} H \begin{pmatrix} 1 \\ 0 \end{pmatrix} &= \frac{1}{\sqrt{2}} \begin{pmatrix} 1 & 1 \\ 1 & -1 \end{pmatrix} \begin{pmatrix} 1 \\ 0 \end{pmatrix} = \frac{1}{\sqrt{2}} \begin{pmatrix} 1 \\ 1 \end{pmatrix}, \\ H \begin{pmatrix} 0 \\ 1 \end{pmatrix} &= \frac{1}{\sqrt{2}} \begin{pmatrix} 1 & 1 \\ 1 & -1 \end{pmatrix} \begin{pmatrix} 0 \\ 1 \end{pmatrix} = \frac{1}{\sqrt{2}} \begin{pmatrix} 1 \\ -1 \end{pmatrix}. \end{aligned} \quad (1.5)$$

Namely, one has

$$\hat{H} |0\rangle = |+\rangle, \quad \text{and} \quad \hat{H} |1\rangle = |-\rangle, \quad (1.6)$$

where  $|\pm\rangle = (|0\rangle \pm |1\rangle)/\sqrt{2}$ . Notably, the Hadamard gate maps the basis of  $\hat{\sigma}_z$  in that of  $\hat{\sigma}_x$ , and back.

**Exercise 1.1**

Express the Hadamard gate as a rotation.

**Exercise 1.2**

Prove that, given two fixed non-parallel normalised vectors  $\mathbf{n}$  and  $\mathbf{m}$ , any unitary single qubit gate  $\hat{U}$  can be expressed as

$$\hat{U} = e^{i\alpha} \hat{R}^{\mathbf{n}}(\beta) \hat{R}^{\mathbf{m}}(\gamma) \hat{R}^{\mathbf{n}}(\delta), \quad (1.7)$$

with  $\alpha, \beta, \gamma, \delta \in \mathbb{R}$ .

It is common to represent quantum circuits with diagrams with the time running from left to right, where lines correspond to qubits and boxes to gates. For example, the following diagram

$$|0\rangle \longrightarrow \boxed{H} \longrightarrow \boxed{R_Z(\theta)} \longrightarrow \boxed{\text{Measure}} \quad (1.8)$$

corresponds to the following logical consecutive operations

- 0) Prepare the qubit in the ground state  $|0\rangle$ .
- 1) Apply the Hadamard gate  $H$ .
- 2) Apply a rotation of an angle  $\theta$  around the  $z$  axis.
- 3) Measure the state of the qubit.

When one is working with more than one qubit, there is the need to construct the representation of the states in the common computational basis. In the case of two qubits, the basis is given by  $\{|00\rangle, |01\rangle, |10\rangle, |11\rangle\}$ , whose representation in the common computational basis is

$$|00\rangle \sim \begin{pmatrix} 1 \\ 0 \\ 0 \\ 0 \end{pmatrix}, \quad |01\rangle \sim \begin{pmatrix} 0 \\ 1 \\ 0 \\ 0 \end{pmatrix}, \quad |10\rangle \sim \begin{pmatrix} 0 \\ 0 \\ 1 \\ 0 \end{pmatrix}, \quad |11\rangle \sim \begin{pmatrix} 0 \\ 0 \\ 0 \\ 1 \end{pmatrix}, \quad (1.9)$$

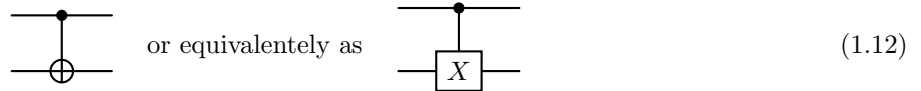
where the symbol  $\sim$  indicates that the state  $|\psi\rangle$  was represented on the computational basis. This is constructed through the tensor product, i.e.

$$|\psi\phi\rangle \sim \begin{pmatrix} \psi_1 \\ \psi_2 \end{pmatrix} \otimes \begin{pmatrix} \phi_1 \\ \phi_2 \end{pmatrix} = \begin{pmatrix} \psi_1\phi_1 \\ \psi_1\phi_2 \\ \psi_2\phi_1 \\ \psi_2\phi_2 \end{pmatrix}. \quad (1.10)$$

Owning the computational representation, we can introduce some 2-qubit gates. One of the most useful among these gates is the CNOT or control-NOT gate:

$$CNOT = \begin{pmatrix} 1 & 0 & 0 & 0 \\ 0 & 1 & 0 & 0 \\ 0 & 0 & 0 & 1 \\ 0 & 0 & 1 & 0 \end{pmatrix}, \quad (1.11)$$

and is represented as



It acts on a target qubit (qubit 1) in a way that depends on the state of a control qubit (qubit 0). Namely, it applies an  $X$  gate to the qubit 1 if the state of qubit 0 is 1, otherwise it does not change the state:

$$CNOT|00\rangle = |00\rangle, \quad CNOT|01\rangle = |01\rangle, \quad CNOT|10\rangle = |11\rangle, \quad CNOT|11\rangle = |10\rangle. \quad (1.13)$$

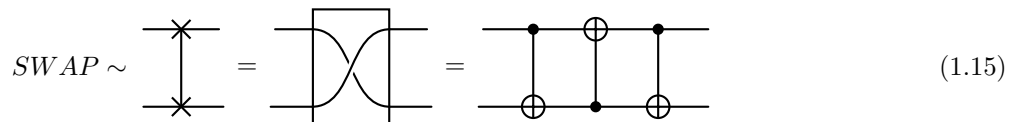
**Exercise 1.3**

Prove that CNOT can generate entanglement.

A second important 2-qubit gate is the SWAP, which swaps the state between two qubits. Namely

$$SWAP|a\rangle \otimes |b\rangle = |b\rangle \otimes |a\rangle. \quad (1.14)$$

A SWAP operation can be constructed using a concatenation of CNOT gates. In particular:



Similarly as the CNOT, one can construct a controlled unitary gate, where the state of the control qubit determines if a unitary gate  $\hat{U}$  is applied to the target qubit:

$$C(U) \sim \begin{pmatrix} 1 & 0 & 0 & 0 \\ 0 & 1 & 0 & 0 \\ 0 & 0 & U_{00} & U_{01} \\ 0 & 0 & U_{10} & U_{11} \end{pmatrix} \sim \begin{array}{c} \text{---} \\ \bullet \\ \text{---} \\ \text{---} \\ \text{---} \\ \text{---} \end{array} \quad (1.16)$$

where  $U_{ij}$  are the matrix elements of  $\hat{U}$ .

### 1.1.1 Hadamard test

The Hadamard test is a useful tool for computing expectation values of a unitary, black-box operator  $\hat{U}$  with respect to a state  $|\psi\rangle$ , which can be in principle a multi-qubit state. Since in general  $\hat{U}$  is not Hermitian, one measures independently the real and immaginary part of  $\langle\psi|\hat{U}|\psi\rangle$ .

The circuit for the real Hadamard test is



and it performs as follows. The first step is to generate a superposition in the first qubit (qubit 0):

$$|0\rangle|\psi\rangle \xrightarrow{\hat{H} \otimes \hat{1}} \frac{1}{\sqrt{2}}(|0\rangle + |1\rangle)|\psi\rangle. \quad (1.18)$$

Then, we entangle the qubits with the  $C(U)$  gate:

$$\frac{1}{\sqrt{2}}(|0\rangle + |1\rangle)|\psi\rangle \xrightarrow{C(U)} \frac{1}{\sqrt{2}}(|0\rangle|\psi\rangle + |1\rangle\hat{U}|\psi\rangle), \quad (1.19)$$

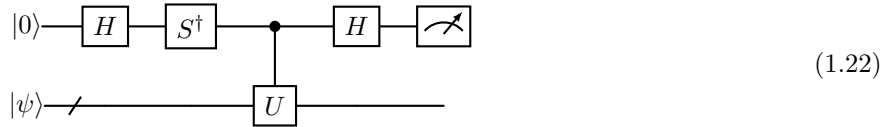
and apply the Hadamard gate to qubit 0:

$$\xrightarrow{\hat{H} \otimes \hat{1}} \frac{1}{2}\left[ (|0\rangle + |1\rangle)|\psi\rangle + (|0\rangle - |1\rangle)\hat{U}|\psi\rangle \right] = \frac{1}{2}\left[ |0\rangle(\hat{1} + \hat{U})|\psi\rangle + |1\rangle(\hat{1} - \hat{U})|\psi\rangle \right]. \quad (1.20)$$

Finally, one measures qubit 0, and the probability of finding the qubit in  $|0\rangle$  is

$$P(|0\rangle) = \frac{1}{4}\langle\psi|(\hat{1} + \hat{U}^\dagger)(\hat{1} + \hat{U})|\psi\rangle = \frac{1}{2}\left(1 + \Re\langle\psi|\hat{U}|\psi\rangle\right). \quad (1.21)$$

Thus, by measuring only one qubit (qubit 0) one has an indication of the real part of  $\langle\psi|\hat{U}|\psi\rangle$ . To estimate the imaginary part, the circuit is modified as follows:



Then, the state before the measurement is

$$\frac{1}{2}\left[ |0\rangle(\hat{1} - i\hat{U})|\psi\rangle + |1\rangle(\hat{1} + i\hat{U})|\psi\rangle \right], \quad (1.23)$$

and correspondingly one has

$$\tilde{P}(|0\rangle) = \frac{1}{2}\left(1 + \Im\langle\psi|\hat{U}|\psi\rangle\right). \quad (1.24)$$

Notably, to well characterise these probabilities, there is the need to run the protocol several times to construct a statistics.

#### Exercise 1.4

Prove that the circuit in Eq. (1.22) provides the result in Eq. (1.24).

## 1.2 No-cloning theorem

For different computational reasons, one would like to create an independent and identical copy of an arbitrary state with a unitary operation. Nevertheless, the following theorem prevents it.

### Theorem 1.1 (No-cloning).

Consider two quantum systems  $\mathcal{A}$  and  $\mathcal{B}$  with corresponding Hilbert spaces of the same dimensions  $\mathbb{H}_{\mathcal{A}}$  and  $\mathbb{H}_{\mathcal{B}}$ . Then, it is not possible to construct a unitary operation  $\hat{U}$  acting on  $\mathbb{H}_{\mathcal{A}} \otimes \mathbb{H}_{\mathcal{B}}$  that copies an arbitrary state of  $\mathcal{A}$  over an initial, reference state of  $\mathcal{B}$ . Namely,  $\nexists \hat{U}$  such that

$$\hat{U} |\psi\rangle |e\rangle = |\psi\rangle |\psi\rangle, \quad (1.25)$$

where  $|\psi\rangle$  is an arbitrary state and  $|e\rangle$  is a reference state.

*Proof.* A simple proof goes as follows. Suppose there exists  $\hat{U}$  such that described in Eq. (1.25). Then, one considers the scalar product between the state  $|\psi, e\rangle = |\psi\rangle |e\rangle$  and  $|\phi, e\rangle = |\phi\rangle |e\rangle$ , where  $|\phi\rangle$  is a second arbitrary state. This gives

$$\langle \phi, e | \psi, e \rangle = \langle \phi | \psi \rangle \langle e | e \rangle. \quad (1.26)$$

Exploiting the unitarity of  $\hat{U}$  we have

$$\langle \phi, e | \psi, e \rangle = \langle \phi, e | \hat{U}^\dagger \hat{U} | \psi, e \rangle \quad (1.27)$$

Now, we apply Eq. (1.25) to both these states:

$$\langle \phi, e | \hat{U}^\dagger \hat{U} | \psi, e \rangle = \langle \phi, \phi | \psi, \psi \rangle = \langle \phi | \psi \rangle^2. \quad (1.28)$$

By putting together the last three expressions we find

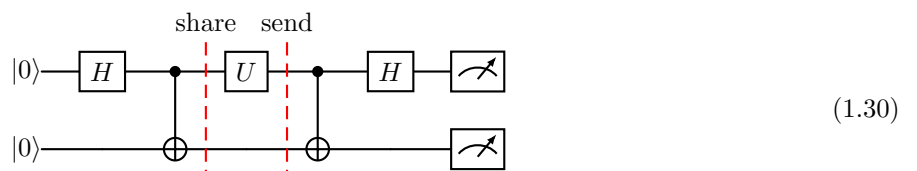
$$\langle \phi | \psi \rangle \langle e | e \rangle = \langle \phi | \psi \rangle^2, \quad (1.29)$$

which holds true only if  $\langle \phi | \psi \rangle = 0$  or  $|\phi\rangle = e^{i\alpha(\phi,\psi)} |\psi\rangle$  with  $\alpha(\phi, \psi)$  being a phase possibly depending on the two input states. In both cases, one does not allow for full arbitrariness, thus proving the no-cloning theorem.

Importantly for the quantum computation field, the no-cloning theorem prevents the employment of classical error correction techniques on quantum states. One needs to employ quantum error corrections, which will be subject of Chapter 4, that effectively circumvent the no-cloning theorem.

## 1.3 Dense coding

An interesting quantum algorithm is that of dense coding. Suppose Alice has two classical bits  $x$  and  $y$  that wants to communicate (securely) to Bob, and can do it only via a single qubit. The following protocol allows for it. It assumes to have two qubits on which six operations are performed:



The first operation is to prepare an initial entangled state

$$|0\rangle |0\rangle \xrightarrow{\hat{H} \otimes \hat{\mathbb{1}}} \frac{1}{\sqrt{2}}(|0\rangle + |1\rangle) |0\rangle \xrightarrow{CNOT} \frac{1}{\sqrt{2}}(|0\rangle |0\rangle + |1\rangle |1\rangle) = |\psi_+\rangle. \quad (1.31)$$

The second operation is to share the state among Alice (qubit 0) and Bob (qubit 1). Then, the third operation is the encoding: Alice encodes the state of  $(x, y)$  in the operation performed with the gate  $\hat{U}$ :

$x, y$	$\hat{U}$
0, 0	$\hat{\mathbb{1}} \otimes \hat{\mathbb{1}}$
0, 1	$\hat{\sigma}_x \otimes \hat{\mathbb{1}}$
1, 0	$\hat{\sigma}_z \otimes \hat{\mathbb{1}}$
1, 1	$i\hat{\sigma}_y \otimes \hat{\mathbb{1}}$

This leads to

$$|\psi_+\rangle \xrightarrow{\hat{U} \otimes \hat{\mathbb{1}}} \begin{cases} \frac{1}{\sqrt{2}}(|0\rangle |0\rangle + |1\rangle |1\rangle) = |\psi_+\rangle, & \text{if } (x, y) = (0, 0), \\ \frac{1}{\sqrt{2}}(|1\rangle |0\rangle + |0\rangle |1\rangle) = |\phi_+\rangle, & \text{if } (x, y) = (0, 1), \\ \frac{1}{\sqrt{2}}(|0\rangle |0\rangle - |1\rangle |1\rangle) = |\psi_-\rangle, & \text{if } (x, y) = (1, 0), \\ \frac{1}{\sqrt{2}}(|0\rangle |1\rangle - |1\rangle |0\rangle) = |\phi_-\rangle, & \text{if } (x, y) = (1, 1), \end{cases} \quad (1.32)$$

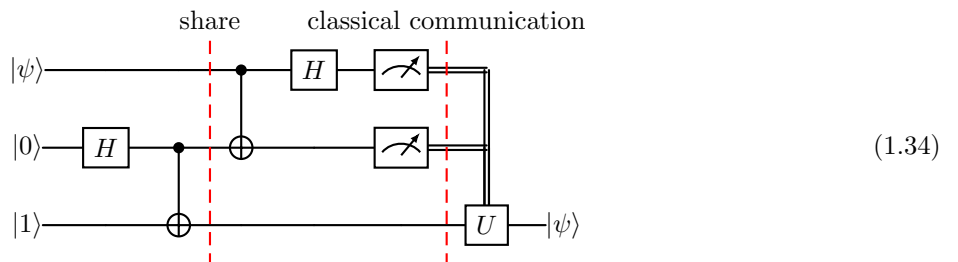
where  $|\psi_{\pm}\rangle$  and  $|\phi_{\pm}\rangle$  are the four Bell states (fully entangled state, being a basis of the common Hilbert space). The fourth operation consists in Alice sending the qubit 0 to Bob. Any operation performed on the two qubits by Bob is now fully local. The fifth operation is the decoding. Bob applies the last two operations (CNOT and  $\hat{H} \otimes \hat{\mathbb{1}}$ ) which together form the inverse operation of the encoding:

$$\begin{aligned} |\psi_+\rangle &\rightarrow |0\rangle |0\rangle, \\ |\phi_+\rangle &\rightarrow |0\rangle |1\rangle, \\ |\psi_-\rangle &\rightarrow |1\rangle |0\rangle, \\ |\phi_-\rangle &\rightarrow |1\rangle |1\rangle. \end{aligned} \quad (1.33)$$

The last operation is to Bob to measure the state of both qubits, which will identify which bits Alice encoded in her qubit.

## 1.4 Quantum teleportation

An application of the dense coding protocol is the quantum teleportation, that allows for sending a generic state  $|\psi\rangle = \alpha|0\rangle + \beta|1\rangle$  from Alice to Bob without knowing a priori the state. The protocol is based on the use of three qubits and six operations:



The first operation is to prepare an entangled state between qubit 1 and 2 (similarly as in the dense coding protocol):

$$|\psi 01\rangle \xrightarrow{\hat{\mathbb{1}} \otimes \hat{H} \otimes \hat{\mathbb{1}}} |\psi\rangle \frac{1}{\sqrt{2}}(|0\rangle + |1\rangle) |1\rangle \xrightarrow{\hat{\mathbb{1}} \otimes CNOT} |\psi\rangle \frac{1}{\sqrt{2}}(|01\rangle + |10\rangle) = |\psi\rangle |\phi_+\rangle. \quad (1.35)$$

Then, the second operation is to shared the qubits among Alice (qubit 0 and 1) and Bob (qubit 2). The third operation consists in applying a decoding operation (see dense coding) to the first two qubits. Namely, the decoding operation acts as in Eq. (1.33). Thus, owning that  $|\psi\rangle = \alpha|0\rangle + \beta|1\rangle$ , one obtains

$$\begin{aligned} |\psi\rangle |\phi_+\rangle &\xrightarrow{CNOT \otimes \hat{\mathbb{I}}} \frac{1}{\sqrt{2}} [\alpha|0\rangle(|01\rangle + |10\rangle) + \beta|1\rangle(|11\rangle + |00\rangle)] \\ &\xrightarrow{\hat{H} \otimes \hat{\mathbb{I}} \otimes \hat{\mathbb{I}}} \frac{1}{2} [|00\rangle(\alpha|1\rangle + \beta|0\rangle) + |01\rangle(\alpha|0\rangle + \beta|1\rangle) + |10\rangle(\alpha|1\rangle - \beta|0\rangle) + |11\rangle(\alpha|0\rangle - \beta|1\rangle)]. \end{aligned} \quad (1.36)$$

The fourth operation consists in Alice measuring her qubits. There are 4 possible couples, and thus four possible collapses (according to the measurement postulate of quantum mechanics). These are  $|00\rangle$ ,  $|01\rangle$ ,  $|10\rangle$  and  $|11\rangle$  with probability  $1/4$  each. The fundamental point of the protocol is that the collapse of the state of the first 2 qubit implies that of the last qubit, being in Bob's hands. In particular, if Alice measures the couple  $(0, 0)$ , then qubit 2 collapses in  $\alpha|1\rangle + \beta|0\rangle$ ; and similarly for the other three measurement outcomes. The fifth operation is the classical communication of the outcomes of the measurement to Bob. Consequently, the sixth operation is a unitary operation  $\hat{U}$  on qubit 2 that depends on the outcomes ( $q_0$  and  $q_1$ ) of the measurement:

$q_0$	$q_1$	$ q_2\rangle$	$\hat{U}$
0	0	$\alpha 1\rangle + \beta 0\rangle$	$\hat{\sigma}_x$
0	1	$\alpha 0\rangle + \beta 1\rangle$	$\hat{\mathbb{I}}$
1	0	$\alpha 1\rangle - \beta 0\rangle$	$i\hat{\sigma}_y$
1	1	$\alpha 0\rangle - \beta 1\rangle$	$\hat{\sigma}_z$

(1.37)

where  $|q_2\rangle$  is the state on which qubit 2 has collapsed after the measurement. By applying the unitary we obtain

$$\begin{aligned} \alpha|1\rangle + \beta|0\rangle &\xrightarrow{\hat{\sigma}_x} |\psi\rangle, \\ \alpha|0\rangle + \beta|1\rangle &\xrightarrow{\hat{\mathbb{I}}} |\psi\rangle, \\ \alpha|1\rangle - \beta|0\rangle &\xrightarrow{i\hat{\sigma}_y} |\psi\rangle, \\ \alpha|0\rangle - \beta|1\rangle &\xrightarrow{\hat{\sigma}_z} |\psi\rangle. \end{aligned} \quad (1.38)$$

In such a way, Bob retrieves the state  $|\psi\rangle$  without that neither Bob or Alice had measure it.

We notice that there is a strong difference with the case studied in the no cloning theorem. Here, one needs to measure two qubits to perform the protocol: this a fundamentally different procedure with respect to a unitary operation.

## 1.5 Quantum Phase estimation

The framework of quantum phase estimation (QPE) is the following. Consider a unitary operation  $\hat{U}$  where the state  $|\psi\rangle$  is one of its eigenstates. In particular, one has

$$\hat{U}|\psi\rangle = e^{2\pi i\varphi}|\psi\rangle. \quad (1.39)$$

Then, the task is to determine the phase  $\varphi$  with a certain given precision.

### 1.5.1 Single-qubit quantum phase estimation

The Hadamard test described in Sec. 1.1.1 can be used to implement a single qubit phase estimation. Indeed, from Eq. (1.39) one gets that

$$\langle \psi | \hat{U} | \psi \rangle = e^{2\pi i \varphi}. \quad (1.40)$$

Then, by merging with Eq. (1.21) one has

$$P(|0\rangle) = \frac{1}{2}(1 + \cos(2\pi\varphi)), \quad (1.41)$$

which implies

$$\varphi = \pm \frac{\arccos(1 - 2P(|0\rangle))}{2\pi} + 2\pi k, \quad (1.42)$$

where  $k \in \mathbb{N}$ . Notice that such a circuit cannot distinguish the sign of  $\varphi$ . Conversely, using both Eq. (1.21) and Eq. (1.24), one has

$$\varphi = \arctan \left( \frac{1 - 2P(|0\rangle)}{1 - 2\tilde{P}(|0\rangle)} \right). \quad (1.43)$$

Now, for the sake of simplicity, let us restrict to the case of  $\varphi \in [0, 1[$ . Suppose we would like to estimate the value of  $\varphi$  with a single run of the circuit in Eq. (1.17). Then, if the outcome is  $+1$  (i.e., the state collapses on  $|0\rangle$ ), we have  $P(|0\rangle) = 1$ . Conversely, with the outcome being  $-1$  we have  $P(|0\rangle) = 0$ . Then, by employing Eq. (1.42) we obtain

outcome	$P( 0\rangle)$	$\bar{\varphi}$	$\varphi_v$
$+1$	1	0	$[0, 1/2[$
$-1$	0	$1/2$	$[1/2, 1[$

(1.44)

where  $\bar{\varphi}$  gives the best estimation for the real value of the phase  $\varphi_v$ . Since there are no other possible outcomes with a single run, the phase is estimated with an error  $\epsilon = 1/2$ , namely  $\varphi_v \in [\bar{\varphi}, \bar{\varphi} + \epsilon[$ . This is a really low accuracy for a deterministic algorithm. To improve this accuracy, one should run the algorithm several times (namely, a number of times that scales as  $\mathcal{O}(1/\epsilon^2)$ , where  $\epsilon$  is the target error bound), or consider alternative methods, as the N-qubit quantum phase estimation described below.

### 1.5.2 Kitaev's method for single-qubit quantum phase estimation

In the fixed point representation, a natural number  $k$  can be represented with a real number  $\varphi \in [0, 1[$  by employing  $d$  bits, i.e.

$$\varphi = (\varphi_{d-1} \dots \varphi_0), \quad (1.45)$$

where  $\varphi_k \in \{0, 1\}$ , as far as  $k \leq 2^d - 1$ .

#### Example 1.3

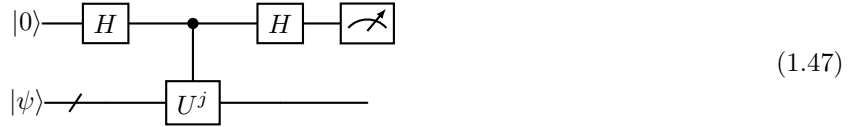
To make an explicit example of the fixed point representation, the value of  $k = 41$  corresponds to the  $d = 6$  bit's string  $[101001]$  and can be represented with  $\varphi = 0.640625$  being equivalent to  $(.101001)$ . Indeed, by employing the following expression with the string  $\varphi = (\varphi_{d-1} \dots \varphi_0) = (.101001)$  one has

$$\sum_{i=0}^{d-1} \varphi_i 2^{i-d} = \varphi_5 2^{-1} + \varphi_4 2^{-2} + \varphi_3 2^{-3} + \varphi_2 2^{-4} + \varphi_1 2^{-5} + \varphi_0 2^{-6} = 2^{-1} + 2^{-3} + 2^{-6} = 0.640625. \quad (1.46)$$

Such a value, when multiplied by  $2^6$  gives exactly 41.

In the simplest scenario of  $d = 1$ , one has  $\varphi = (\varphi_0)$  with  $\varphi_0 \in \{0, 1\}$ . Thus, when performing once the real Hadamard test, one has  $P(|0\rangle) = 1$  if  $\varphi_0 = 0$  (i.e.,  $\bar{\varphi} = 0$ ), and  $P(|0\rangle) = 0$  if  $\varphi_0 = 1$  (i.e.,  $\bar{\varphi} = 1/2$ ).

Next, we consider the case of  $d$  bits, where  $\varphi = (.0 \dots 0\varphi_0)$ . Here, the first  $d$  bits are 0 and the last one is  $\varphi_0$ . To determine the value of  $\varphi_0$  one needs to reach a precision of  $\epsilon < 2^{-d}$ . This would require  $\mathcal{O}(1/\epsilon^2) = \mathcal{O}(2^{2d})$  repeated applications of the single-qubit quantum phase estimation, or number of queries to  $\hat{U}$ . The observation from Kitaev's method is that if we can have access to  $\hat{U}^j$  for a suitable power  $j$ , then the number of queries to  $\hat{U}$  can be reduced. If one substitutes  $\hat{U}^j$  to  $\hat{U}$ , with the corresponding circuit being



then the probability changes in

$$P(|0\rangle) = \frac{1}{2}(1 + \cos(2\pi j\varphi)). \quad (1.48)$$

Importantly, every time one multiplies a number by a factor 2, the bits in the fixed point representation are shifted to the left. To make an example,

$$2 \times (.00\varphi_0) = (.0\varphi_0). \quad (1.49)$$

Then, one has that  $2^{d-1}\varphi = 2^{d-1}(.0 \dots 0\varphi_0) = (.varphi_0)$ . Thus, applying the circuit in Eq. (1.47) with  $j = d - 1$  to estimate  $(.0 \dots 0\varphi_0)$  is equivalent to apply the circuit in Eq. (1.17) to estimate  $(.\varphi_0)$ .

This idea can be extended to general phases with  $d$  bits, i.e.  $\varphi = (.varphi_{d-1} \dots \varphi_0)$ . Indeed, one has

$$\hat{U}e^{2\pi i\varphi}|\psi\rangle = \hat{U}e^{2\pi i(.varphi_{d-1} \dots \varphi_0)}|\psi\rangle = e^{2\pi i(\varphi_{d-1} \cdot \varphi_{d-2} \dots \varphi_0)}|\psi\rangle = e^{2\pi i\varphi_{d-1}}e^{2\pi i(.varphi_{d-2} \dots \varphi_0)}|\psi\rangle, \quad (1.50)$$

but  $e^{2\pi i\varphi_{d-1}} = 1$  independently from the value of  $\varphi_{d-1}$ . Thus

$$\hat{U}e^{2\pi i\varphi}|\psi\rangle = e^{2\pi i(.varphi_{d-2} \dots \varphi_0)}|\psi\rangle, \quad (1.51)$$

i.e. the application of  $\hat{U}$  shifts the bits and allows the evaluation of the first bit after the decimal point.

### 1.5.3 *n*-qubit quantum phase estimation

Notably, both the previous algorithms necessitate an important classical post-processing. Employing  $n$  ancillary qubits allow the reduction of such post-processing. This is based on the application of the Inverse Quantum Fourier Transform  $\hat{F}^\dagger$ .

#### **Recall 1.1 (Quantum Fourier transform)**

The discrete Fourier transform of a  $N$ -component vector with complex components  $\{f(0), \dots, f(N-1)\}$  is a new complex vector  $\{\tilde{f}(0), \dots, \tilde{f}(N-1)\}$ , defined as

$$F(f(j), k) = \tilde{f}(k) = \frac{1}{\sqrt{N}} \sum_{j=0}^{N-1} e^{2\pi ijk/N} f(j). \quad (1.52)$$

The Quantum Fourier transform (QFT) acts similarly: it acts as the unitary operator  $\hat{F}$  on a quantum register of  $n$  qubits, where  $N = 2^n$ , in the computational basis as

$$\hat{F}|j\rangle = \frac{1}{\sqrt{2^n}} \sum_{k=0}^{2^n-1} e^{2\pi ijk/2^n} |k\rangle, \quad (1.53)$$

where  $|j\rangle = |j_{n-1} \dots j_0\rangle$  and  $|k\rangle = |k_{n-1} \dots k_0\rangle$ . Namely, the application of the quantum Fourier transform  $\hat{F}$  to the state  $|j\rangle = |j_{n-1} \dots j_0\rangle$  gives

$$\hat{F}|j\rangle = \frac{1}{\sqrt{2^n}} \left( |0\rangle + e^{2\pi i(0.j_0)} |1\rangle \right) \left( |0\rangle + e^{2\pi i(0.j_1 j_0)} |1\rangle \right) \dots \left( |0\rangle + e^{2\pi i(0.j_{n-1} \dots j_0)} |1\rangle \right). \quad (1.54)$$

In the case of a superposition  $|\psi\rangle = \sum_j f(j)|j\rangle$ , one has

$$|\tilde{\psi}\rangle = \hat{F}|\psi\rangle = \sum_{k=0}^{2^n-1} \tilde{f}(k)|k\rangle, \quad (1.55)$$

where the coefficients  $\tilde{f}(k)$  are the discrete Fourier transform of the coefficients  $f(j)$ .

The inverse quantum Fourier transform  $\hat{F}^\dagger$  acts as

$$\hat{F}^\dagger|j\rangle = \frac{1}{\sqrt{2^n}} \sum_{j=0}^{2^n-1} e^{-2\pi ijk/2^n} |k\rangle, \quad (1.56)$$

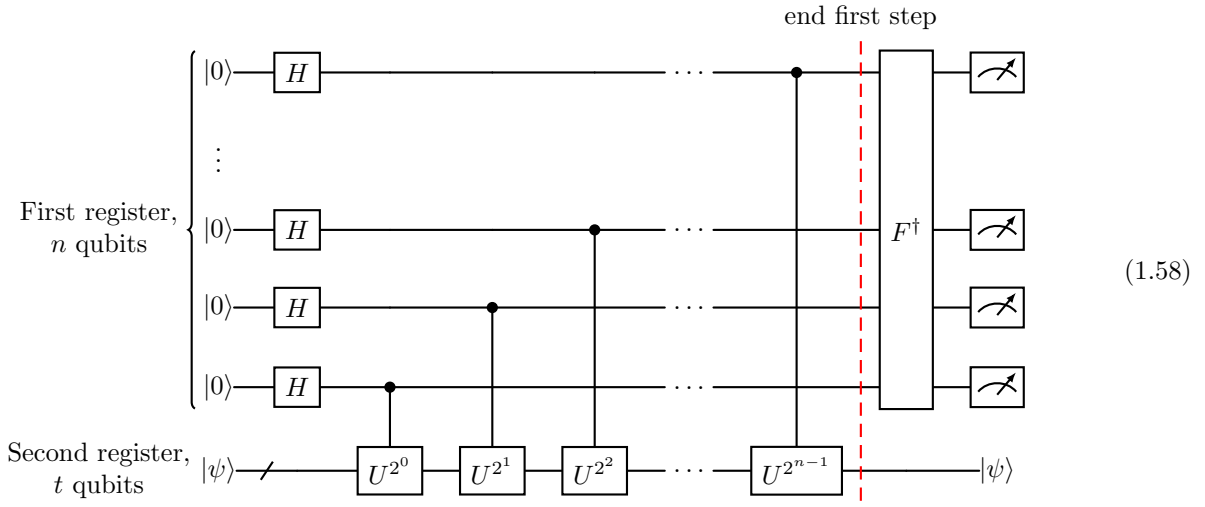
in a completely similar way as Eq. (1.53) but with negative phases.

#### Example 1.4

The application of the quantum Fourier transform  $\hat{F}$  to the state  $|j\rangle = |10\rangle = |j_1 = 1, j_0 = 0\rangle$  gives

$$\begin{aligned} \hat{F}|j\rangle &= \frac{1}{2} \left( |0\rangle + e^{2\pi i(0.j_0)} |1\rangle \right) \left( |0\rangle + e^{2\pi i(0.j_1 j_0)} |1\rangle \right), \\ &= \frac{1}{\sqrt{2}} (|0\rangle + |1\rangle) \frac{1}{\sqrt{2}} (|0\rangle - |1\rangle). \end{aligned} \quad (1.57)$$

The algorithm implementing the (standard) quantum phase estimation uses a first register of  $n$  ancillary qubits and a second register of which we want to compute the phase. The first register is initially prepared in the  $|0\rangle$  state for all the qubits. The circuit implementing the algorithm is the following



In particular, the state of the first register after the end of the first part of the algorithm (see red dashed line) reads

$$\frac{1}{\sqrt{2^n}} \left( |0\rangle + e^{2\pi i(2^{n-1}\varphi)} |1\rangle \right) \dots \left( |0\rangle + e^{2\pi i(2^0\varphi)} |1\rangle \right). \quad (1.59)$$

Now, by considering the binary representation of  $\varphi = (\varphi_{n-1} \dots \varphi_0)$ , the latter expression becomes

$$\frac{1}{\sqrt{2^n}} \left( |0\rangle + e^{2\pi i (0 \cdot \varphi_0)} |1\rangle \right) \left( |0\rangle + e^{2\pi i (0 \cdot \varphi_1 \varphi_0)} |1\rangle \right) \dots \left( |0\rangle + e^{2\pi i (0 \cdot \varphi_{n-1} \dots \varphi_0)} |1\rangle \right), \quad (1.60)$$

which is exactly equal to  $\hat{F}|j\rangle$  in Eq. (1.54) for  $|j\rangle = |\varphi\rangle$ . Thus, applying the inverse Fourier transform  $\hat{F}^\dagger$  one gets  $|\varphi\rangle$ , which is then measured.

## 1.6 Harrow-Hassidim-Lloyd algorithm

The Harrow-Hassidim-Lloyd (HHL) algorithm allows for the resolution of linear system problems on a quantum computer. To be precise, the problem to be solved is described as finding the  $N_b$  complex entries of  $\mathbf{x}$  that solve the following problem

$$A\mathbf{x} = \mathbf{b}, \quad (1.61)$$

where  $A$  is an hermitian and non-singular  $N_b \times N_b$  matrix and  $\mathbf{b}$  is a  $N_b$  vector, both defined on  $\mathbb{C}$ . Classically, the solution is given by

$$\mathbf{x} = A^{-1}\mathbf{b}. \quad (1.62)$$

The question is then how one can implement this on a quantum computer.

First, let us assume that the entries of  $\mathbf{b}$  are such that  $\|\mathbf{b}\| = 1$ . Then,  $\mathbf{b}$  can be stored in a  $n_b$ -qubit state  $|b\rangle$ , through the following mapping:

$$\mathbf{b} = \begin{pmatrix} b_0 \\ \vdots \\ b_{N_b-1} \end{pmatrix} \leftrightarrow b_0 |0\rangle + \dots + b_{N_b-1} |N_b-1\rangle = |b\rangle, \quad (1.63)$$

where  $N_b = 2^{n_b}$ . For example, this can be done via a unitary operation  $\hat{U}_b$ . Now, we define  $|x\rangle = \hat{A}^{-1}|b\rangle$ , where  $\hat{A}$  in the computational representation gives the classical matrix  $A$ . Notably, the state  $|x\rangle$  needs to be normalised to be stored in a quantum register. Thus, one has

$$|x\rangle = \frac{\hat{A}^{-1}|b\rangle}{\|\hat{A}^{-1}|b\rangle\|}, \quad (1.64)$$

where the normalisation problem can be tackled in a second moment.

Consider the spectral decomposition of  $\hat{A}$ :

$$\hat{A}|v_j\rangle = \lambda_j|v_j\rangle, \quad (1.65)$$

where  $\lambda_j$  and  $|v_j\rangle$  are respectively the eigenvalues and eigenstates of  $\hat{A}$ . We also assume that the ordering of the eigenvalues is such that

$$0 < \lambda_0 \leq \dots \leq \lambda_{N_b-1} < 1. \quad (1.66)$$

In general this will not be the case, but one can remap the problem in order to fall within this case. We also assume that all the  $N_b$  eigenvalues have an exact  $d$ -bit representation.

By applying what in Sec. 1.5, we can query  $\hat{A}$  via an unitary operation  $\hat{U} = e^{2\pi i \hat{A}}$  using QPE. For example, suppose  $|b\rangle = |v_j\rangle$ , then we have

$$\hat{U}_{\text{QPE}}|0\rangle^{\otimes d}|v_j\rangle = |\lambda_j\rangle|v_j\rangle. \quad (1.67)$$

In particular, the (not-normalised) solution of the linear system problem would be

$$\hat{A}^{-1}|b\rangle = \hat{A}^{-1}|v_j\rangle = \frac{1}{\lambda_j}|v_j\rangle. \quad (1.68)$$

More generally, one can decompose the state  $|b\rangle$  on the basis of  $\hat{A}$ , i.e.

$$|b\rangle = \sum_{j=0}^{2^{n_b}-1} \beta_j |v_j\rangle, \quad (1.69)$$

where  $\beta_j$  are a linear combination of  $b_j$ . Then the QPE procedure gives

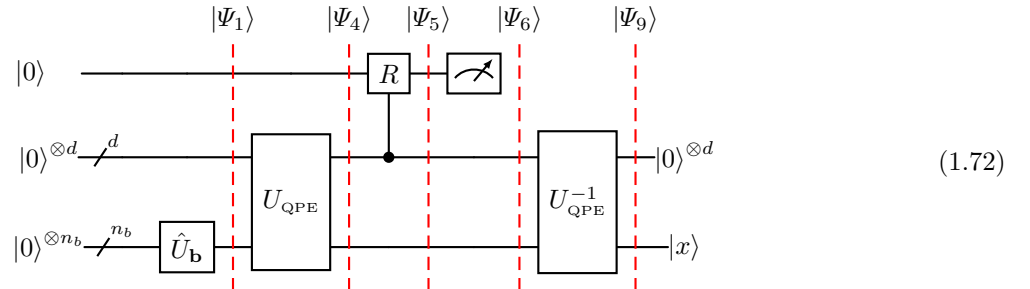
$$\hat{U}_{\text{QPE}} |0\rangle^{\otimes d} |b\rangle = \sum_j \beta_j |\lambda_j\rangle |v_j\rangle, \quad (1.70)$$

and the solution of the problem is given by

$$\hat{A}^{-1} |b\rangle = \sum_{j=0}^{2^{n_b}-1} \frac{\beta_j}{\lambda_j} |v_j\rangle. \quad (1.71)$$

The aim of the HHL algorithm is to generate the normalised version of the state in Eq. (1.71) from the general state  $|b\rangle$  as shown in Eq. (1.69).

The algorithm works with three registers. The first one is an ancillary register made of a single qubit, the second is also an ancillary register but made of  $d$  qubits, the third register is made of  $n_b$  qubits and will encode the solution of the problem. The HHL circuit is the following



The algorithm works as the following. Initially, all the qubits are prepared in  $|0\rangle$ :

$$|\Psi_0\rangle = |0\rangle |0\rangle^{\otimes d} |0\rangle^{\otimes n_b}, \quad (1.73)$$

then the information about  $\mathbf{b}$  is encoded in the last register:

$$|\Psi_1\rangle = \hat{\mathbb{1}} \otimes \hat{\mathbb{1}}^{\otimes d} \otimes \hat{U}_b |\Psi_0\rangle = |0\rangle |0\rangle^{\otimes d} |b\rangle. \quad (1.74)$$

We apply the QPE procedure, which is here broke down in the corresponding three steps. The first is the application of the Hadamard gate:

$$|\Psi_2\rangle = \hat{\mathbb{1}} \otimes \hat{H}^{\otimes d} \otimes \hat{\mathbb{1}} |\Psi_1\rangle = |0\rangle \frac{1}{2^{d/2}} (|0\rangle + |1\rangle)^{\otimes d} |b\rangle. \quad (1.75)$$

This is followed by the controlled unitary  $\hat{U}^j$ :

$$|\Psi_3\rangle = \hat{\mathbb{1}} \otimes C(U^j) |\Psi_2\rangle = |0\rangle \frac{1}{2^{d/2}} \sum_{k=0}^{2^d-1} e^{2\pi i k \varphi} |k\rangle |b\rangle, \quad (1.76)$$

where  $\hat{U} |b\rangle = e^{2\pi i \varphi} |b\rangle$  with  $\varphi \in [0, 1[$ . Finally, we apply the inverse Fourier transform to the second register

$$\begin{aligned}
|\Psi_4\rangle &= \hat{\mathbb{1}} \otimes \hat{F}^\dagger \otimes \hat{\mathbb{1}}^{\otimes n_b} |\Psi_3\rangle, \\
&= |0\rangle \frac{1}{2^{d/2}} \sum_{k=0}^{2^d-1} e^{2\pi i k \varphi} \hat{F}^\dagger |k\rangle |b\rangle, \\
&= |0\rangle \frac{1}{2^d} \sum_{k=0}^{2^d-1} e^{2\pi i k \varphi} \sum_{y=0}^{2^d-1} e^{-2\pi i y k / 2^d} |y\rangle |b\rangle.
\end{aligned} \tag{1.77}$$

However, one has that

$$\sum_{k=0}^{2^d-1} e^{2\pi i k (\varphi - y / 2^d)} = \begin{cases} \sum_{k=0}^{2^d-1} e^0 = 2^d, & \text{if } \varphi = y / 2^d, \\ 0, & \text{if } \varphi \neq y / 2^d, \end{cases} \tag{1.78}$$

meaning that the  $k$  sum selects the value of  $y = \varphi 2^d$ . Thus,

$$|\Psi_4\rangle = |0\rangle |\varphi 2^d\rangle |b\rangle. \tag{1.79}$$

In general,  $|b\rangle$  is in a superposition of  $|v_j\rangle$ , then

$$\hat{U} |v_j\rangle = e^{2\pi i \hat{A}} |v_j\rangle = e^{2\pi i \lambda_j} |v_j\rangle. \tag{1.80}$$

Then, the entire QPE gate maps

$$|\Psi_1\rangle = |0\rangle |0\rangle^{\otimes d} \sum_{j=0}^{2^{n_b}-1} \beta_j |v_j\rangle \xrightarrow{U_{\text{QPE}}} |\Psi_4\rangle = |0\rangle \sum_{j=0}^{2^{n_b}-1} \beta_j |\lambda_j 2^d\rangle |v_j\rangle. \tag{1.81}$$

We apply a controlled rotation on the first register, such that

$$|\Psi_5\rangle = C(R) \otimes \hat{\mathbb{1}}^{\otimes n_b} |\Psi_4\rangle = \sum_{j=0}^{2^{n_b}-1} \beta_j \left( \sqrt{1 - \frac{C^2}{\lambda_j^2}} |0\rangle + \frac{C}{\lambda_j} |1\rangle \right) |\lambda_j 2^d\rangle |v_j\rangle, \tag{1.82}$$

where  $C \in \mathbb{R}$  is an arbitrary constant. At this point we perform the measurement of the first register. If the outcome is  $+1$  and the state collapses in  $|0\rangle$  then we discard the run; if the outcome is  $-1$  with the state collapsed in  $|1\rangle$  then we retain the run. To increase the probabilities of having the outcome  $-1$ , we make  $C$  as large as possible. After the collapse of the first register in  $|1\rangle$ , the state of the second and third register is

$$|\Psi_6\rangle = \frac{1}{\left( \sum_{j=0}^{2^{n_b}-1} |\beta_j / \lambda_j|^2 \right)^{1/2}} \sum_{j=0}^{2^{n_b}-1} \frac{\beta_j}{\lambda_j} |\lambda_j 2^d\rangle |v_j\rangle, \tag{1.83}$$

where we exploited that  $C \in \mathbb{R}$ . Now, we apply the inverse QPE, which has also three steps. The first is the application of the QFT:

$$\begin{aligned}
|\Psi_7\rangle &= \hat{F} \otimes \hat{\mathbb{1}}^{\otimes n_b} |\Psi_6\rangle, \\
&= \frac{1}{\left( \sum_{j=0}^{2^{n_b}-1} |\beta_j / \lambda_j|^2 \right)^{1/2}} \sum_{j=0}^{2^{n_b}-1} \frac{\beta_j}{\lambda_j} \hat{F} |\lambda_j 2^d\rangle |v_j\rangle, \\
&= \frac{1}{\left( \sum_{j=0}^{2^{n_b}-1} |\beta_j / \lambda_j|^2 \right)^{1/2}} \sum_{j=0}^{2^{n_b}-1} \frac{\beta_j}{\lambda_j} \frac{1}{2^{d/2}} \sum_{y=0}^{2^d-1} e^{2\pi i y (\lambda_j 2^d) / 2^d} |y\rangle |v_j\rangle.
\end{aligned} \tag{1.84}$$

Then, we apply the controlled unitary  $C(U^{-j})$ , which gives

$$\begin{aligned}
|\Psi_8\rangle &= C(U^{-j}) |\Psi_7\rangle, \\
&= \frac{1}{\left(\sum_{j=0}^{2^{n_b}-1} |\beta_j/\lambda_j|^2\right)^{1/2}} \sum_{j=0}^{2^{n_b}-1} \frac{\beta_j}{\lambda_j} \frac{1}{2^{d/2}} \sum_{y=0}^{2^d-1} e^{2\pi i y \lambda_j} |y\rangle e^{-2\pi i \lambda_j y} |v_j\rangle,
\end{aligned} \tag{1.85}$$

where the two phases cancel and thus

$$|\Psi_8\rangle = \frac{1}{2^{d/2}} \sum_{y=0}^{2^d-1} |y\rangle \sum_{j=0}^{2^{n_b}-1} \frac{\beta_j}{\lambda_j} \frac{1}{\left(\sum_{j=0}^{2^{n_b}-1} |\beta_j/\lambda_j|^2\right)^{1/2}} |v_j\rangle. \tag{1.86}$$

Finally, the application of Hadamard's gates on the second register gives

$$|\Psi_9\rangle = \hat{H}^{\otimes d} \otimes \hat{\mathbb{1}}^{\otimes n_b} |\Psi_8\rangle = |0\rangle^{\otimes d} \sum_{j=0}^{2^{n_b}-1} \frac{\beta_j}{\lambda_j} \frac{1}{\left(\sum_{j=0}^{2^{n_b}-1} |\beta_j/\lambda_j|^2\right)^{1/2}} |v_j\rangle, \tag{1.87}$$

where the third register is exactly in the form in Eq. (1.71) after the proper normalisation. Thus,

$$|\Psi_9\rangle = |0\rangle^{\otimes d} |x\rangle, \tag{1.88}$$

embeds the solution of the linear system  $A\mathbf{x} = \mathbf{b}$ .

## Chapter 2

# Variational Quantum Algorithms

This class of algorithms employs a quantum and a classical computer to solve some optimisation problems. The quantum computer performs the quantum evolution of a state with respect to an Hamiltonian that is transformed, say from  $\hat{H}_0$  to  $\hat{H}_1$ . The classical computer determines how such a transformation should take place employing the variational principle. Typically, the problem is to map the state from the ground state of  $\hat{H}_0$  to that of  $\hat{H}_1$ , whose ground state is unknown. Thus, one wants to have a well-known  $\hat{H}_0$ . This is often taken as that of the Ising model.

### 2.1 The Ising model

In a combinatorial optimisation problem, one has a string of  $n$  bits and wants to optimise a particular problem. The problem is mapped in a minimisation (or maximisation) of a cost function  $C : \{0, 1\}^n \rightarrow \mathbb{R}$ . Notably, the maximisation problem can be obtained from the minimisation one by a minus sign:  $C \rightarrow -C$ .

To solve a combinatorial optimisation problem via a quantum algorithm, one needs to encode the problem onto a quantum system. In the following, we show how the Ising Hamiltonian can be used to embed such an optimisation problem.

The Ising model was developed to study the phase transition in magnetic materials. It consists in  $n$  spins that can be coupled via long-range interactions. The corresponding Hamiltonian is

$$\hat{H}_C = - \sum_{i=1}^n h_i \hat{\sigma}_z^{(i)} - \sum_{1 \leq i < j \leq n} J_{ij} \hat{\sigma}_z^{(i)} \hat{\sigma}_z^{(j)}, \quad (2.1)$$

where  $h_i$  are the single spin magnetic fields describing the single spin evolution and  $J_{ij}$  the spin-spin couplings. The choice of the latter encodes if the spins are encouraged to be aligned (ferromagnetic phase) or anti-aligned (antiferromagnetic phase). Since only  $\hat{\sigma}_z$  are appearing in  $\hat{H}_C$ , then its spectral decomposition can be expressed in the computational basis:

$$\hat{H}_C = \sum_{z=0}^{2^n - 1} C(z) |z\rangle \langle z|, \quad (2.2)$$

where  $C(z)$  is the energy of the specific spin configuration  $|z\rangle$ . Then, by properly mapping a combinatorial problem in the choice of  $\{h_i\}$  and  $\{J_{ij}\}$ , one can find the optimal solution by minimizing the energy, i.e. by finding the configuration  $|z\rangle$  that corresponds to minimal energy (or cost)  $C(z)$ .

## 2.2 Mapping combinatorial optimisation problems into the Ising model

Many problems can be mapped in the form in Eq. (2.1), and hence solve with a quantum computer, by choosing the appropriate values of  $\{ h_i \}$  and  $\{ J_{ij} \}$ . Here we consider some explicit examples.

**Subset sum problem.** Given an integer number  $m$  (total value) and a set of  $N$  positive and negative integers  $n = \{ n_1, \dots, n_N \}$ , which is the subset of the latter integers whose sum gives  $m$ ?

**Example 2.1**

Consider the case of  $m = 7$  and  $n = \{ -5, -3, 1, 4, 9 \}$ . The subset  $\{ -3, 1, 9 \}$  solves the problem:  $-3 + 1 + 9 = 7 = m$ .

**Exercise 2.1**

Consider the case of  $m = 13$  and  $n = \{ -3, 2, 8, 4, 20 \}$ . Show that the corresponding subset sum problem has no solution.

The subset sum problem can be framed as an energy minimisation problem as follows. Consider the sum  $\sum_{i=1}^N n_i z_i - m$ , where  $n_i$  are the elements of  $n$  and  $z_i \in \{ 0, 1 \}$  are weights that select or not the corresponding element  $n_i$  in the sum (effectively, this is the way to select a specific subsection). We define  $\mathcal{E}(z)$  as the square of such a sum:

$$\mathcal{E}(z) = \mathcal{E}(z_1, \dots, z_N) = \left( \sum_{i=1}^N n_i z_i - m \right)^2. \quad (2.3)$$

Then, if there is a subset solving the problem, one has that exists a value of  $z = \{ z_1, \dots, z_N \}$  such that  $\mathcal{E}(z) = 0$ . Conversely, if all the possible values of  $z$  give  $\mathcal{E}(z) \neq 0$ , then there is no subset that can solve the subset sum problem. One can already see that the  $z$  corresponding to the solution of the problem is the one minimising  $\mathcal{E}(z)$ . We now show the connection with the Ising model. We introduce the classical spins  $s_i = \pm 1$ , which will be employed in place of the weights  $z_i$ . Namely, one uses

$$z_i = \frac{1}{2}(1 - s_i), \quad (2.4)$$

so that  $s_i = +1$  (spin up) corresponds to  $z_i = 0$  and  $s_i = -1$  (spin down) to  $z_i = 1$ . We define the corresponding classical Hamiltonian

$$\begin{aligned} \mathcal{H}(s_1, \dots, s_N) &= \left( \sum_{i=1}^N n_i \frac{1}{2}(1 - s_i) - m \right)^2, \\ &= \frac{1}{4} \sum_{i,j=1}^N n_i n_j s_i s_j - \sum_{i=1}^N \left( \frac{1}{2} \sum_{j=1}^N n_j - m \right) n_i s_i + \left( \frac{1}{2} \sum_{i=1}^N n_i - m \right)^2, \end{aligned} \quad (2.5)$$

where the last term is independent from  $s_i$  and thus is a negligible constant of the problem. After having defined

$$J_{ij} = -\frac{n_i n_j}{4}, \quad \text{and} \quad h_i = \left( \frac{1}{2} \sum_{j=1}^N n_j - m \right) n_i, \quad (2.6)$$

the Hamiltonian becomes

$$\mathcal{H}(s_1, \dots, s_N) = - \sum_{1 \leq i < j \leq n} J_{ij} s_i s_j - \sum_{i=1}^n h_i s_i + \text{const}, \quad (2.7)$$

where

$$\text{const} = \left( \frac{1}{2} \sum_{i=1}^N n_i - m \right)^2 - \sum_{i=1}^N J_{ii} s_i^2, \quad (2.8)$$

is  $s_i$  independent since  $s_i^2 = 1$  for any value of  $i$ . To solve the problem on a quantum computer, one quantises the Hamiltonian in Eq. (2.7) by substituting  $s_i \rightarrow \hat{\sigma}_z^{(i)}$  and gets Eq. (2.1).

**Number partitioning problem.** Another combinatorial problem that can be mapped in an Ising Hamiltonian is the number partitioning problem. It asks if a set of  $N$  integers  $\{n_1, \dots, n_N\}$  can be partitioned in two subsets such that the sum of the elements in the individual subsets is equal.

**Example 2.2**

Consider the set  $n = \{1, 2, 3, 4, 6, 10\}$ . In such a case, one can consider the case of  $\{1, 2, 4, 6\}$  and  $\{3, 10\}$ , whose individual sums are both equal to 13.

The classical Hamiltonian for this problem can be straightforwardly constructed as

$$\mathcal{H}(s_1, \dots, s_N) = \left( \sum_{i=1}^N n_i s_i \right)^2, \quad (2.9)$$

with  $s_i = \pm 1$ . Clearly, the solution  $s = \{s_1, \dots, s_N\}$  is such that  $\mathcal{H}(s) = 0$ . Expanding the square, we find

$$\mathcal{H}(s) = - \sum_{1 \leq i < j \leq N} J_{ij} s_i s_j - \text{Tr}[J_{ij}], \quad (2.10)$$

where

$$J_{ij} = -\frac{n_i n_j}{2}, \quad \text{and} \quad \text{Tr}[J_{ij}] = \sum_{i=1}^N J_{ii} s_i^2. \quad (2.11)$$

The classical Hamiltonian in Eq. (2.10) can be quantised and one obtains that in Eq. (2.1) with no need to introduce the magnetic fields, i.e.  $h_i = 0$ .

## 2.3 Adiabatic Theorem

Adiabatic quantum computation is based on the adiabatic theorem. The latter considers the case of a time dependent Hamiltonian, that changes from  $\hat{H}_0$  at time  $t = 0$  to  $\hat{H}_1$  at time  $t = \tau$ . We also assume that the two Hamiltonians do not commute, i.e.  $[\hat{H}_0, \hat{H}_1] \neq 0$ . The theorem states that a system prepared in the  $n$ -th eigenstate of  $\hat{H}_0$  goes in the  $n$ -th eigenstate of  $\hat{H}_1$  if the transformation is made slowly enough, i.e. adiabatically. The application to quantum computation then is to take an initial Hamiltonian with a ground state that can be easily prepared and then adiabatically change the Hamiltonian to that of the problem one wants to optimise. If the system is initially in the ground state of  $\hat{H}_0$ , then will remain in the ground state of the target Hamiltonian  $\hat{H}_1$  and it will encode the solution of the optimisation problem.

The proof of the adiabatic theorem is the following. Consider the instantaneous spectralisation of a time-dependent Hamiltonian  $\hat{H}(t)$ , which is

$$\hat{H}(t) |n(t)\rangle = E_n(t) |n(t)\rangle, \quad (2.12)$$

where  $E_n(t)$  and  $|n(t)\rangle$  are respectively the corresponding instantaneous eigenvalues and eigenstates. Given a state  $|\psi(t)\rangle$  at time  $t$ , one can always express it as a superposition of the instantaneous eigenstates as

$$|\psi(t)\rangle = \sum_n c_n(t) |n(t)\rangle, \quad (2.13)$$

where

$$c_n(t) = \langle n(t) | \psi(t) \rangle, \quad (2.14)$$

determine the probabilities  $P_n(t) = |c_n(t)|^2$  of being in  $|n(t)\rangle$  at time  $t$ . The evolution of  $c_n(t)$  can be determined via

$$\begin{aligned} \dot{c}_n(t) &= \langle \dot{n}(t) | \psi(t) \rangle + \langle n(t) | \dot{\psi}(t) \rangle, \\ &= \langle \dot{n}(t) | \psi(t) \rangle - \frac{i}{\hbar} \langle n(t) | \hat{H}(t) | \psi(t) \rangle, \\ &= \langle \dot{n}(t) | \psi(t) \rangle - \frac{i}{\hbar} E_n(t) \langle n(t) | \psi(t) \rangle, \end{aligned} \quad (2.15)$$

where we defined  $|\dot{n}(t)\rangle = \frac{d}{dt}|n(t)\rangle$ , and we applied the Schrödinger equation and applied the Hamiltonian to its eigenstate. Then, by imposing Eq. (2.13), we get

$$\dot{c}_n(t) = \sum_m c_m(t) \langle \dot{n}(t) | m(t) \rangle - \frac{i}{\hbar} E_n(t) c_n(t), \quad (2.16)$$

which determines a system of coupled differential equations. In complete generality, the evolution of  $c_n(t)$  depends on  $c_m(t)$  for all values of  $m$ . To determine the first term of Eq. (2.16), we consider the time derivative of Eq. (2.12) with  $|n(t)\rangle$  substituted with  $|m(t)\rangle$  and projecting it on  $\langle n(t)|$ . This gives

$$\langle n(t) | \frac{d}{dt} \hat{H}(t) | m(t) \rangle + \langle n(t) | \hat{H} | \dot{m}(t) \rangle = \dot{E}_m(t) \delta_{nm} + E_m(t) \langle n(t) | \dot{m}(t) \rangle, \quad (2.17)$$

which can be recasted as

$$(E_n(t) - E_m(t)) \langle n(t) | \dot{m}(t) \rangle = \dot{E}_m(t) \delta_{nm} - \langle n(t) | \frac{d}{dt} \hat{H}(t) | m(t) \rangle. \quad (2.18)$$

For  $m \neq n$ , one then has

$$\langle \dot{n}(t) | m(t) \rangle = \frac{\langle n(t) | \frac{d}{dt} \hat{H}(t) | m(t) \rangle}{(E_n(t) - E_m(t))}, \quad (2.19)$$

where we exploited that  $\langle \dot{n}(t) | m(t) \rangle = -\langle n(t) | \dot{m}(t) \rangle$ . Thus, by separating the case of  $m = n$  and  $m \neq n$  in Eq. (2.16), we have

$$\dot{c}_n(t) = \left( \langle \dot{n}(t) | n(t) \rangle - \frac{i}{\hbar} E_n(t) \right) c_n(t) + \sum_{m \neq n} c_m(t) \frac{\langle n(t) | \frac{d}{dt} \hat{H}(t) | m(t) \rangle}{(E_n(t) - E_m(t))}. \quad (2.20)$$

In the limit where the Hamiltonian  $\hat{H}(t)$  changes slowly enough, i.e. for  $\langle n(t) | \frac{d}{dt} \hat{H}(t) | m(t) \rangle \ll (E_n(t) - E_m(t))$  for all  $n$  and  $m$ , then one can neglect the last term in Eq. (2.20). This is the so-called adiabatic approximation, which gives the following solutions

$$c_n(t) = e^{i\theta_n(t)} e^{i\gamma_n(t)} c_n(0), \quad (2.21)$$

where we defined

$$\theta_n(t) = -\frac{1}{\hbar} \int_0^t ds E_n(s), \quad \text{and} \quad \gamma_n(t) = -i \int_0^t ds \langle \dot{n}(s) | n(s) \rangle. \quad (2.22)$$

In particular,  $\gamma_n(t) \in \mathbb{R}$  is known as the Berry phase.

Importantly, under the adiabatic approximation, one has that the probabilities evolve as

$$P_n(t) = |c_n(t)|^2 = |c_n(0)|^2 = P_n(0), \quad (2.23)$$

which is the final proof of the theorem.

*Remark 2.1.* It is important to understand the limits in which the adiabatic approximation is valid. To prove it in complete generality, one should require that the time-scale  $\tau$  of the transformation is such that

$$\tau \gg \max_{n \neq m} \max_{0 \leq t \leq \tau} \left| \frac{\langle n(t) | \frac{d}{dt} \hat{H}(t) | m(t) \rangle}{(E_n(t) - E_m(t))} \right|. \quad (2.24)$$

For the perspective of quantum computation, one can restrict to the case of  $n = 0$  and  $m = 1$ . This is the case where the system is initially prepared in the ground state  $n = 0$  and one does not want a jump in the first excited state  $m = 1$ . In such a case, the approximation is valid if

$$\tau \gg \max_{0 \leq t \leq \tau} \left| \frac{\langle \psi_0(t) | \frac{d}{dt} \hat{H}(t) | \psi_1(t) \rangle}{(E_0(t) - E_1(t))} \right|. \quad (2.25)$$

Notably, the more the energy gap  $E_1 - E_0$  closes, the larger value of  $\tau$  one has to consider. In the case of a linear transition between the initial  $\hat{H}_0$  and final Hamiltonian  $\hat{H}_1$  (i.e.  $\hat{H}(t) = (1-t/\tau)\hat{H}_0 + t/\tau\hat{H}_1$ ), a necessary condition for keeping the energy gap open is that  $[\hat{H}_0, \hat{H}_1] \neq 0$ . Figure 2.1 represents graphically how the gap should remain open during the Hamiltonian change so that the initial state being the ground state of  $\hat{H}_0$  is mapped to the ground state of  $\hat{H}_1$ , which encodes the solution of the problem.

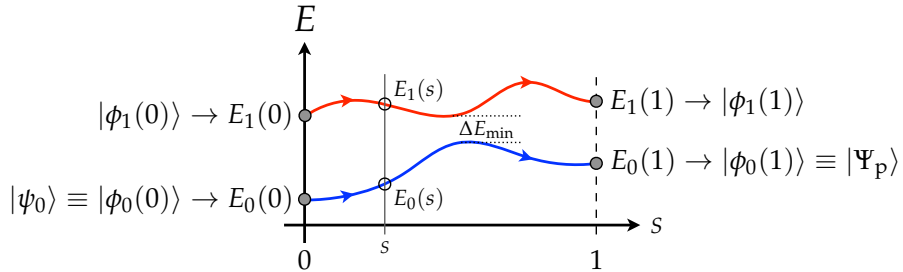


Fig. 2.1: Graphical representation of how the energy levels of  $\hat{H}(t)$  change in time. As long as the minimum energy gap  $\Delta E_{\min}$  is finite, one can employ the adiabatic theorem to go from the ground state of  $\hat{H}_0$  (here denoted as  $|\psi_0\rangle$ ) to that of  $\hat{H}_1$  ( $|\Psi_p\rangle$ ). Here, we used the parameter  $s$  to parametrise the time flow:  $t = s\tau$ .

## 2.4 Quantum Annealing

The quantum annealing is an heuristic quantum algorithm based on the adiabatic theorem. It aims at solving hard combinatorial optimisation problems using the Ising Hamiltonian as a target Hamiltonian.

The algorithm exploits an Hamiltonian transformation of the form

$$\hat{H}(t) = (1 - s(t)) \hat{H}_0 + s(t) \hat{H}_C, \quad (2.26)$$

where  $s(t)$  is a suitable smooth function of time with  $s(0) = 0$  and  $s(\tau) = 1$ , and  $\hat{H}_C$  is the Ising Hamiltonian in Eq. (2.1) whose ground state encodes the solution of the problem. Moreover, one requires that  $H_0$  has a non-degenerate ground state that is easy to prepare and that  $[\hat{H}_0, \hat{H}_1] \neq 0$ . A simple choice is

$$\hat{H}_0 = - \sum_{i=1}^n \hat{\sigma}_x^{(i)}, \quad (2.27)$$

which has  $|+\rangle^{\otimes n}$  as ground state. This can be easily prepared via Hadamard gates:  $|+\rangle^{\otimes n} = \hat{H}^{\otimes n} |0\rangle^{\otimes n}$ .

If the quantum annealing time  $\tau$  is not sufficiently long (i.e. the transformation is not sufficiently adiabatic), which is essentially always the case, then one reach a state  $|\psi(\tau)\rangle$ , which has a probability  $p$  of being the solution

of the problem. Such a probability (of success) is given by  $p = |\langle z_{\text{sol}} | \psi(\tau) \rangle|^2$ , where  $|z_{\text{sol}}\rangle$  is the state encoding the exact solution. To obtain the solution with a 99% certainty, one has to repeat the annealing procedure  $m$  times. Indeed,

$$P_{\text{succ}}^m = 1 - (1 - p)^m = 0.99. \quad (2.28)$$

The corresponding total time required is given by

$$T_{99\%} = m\tau = \frac{\ln(1 - 0.99)}{\ln(1 - p)}\tau \quad (2.29)$$

A strong challenge for the quantum annealing is the full connectivity of the qubits. Indeed, in a quantum computer, the qubits interactions, which are parameterised by  $J_{ij}$ , are typically null beyond nearest-neighbour sites. This strongly limits the scaling of universally annealing where one can suitably tune all the values of  $J_{ij}$ .

## 2.5 Quantum Approximate Optimisation Algorithm (QAOA)

The Quantum Approximate Optimisation Algorithm (QAOA) is a hybrid quantum-classical algorithm that allows for optimising a cost function and finding an approximated solution. It is an application of the adiabatic theorem, similarly as the quantum annealing, which is run on a quantum computer, while a classical computer optimises the cost function.

We start from a quantum annealing Hamiltonian of the form

$$\hat{H}(t) = (1 - s(t))\hat{H}_{\text{M}} + s(t)\hat{H}_{\text{C}}, \quad (2.30)$$

where  $s(t)$  is an arbitrary function such that  $s(0) = 0$  and  $s(\tau) = 1$  with  $\tau$  being the total time of the algorithm. The initial Hamiltonian  $\hat{H}_{\text{M}}$  is such that its ground state can be prepared easily.  $\hat{H}_{\text{C}}$  is instead the cost Hamiltonian whose ground state encodes the solution to the problem. The QAOA is based on the observation that the best way to implement the annealing Hamiltonian in Eq. (2.30) is a Trotter procedure. Namely, this is to consider the unitary evolution with respect to  $\hat{H}(t)$  and decompose it in small time steps. Then, we have

$$\hat{U}(\tau) = \text{T exp} \left[ -\frac{i}{\hbar} \int_0^\tau dt \hat{H}(t) \right] \simeq \prod_{k=1}^p \exp \left[ -\frac{i}{\hbar} \hat{H}(k\Delta t) \Delta t \right], \quad (2.31)$$

where T indicates the time ordering, one assumes a large number of steps  $p \gg 1$  of length  $\Delta = \tau/p$ . Owing that for  $[\hat{A}, \hat{B}] \neq 0$  one has

$$e^{i(\hat{A}+\hat{B})\Delta t} = e^{i\hat{A}\Delta t} e^{i\hat{B}\Delta t} + \mathcal{O}((\Delta t)^2), \quad (2.32)$$

and since we require that  $[\hat{H}_{\text{C}}, \hat{H}_{\text{M}}] \neq 0$ , one has that at each time step the following approximation is valid to the order  $(\Delta t)^2$ :

$$\hat{U}(\tau) \simeq \prod_{k=1}^p \exp \left[ -\frac{i}{\hbar} (1 - s(k\Delta t)) \hat{H}_{\text{M}} \Delta t \right] \exp \left[ -\frac{i}{\hbar} s(k\Delta t) \hat{H}_{\text{C}} \Delta t \right]. \quad (2.33)$$

Now, the key idea of QAOA is to redefine the time dependence in the following way:

$$\frac{1}{\hbar} (1 - s(k\Delta t)) \Delta t \rightarrow \beta_k, \quad \text{and} \quad \frac{1}{\hbar} s(k\Delta t) \Delta t \rightarrow \gamma_k. \quad (2.34)$$

Thus, we have

$$\hat{U}(\tau) \simeq \prod_{k=1}^p \exp \left[ -i\beta_k \hat{H}_{\text{M}} \right] \exp \left[ -i\gamma_k \hat{H}_{\text{C}} \right], \quad (2.35)$$

where the parameters  $\beta = (\beta_1, \dots, \beta_p)$  and  $\gamma = (\gamma_1, \dots, \gamma_p)$  become the variational parameters to be optimised. Crucial difference with respect to the quantum annealing case is that one optimises over a set of  $2p$  parameters

instead of a fixed time segments. Finally, one constructs the variational state

$$|\gamma, \beta\rangle = \prod_{k=1}^p e^{-i\beta_k \hat{H}_M} e^{-i\gamma_k \hat{H}_C} |\text{init}\rangle, \quad (2.36)$$

where the initial state  $|\text{init}\rangle$  is the ground state of  $\hat{H}_M$ . In the case of  $\hat{H}_M$  being equal to Eq. (2.27), one has

$$|\text{init}\rangle = \hat{H}^{\otimes n} |0\rangle^{\otimes n}. \quad (2.37)$$

In the computational basis, the variational state reads

$$|\gamma, \beta\rangle = \sum_{z=0}^{2^n-1} d_z(\gamma, \beta) |z\rangle, \quad (2.38)$$

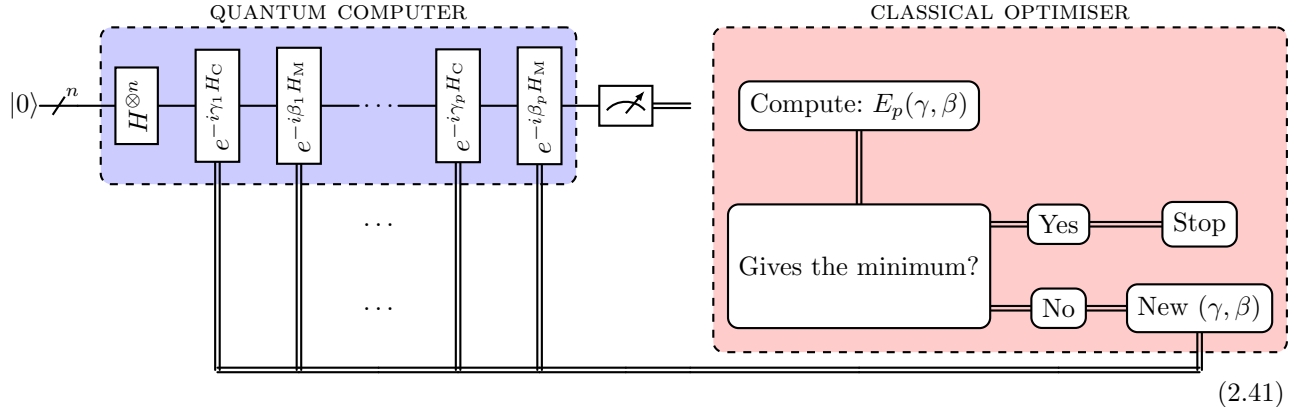
where  $d_z(\gamma, \beta)$  defines the superposition in the  $Z$  basis. Notably, since  $\hat{H}_C$  encodes in its ground state the solution of the problem, one needs to minimise the expectation value of  $\hat{H}_C$  computed on the variational state. Namely

$$E_p(\gamma, \beta) = \langle \gamma, \beta | \hat{H}_C | \gamma, \beta \rangle = \sum_{z=0}^{2^n-1} P_z(\gamma, \beta) C(z), \quad (2.39)$$

where  $P_z(\gamma, \beta) = |d_z(\gamma, \beta)|^2$  is the probability of having the  $|z\rangle$  state and  $C(z) = \langle z | \hat{H}_C | z \rangle$  is the corresponding cost. The best  $(\gamma, \beta)$  are such that

$$(\gamma^*, \beta^*) = \arg \min_{\gamma, \beta} E_p(\gamma, \beta). \quad (2.40)$$

Such an optimisation is performed on classical computer (classical optimiser). The circuit representation of the QAOA is



### Exercise 2.2

Derive the explicit expression of the cost function  $C(z)$  in terms of the coefficients  $J_{ij}$  and  $h_i$ .

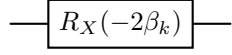
The single  $k$  step of the QAOA, when considering  $\hat{H}_M$  as in Eq. (2.27) and  $\hat{H}_C$  being the Ising Hamiltonian, is implemented as the following. First we consider  $\hat{H}_M$ ,

$$\hat{H}_M = - \sum_{i=1}^n \hat{\sigma}_x^{(i)}. \quad (2.42)$$

Then, the corresponding unitary acts independently on each qubit

$$e^{-i\beta_k \hat{H}_M} = e^{i\beta_k \sum_{i=1}^n \hat{\sigma}_x^{(i)}} = \prod_{i=1}^n e^{i\beta_k \hat{\sigma}_x^{(i)}}. \quad (2.43)$$

Then, the corresponding action can be implemented with a rotation on the single  $i$ -th qubit. The circuit implementing it is

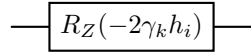


$$(2.44)$$

Indeed a rotation around  $\mathbf{n}$  by an angle  $\theta$  is defined a  $\hat{R}^{\mathbf{n}}(\theta) = e^{-i\theta\mathbf{n}\cdot\hat{\sigma}/2}$ . The implementation of the unitary related to  $\hat{H}_C$  can be divided in two steps, indeed the two terms of  $\hat{H}_C$  in Eq. (2.1) commute. Then, one writes

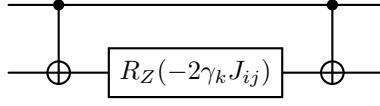
$$e^{-i\gamma_k \hat{H}_C} = e^{i\gamma_k (\sum_{i=1}^n h_i \hat{\sigma}_z^{(i)} + \sum_{1 \leq i < j \leq n} J_{ij} \hat{\sigma}_z^{(i)} \hat{\sigma}_z^{(j)})} = \prod_{1 \leq i < j \leq n} e^{i\gamma_k J_{ij} \hat{\sigma}_z^{(i)} \hat{\sigma}_z^{(j)}} \prod_{i=1}^n e^{i\gamma_k h_i \hat{\sigma}_z^{(i)}}. \quad (2.45)$$

Here, the single qubits factors act as rotations, with a circuit being



$$(2.46)$$

On the other hand, the two qubits interactions are 2-local gates, which can be implemented via a rotation between two CNOT gates. Namely, the corresponding circuit will read



$$(2.47)$$

thus becoming very easy to be implemented.

## 2.6 Variational Quantum Eigensolver (VQE)

Similarly as the QAOA, the Variational Quantum Eigensolver (VQE) is an heuristic approach to solve combinatorial optimisation problem that exploits a combination of quantum computation and classical optimisation. In particular, the QAOA can be seen as a specific implementation of the VQE algorithm.

The algorithm is designed to solve problems that can be stated as finding the ground state energy  $E_0$  of  $n$  qubit Hamiltonian. Namely, to find the configuration corresponding to the state  $|\Psi_0\rangle$  that

$$\hat{H} |\Psi_0\rangle = E_0 |\Psi_0\rangle. \quad (2.48)$$

The generality with respect to QAOA comes in the form of the cost Hamiltonian  $\hat{H}_C$ . Indeed, one assumes for it the most general form, which is

$$\hat{H}_C = \sum_{\alpha} h_{\alpha} \hat{P}_{\alpha} = \sum_{\alpha} h_{\alpha} \bigotimes_{j=1}^n \hat{\sigma}_{\alpha_j}^{(j)}, \quad (2.49)$$

where  $h_{\alpha}$  are coefficients and the  $\hat{P}_{\alpha}$  are called Pauli strings. The latter are product of  $n$  single-qubit Pauli matrices (including the identity). Thus, compared to QAOA (which exploits the Ising model), this Hamiltonian is not limited to two qubit interactions only, but can consider  $n$  qubit interactions. This is particularly relevant when considering more complex systems where the Ising model fails to describe the entire complexity of the problem.

Then, the steps of VQE are the following:

1. Map the problem in a cost Hamiltonian  $\hat{H}_C$  so that the solution is embedded in its ground state.

2. Prepare the initial state as the ground state of  $\hat{H}$ .
3. Generate the trial state  $|\Psi(\theta)\rangle$ , which is determined by a set of parameters  $\theta$ .
4. Measure the expectation values of the Pauli strings in the Hamiltonian, i.e.  $\langle\Psi(\theta)|\hat{P}_\alpha|\Psi(\theta)\rangle$ . This is the end of the computation on the quantum computer
5. Compute the corresponding energy, i.e.  $E(\theta) = \sum_\alpha h_\alpha \langle\Psi(\theta)|\hat{P}_\alpha|\Psi(\theta)\rangle$
6. Update or accept the values of  $\theta$  based on the result.
7. If updated, one goes back to point 2.

Notably, when searching for the ground state energy of the cost Hamiltonian, there are several pitfalls that the update step must deal with. For example, the parameter landscape may have local minima where one does not want to remain stacked.

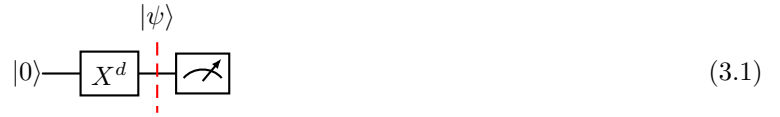
## Chapter 3

# Noisy Intermediate-Scale Quantum (NISQ) computation

For quantum algorithms to function properly, we need to ensure that the basic units of quantum information, the qubits, are as reliable as the bits in classical computers. These qubits must be shielded from environmental noise that can disrupt their states, while still have to be controlled by external agents. This control involves making the qubits entangle and eventually measuring their states to extract the outputs of the quantum computation. Technically, it is feasible to minimise the impact of noise without compromising the quantum information process through the development of Quantum Error Correction (QEC) and Quantum Error Mitigation (QEM) protocols, see Chap. 4.

Many quantum algorithms that come with guaranteed performance need millions of physical qubits to effectively use QEC methods. It could take decades to build fault-tolerant quantum computers capable of reaching this scale. Presently, quantum devices typically have around 100-1000 physical qubits, often referred to as noisy intermediate-scale quantum (NISQ) devices. These devices lack error correction and are imperfect, yet in the NISQ era, the aim is to maximize the quantum computational capabilities of current devices, while working on techniques for fault-tolerant quantum computation.

Here, we study how noises impact quantum circuits. The following circuit will be considered as a basis of the study:



where the gate  $X$  is repeated  $d$  times. The value of  $d$  is also called the depth of the circuit. The state before the measurement, when no noise is considered, is given by

$$|\psi\rangle = (i\hat{R}_x(\theta = \pi))^d |0\rangle = i^d [\cos(d\pi/2) |0\rangle - \sin(d\pi/2) |1\rangle], \quad (3.2)$$

indeed one has that the  $X$  gate can be realised as a rotation of an angle  $\pi$  around the  $x$  axis:  $\hat{\sigma}_x = i\hat{R}_x(\pi)$ . Notably, the factor  $i^d$  is just a negligible global phase. The expectation value of the polarisation is

$$\langle Z \rangle = \langle \psi | \hat{\sigma}_z | \psi \rangle = \cos^2(d\pi/2) - \sin^2(d\pi/2) = \cos(d\pi), \quad (3.3)$$

which is shown in the left panel of Fig. 3.1. Clearly, the value of  $\langle Z \rangle$  jumps from +1 to -1 depending on the value of  $d$ . However, when we perform such a simple experiment the result is quite different due to the noises and errors acting on the system. This is represented in the right panel Fig. 3.1. Such a result account for the presence of different noises and errors. These are listed and studied below.

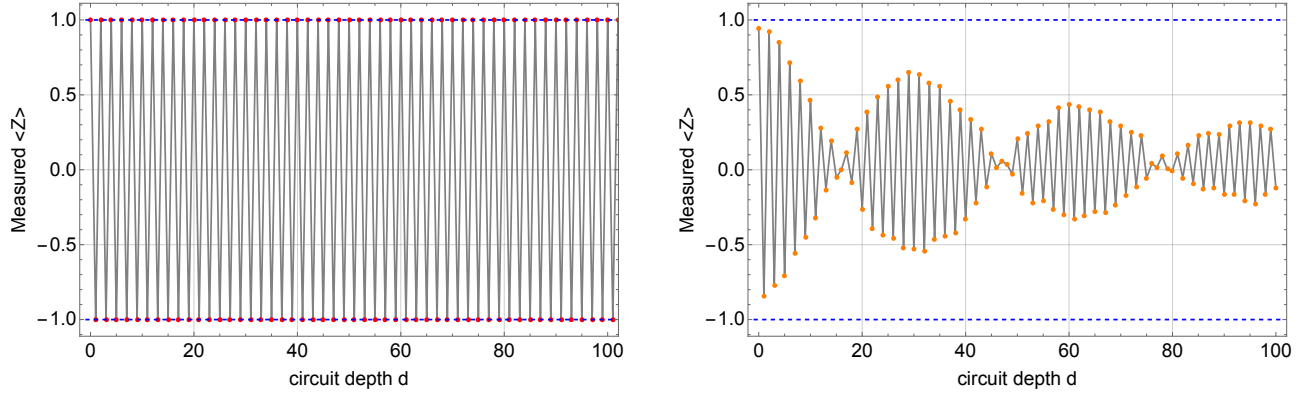


Fig. 3.1: Expectation value of the polarisation  $\langle Z \rangle$  for the circuit in Eq. (3.1) with respect to the depth  $d$  of the circuit: (left panel) in the case of no noises; (right panel) when noises are accounted.

### 3.1 Miscalibrated gates

As we saw previously, the gate  $X$  can be performed as a rotation of an angle  $\pi$  around the  $x$  axis. Now, let us suppose that the gate is systematic miscalibrated. Specifically, one performs a rotation of an angle of  $\pi + \epsilon$  in place of only  $\pi$ . Then, we have that the actual gate  $\tilde{X}$  is given by

$$\text{---} \boxed{\tilde{X}} \text{---} = \text{---} \boxed{X} \text{---} iR_x(\epsilon) \text{---} \quad (3.4)$$

indeed one has that

$$R_x(\pi + \epsilon) = R_x(\pi)R_x(\epsilon). \quad (3.5)$$

Then, when running the circuit with  $d$  repetitions, one simply has

$$|0\rangle \text{---} \boxed{\tilde{X}^d} \text{---} \cancel{\text{---}} = |0\rangle \text{---} \boxed{X^d} \text{---} iR_x(d\epsilon) \text{---} \cancel{\text{---}} |\psi\rangle \quad (3.6)$$

where

$$|\psi\rangle = i^d \left[ \cos\left(d\frac{(\pi+\epsilon)}{2}\right) |0\rangle - i \sin\left(d\frac{(\pi+\epsilon)}{2}\right) |1\rangle \right]. \quad (3.7)$$

Correspondingly, one has that the expectation value for the polarisation is

$$\langle Z \rangle = \cos^2\left(d\frac{(\pi+\epsilon)}{2}\right) - \sin^2\left(d\frac{(\pi+\epsilon)}{2}\right) = \cos(d(\pi + \epsilon)), \quad (3.8)$$

which is shown in the left panel of Fig. 3.2. For small values of  $\epsilon$  and  $d$ , one performs an error of

$$|\langle Z \rangle_{\text{noiseless}} - \langle Z \rangle_{\text{miscalibrated}}| \sim \frac{1}{2}d^2\epsilon^2, \quad (3.9)$$

which scales quadratically with the miscalibration  $\epsilon$ . As it is shown in the right panel of Fig. 3.2, the difference with respect to the noiseless result can be substantial. Indeed, for values of  $d$  such that  $d\epsilon \sim (2n+1)\pi$ , with  $n \in \mathbb{N}$ , we have that

$$\langle Z \rangle_{\text{miscalibrated}} = -\langle Z \rangle_{\text{noiseless}}. \quad (3.10)$$

This means that the error completely inverts the output signal.

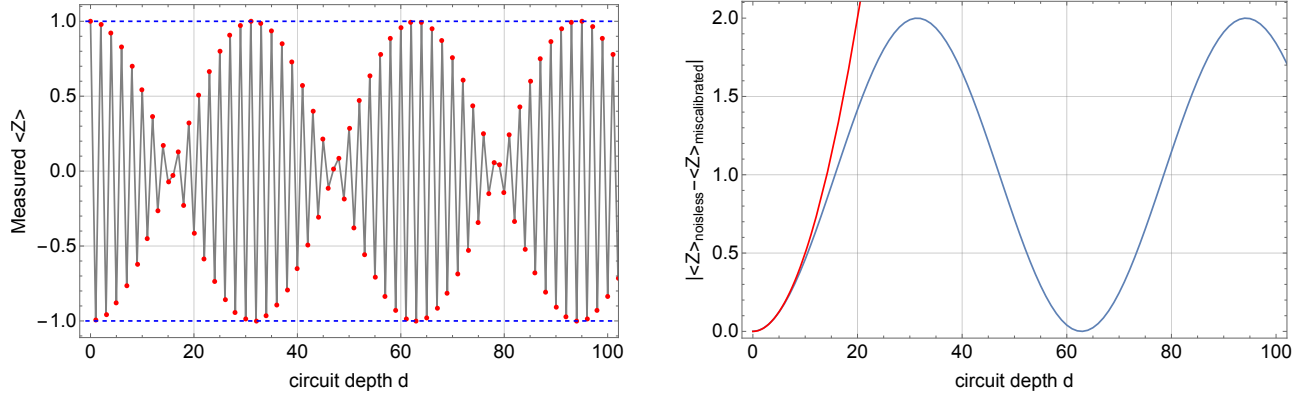


Fig. 3.2: (Left panel) Expectation value (red dots) of the polarisation  $\langle Z \rangle$  for the circuit in Eq. (3.1) with respect to the depth  $d$  of the circuit when miscalibrated gates are considered. (Right panel) Difference with respect to the noiseless case (blue line) and the small  $\epsilon$  and  $d$  expansion (red line). Here we considered  $\epsilon = 0.1$ .

### 3.2 Projection noise and sampling error

Consider the following trivial circuit

$$|\psi\rangle \xrightarrow{\text{gate}} \quad (3.11)$$

whose possible values of the polarisation are  $z = +1$ , meaning that the state after the collapse is  $|0\rangle$ , and  $z = -1$ , with corresponding state  $|1\rangle$ .

Let us define a measurement operator  $\hat{M}$  that indicates if the state of the qubit is in the  $|1\rangle$  state. Such an operator can be constructed as

$$\begin{aligned} \hat{M} &= |1\rangle\langle 1|, \\ &= 1|1\rangle\langle 1| + 0|0\rangle\langle 0|, \\ &= \sum_{m=0,1} m\hat{\Pi}_m, \end{aligned} \quad (3.12)$$

where  $m$  are the eigenvalues of  $\hat{M}$  and  $\hat{\Pi}_m = |m\rangle\langle m|$ , with  $\sum_m \hat{\Pi}_m = \hat{1}$ . Namely, the expectation value of  $\hat{M}$  indicates the probability  $p(m=1)$  that the state  $|\psi\rangle$  is equal to  $|1\rangle$ :

$$\langle\psi|\hat{M}|\psi\rangle = \langle\psi|1\rangle\langle 1|\psi\rangle = |\langle 1|\psi\rangle|^2 = p(m=1). \quad (3.13)$$

Correspondingly, one has  $p(m=0) = 1 - p(m=1)$ . To ease the notation, in the following we use  $p = p(m=1)$ . The outcomes of the operator  $\hat{M}$  are distributed via a binomial distribution  $\mathcal{B}(p)$ . To be more explicit, let us consider the repetition of the above circuit  $N$  times, meaning that we have  $N$  samplings of the protocol. Then, we can construct a series of outputs:  $\{m_n\}_{n=1}^N = \{0, 0, 1, 0, 1, 1, 0, \dots\}$ , where each entry is a random variable. This corresponds in a series of states into which the system has collapsed after the measurement:  $\{|0\rangle, |0\rangle, |1\rangle, |0\rangle, |1\rangle, |1\rangle, |0\rangle, \dots\}$ . Suppose we have  $N = 3$ , then we have a total of  $2^N = 2^3$  outputs  $(m_1, m_2, m_3)$ . Namely

$(m_1, m_2, m_3)   ( m_1\rangle,  m_2\rangle,  m_3\rangle)   S$		
$(0, 0, 0)$	$( 0\rangle,  0\rangle,  0\rangle)$	0
$(0, 0, 1)$	$( 0\rangle,  0\rangle,  1\rangle)$	$1/3$
$(0, 1, 0)$	$( 0\rangle,  1\rangle,  0\rangle)$	$1/3$
$(0, 1, 1)$	$( 0\rangle,  1\rangle,  1\rangle)$	$2/3$
$(1, 0, 0)$	$( 1\rangle,  0\rangle,  0\rangle)$	$1/3$
$(1, 0, 1)$	$( 1\rangle,  0\rangle,  1\rangle)$	$2/3$
$(1, 1, 0)$	$( 1\rangle,  1\rangle,  0\rangle)$	$2/3$
$(1, 1, 1)$	$( 1\rangle,  1\rangle,  1\rangle)$	1

(3.14)

where we also computed the corresponding sampling mean  $S$ , which is defined as

$$S = \frac{1}{N} \sum_{n=1}^N m_n. \quad (3.15)$$

The statement then is that the sampling mean  $S$ , which is also a random variable, is distributed as a binomial distribution  $\mathcal{B}(\mathbb{P})$ , with mean  $\mathbb{E}[S] = \mathbb{P}$  and variance  $\mathbb{V}[S] = \mathbb{P}(1 - \mathbb{P})/N$ . Fig. 3.3 shows some examples. Now,

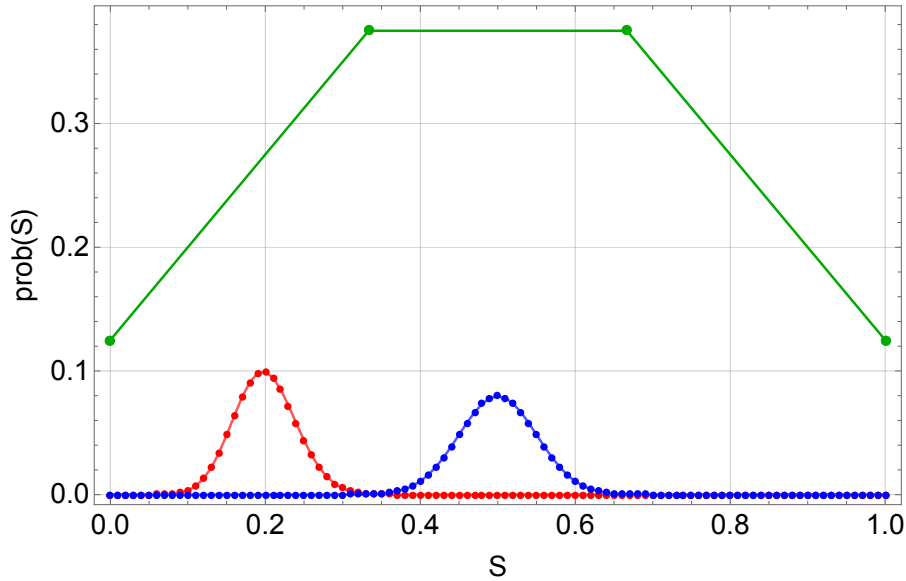


Fig. 3.3: Binomial distribution followed by the sampling mean  $S$  for  $N = 100$  samplings with  $\mathbb{P} = 0.2$  (red plot) and  $\mathbb{P} = 0.5$  (blue plot), and for  $N = 3$  with  $\mathbb{P} = 0.5$  (green plot).

by assuming that the state  $|\psi\rangle$  in Eq. (3.11) is that one has before the measurement in Eq. (3.6), i.e.

$$|\psi\rangle = i^d \left[ \cos\left(d\frac{\pi+\epsilon}{2}\right) |0\rangle - i \sin\left(d\frac{\pi+\epsilon}{2}\right) |1\rangle \right], \quad (3.16)$$

then the corresponding distribution  $\mathcal{B}(\mathbb{P}_d)$  depends on the probability of being in the state  $|1\rangle$  after a depth  $d$  of the circuit. This is given by

$$\mathbb{P}_d = \sin^2\left(d\frac{\pi+\epsilon}{2}\right). \quad (3.17)$$

The corresponding expectation value of the polarisation is shown in Fig. 3.4, where we also report its difference with respect to the case shown in Fig. 3.2.

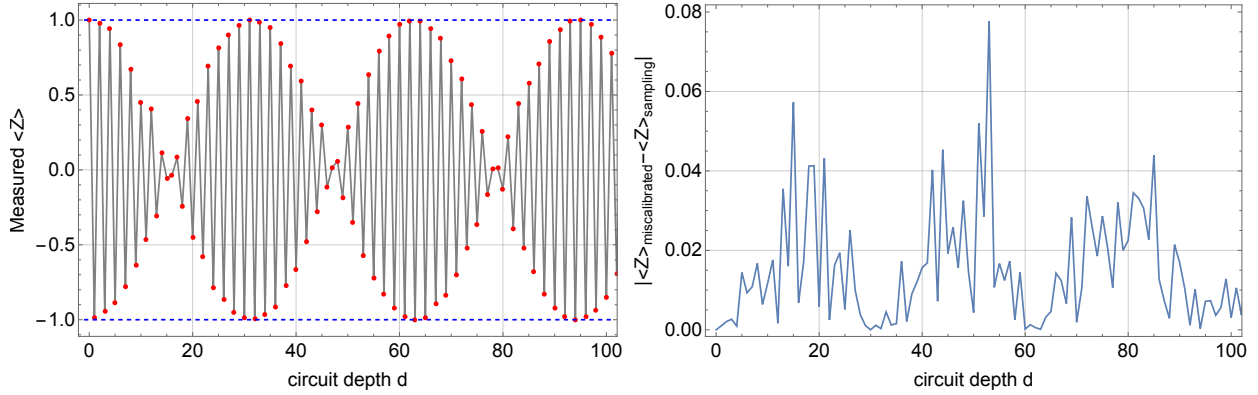


Fig. 3.4: (Left panel) Expectation value (red dots) of the polarisation  $\langle Z \rangle$  for the circuit in Eq. (3.1) with respect to the depth  $d$  of the circuit when miscalibrated gates and error sampling are considered. (Right panel) Difference with respect to the miscalibrated case. Here we considered  $\epsilon = 0.1$  and  $N = 10$ .

### 3.3 Measurement error

Another source of errors is related to the performance of the measurement apparatus. To be explicit, consider the following trivial circuit



Suppose that is the state  $|\psi\rangle = |0\rangle$  to be fed to the measurement apparatus. Then, if the apparatus is perfectly set, it will give as the polarisation value  $z = +1$  corresponding to the output  $m = 0$ . However, there might be errors and there could be a non-null probability  $\mu$  that the measurement apparatus gives as an output  $m = 1$ . Similarly, if  $|\psi\rangle = |1\rangle$ , one could have a probability  $\nu$  to have  $m = 0$ . The following scheme represents the supposed outcome and the actual outcome with the corresponding probabilities:

$$\text{supposed } m = \begin{array}{ccc} 0 & \xrightarrow{(1-\mu)} & 0 \\ & \downarrow \mu & \\ 1 & \xrightarrow{\nu} & 1 \end{array} = \text{actual } \tilde{m}. \quad (3.19)$$

We can define the probability vectors for the supposed and actual outcomes, which respectively are

$$\mathbb{P}_M = \begin{pmatrix} 1 - \mathbb{P} \\ \mathbb{P} \end{pmatrix} \quad \text{and} \quad \mathbb{P}_{\tilde{M}} = \begin{pmatrix} 1 - \tilde{\mathbb{P}} \\ \tilde{\mathbb{P}} \end{pmatrix}, \quad (3.20)$$

where  $\mathbb{P} = \mathbb{P}(m = 1)$  and  $\tilde{\mathbb{P}} = \tilde{\mathbb{P}}(\tilde{m} = 1)$  are the probability of having the outcome  $m = 1$  in the supposed and actual case respectively. Such vectors are related by the matrix  $A$ , which quantifies the performances of measurement apparatus:  $\mathbb{P}_{\tilde{M}} = A\mathbb{P}_M$ , where

$$A = \begin{pmatrix} P(\tilde{m} = 0|m = 0) & P(\tilde{m} = 0|m = 1) \\ P(\tilde{m} = 1|m = 0) & P(\tilde{m} = 1|m = 1) \end{pmatrix}, \quad (3.21)$$

where  $P(\tilde{m}|m)$  is the conditional probability of having the actual outcome  $\tilde{m}$  given the supposed outcome  $m$ . The diagram in Eq. (3.19) sets the entries of  $A$  to

$$A = \begin{pmatrix} 1 - \mu & \nu \\ \mu & 1 - \nu \end{pmatrix}. \quad (3.22)$$

By merging the latter and Eq. (3.20), we find

$$\tilde{p} = p + \mu - (\nu + \mu)p, \quad (3.23)$$

which is represented in Fig. 3.5. To recalibrate the measurement apparatus, i.e. to quantify experimentally the

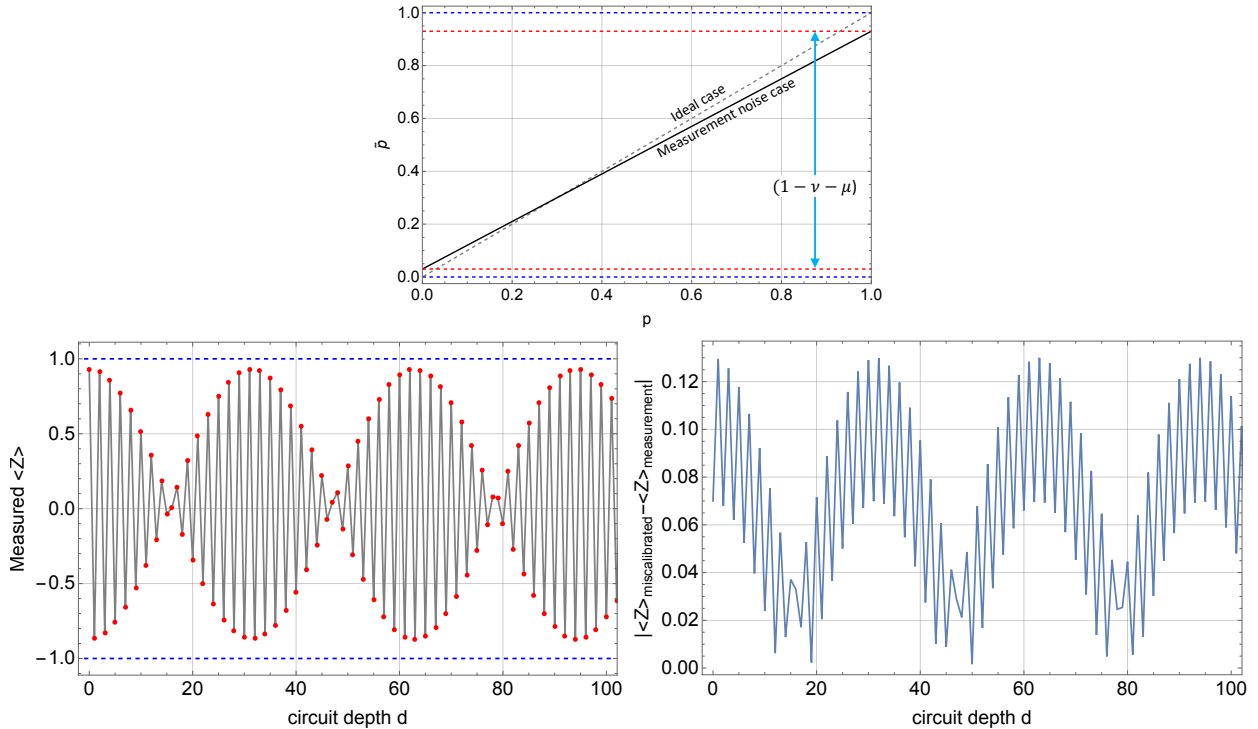


Fig. 3.5: (Top panel) Representation of Eq. (3.23). (Bottom left panel) Expectation value (red dots) of the polarisation  $\langle Z \rangle$  for the circuit in Eq. (3.1) with respect to the depth  $d$  of the circuit when miscalibrated gates and measurement errors are considered. (Bottom right panel) Difference with respect to the miscalibrated case. Here we considered  $\epsilon = 0.1$ ,  $\nu = 0.07$  and  $\mu = 0.03$ .

values of  $\mu$  and  $\nu$  one would need to run the following two trivial circuits:



They should give 100% of the time the outcomes  $m = 0$  and  $m = 1$  respectively. Variations of such percentage will characterise the values of  $\mu$  and  $\nu$ . The bottom panels in Fig. 3.5 show the corresponding polarisation and difference with the miscalibrated case.

### 3.3.1 Environmental noise

We now dwell in the most interesting source of noise, which is the one due to the external environment. In a circuit-based representation of the evolution, one now has

$$|0\rangle \xrightarrow{\tilde{G}} \text{Measurement} \quad (3.25)$$

where  $\tilde{G}$  represents the noisy version of the gate  $G$ . There are different possible ways how one can account for the noise action. Here, we will consider the following way. Every gate  $G$  of the noiseless case is substituted by  $\tilde{G}$ , where an extra gate, say  $\mathcal{E}$ , is added with a probability  $p_E$ . Namely,

Case	Probability	Effective circuit
A	$1 - p_E$	$ 0\rangle \xrightarrow{\mathbb{1}} \tilde{G}_A \xrightarrow{\text{Measurement}}$
B	$p_E$	$ 0\rangle \xrightarrow{\mathcal{E}} \tilde{G}_B \xrightarrow{\text{Measurement}}$

(3.26)

For the sake of simplicity, we will consider the case of  $\mathcal{E} = X$  and  $G = X$ . With this choice, in the case A, one has  $\tilde{G} = \mathbb{1}X = X$ , and the gate is properly implemented. While the case B, one has  $\tilde{G} = XX = \mathbb{1}$ , which nullify the action of the original gate. Now, in the ideal case ( $\mathcal{E} = \mathbb{1}$  always), the state before the measurement is  $|\psi\rangle = |1\rangle$ , so the outcome is

$$\langle m \rangle = \text{Tr} [\hat{M} \hat{\rho}] = 1, \quad (3.27)$$

indeed, the probability of having  $m = 1$  is  $p(m = 1) = 1$ . In the case with the environmental noise, one has

$$\begin{aligned} \langle m \rangle &= \sum_{m=0,1} m p(m), \\ &= (1 - p_E) + p_E \times 0, \\ &= (1 - p_E). \end{aligned} \quad (3.28)$$

In particular, this result can be constructed as follows. Starting from the initial state  $|0\rangle$ , we construct the corresponding initial statistical operator  $\hat{\rho}_0$ . Then, with a probability  $p_A = (1 - p_E)$  evolves as in the case A, and with a probability  $p_B = p_E$  as in the case B. Namely, one has

$$\hat{\rho} = p_A \hat{\rho}_A + p_B \hat{\rho}_B, \quad (3.29)$$

where

$$\hat{\rho}_B = \hat{\sigma}_x \hat{\rho}_0 \hat{\sigma}_x, \quad \text{and} \quad \hat{\rho}_B = \hat{\mathbb{1}} \hat{\rho}_0 \hat{\mathbb{1}}. \quad (3.30)$$

This gives

$$\hat{\rho} = (1 - p_E) |1\rangle \langle 1| + p_E |0\rangle \langle 0|, \quad (3.31)$$

which, in the computational basis, is represented as

$$\rho = \begin{pmatrix} p_E & 0 \\ 0 & (1 - p_E) \end{pmatrix}. \quad (3.32)$$

The corresponding expectation value of the measurement operator  $\hat{M}$  is

$$\begin{aligned}
\langle m \rangle &= \text{Tr} [\hat{M} \hat{\rho}], \\
&= \text{Tr} \left[ \begin{pmatrix} 0 & 0 \\ 0 & 1 \end{pmatrix} \begin{pmatrix} p_E & 0 \\ 0 & (1-p_E) \end{pmatrix} \right], \\
&= \text{Tr} \left[ \begin{pmatrix} 0 & 0 \\ 0 & (1-p_E) \end{pmatrix} \right], \\
&= (1-p_E),
\end{aligned} \tag{3.33}$$

as expected. Conversely, the polarisation is

$$\langle Z \rangle = (2p_E - 1). \tag{3.34}$$

Applying the noisy gate  $d$  times, we find

$$\langle Z \rangle = (2p_E - 1)^d, \tag{3.35}$$

which is represented in Fig. 3.6.

**Exercise 3.1**

Verify the relation in Eq. (3.35).

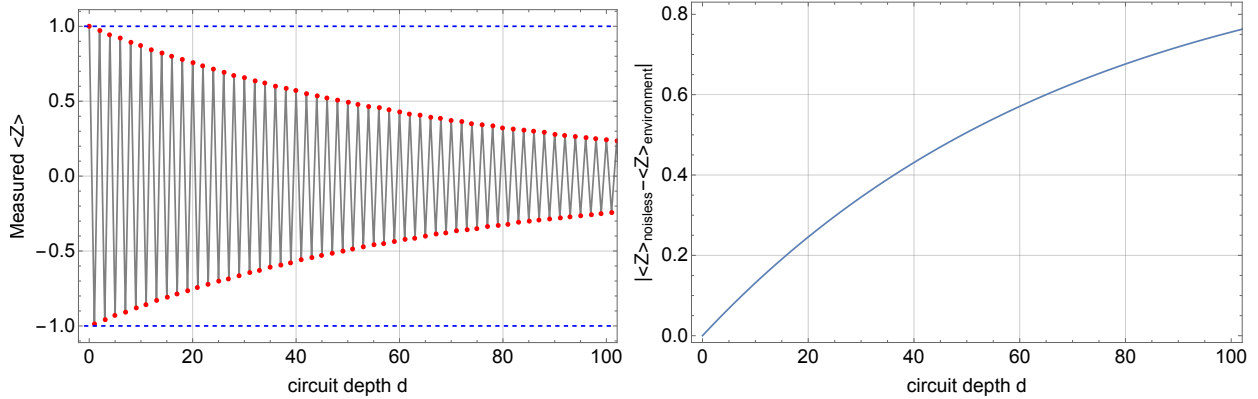
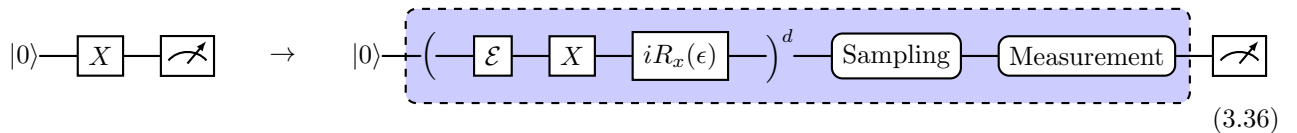


Fig. 3.6: (Left panel) Expectation value (red dots) of the polarisation  $\langle Z \rangle$  for the circuit in Eq. (3.1) with respect to the depth  $d$  of the circuit when the environment noise considered. (Right panel) Difference with respect to the noiseless case. Here we considered  $p_E = 0.007$ .

### 3.3.2 Global noise action

The last step of this section is to put together the different noises and errors discussed here. Namely, when one has a circuit, to account for the error, such a circuit needs to be substituted as represented



The action of the environment noise and miscalibration lead the qubit in the state

$$\hat{\rho} = (1 - p_E) |\psi_A\rangle \langle \psi_A| + p_E |\psi_B\rangle \langle \psi_B|, \quad (3.37)$$

where

$$\begin{aligned} |\psi_A\rangle &= \cos\left(d\frac{(\pi+\epsilon)}{2}\right) |0\rangle - i \sin\left(d\frac{(\pi+\epsilon)}{2}\right) |1\rangle, \\ |\psi_B\rangle &= \cos\left(d\frac{\epsilon}{2}\right) |0\rangle - i \sin\left(d\frac{\epsilon}{2}\right) |1\rangle. \end{aligned} \quad (3.38)$$

Specifically, such a state can be rewritten as

$$\hat{\rho} = (\rho_{00} |0\rangle \langle 0| + \rho_{11} |1\rangle \langle 1| + \rho_{10} |1\rangle \langle 0| + \rho_{01} |0\rangle \langle 1|), \quad (3.39)$$

where the  $\rho_{00}$  and  $\rho_{11}$  populations are fundamental in computing the expectation value of the polarisation:

$$\begin{aligned} \langle Z \rangle &= \rho_{00} - \rho_{11}, \\ &= (1 - p_E) \cos(d(\pi + \epsilon)) + p_E \cos(d\epsilon). \end{aligned} \quad (3.40)$$

On the other hand, to compute the effect of the sampling error, one needs only  $\rho_{11}$ , which is equal to the probability of having  $m = 1$ , i.e. of being in the state  $|1\rangle$ . Thus, Eq. (3.17) becomes

$$p_d = (1 - p_E) \frac{(1 - \cos(d(\pi + \epsilon)))}{2} + p_E \frac{(1 - \cos(d\epsilon))}{2}, \quad (3.41)$$

with respect to which one constructs the statistics of the outcomes that are distributed following a binomial distribution  $\mathcal{B}(p_d)$ .

Finally, the measurement error can be accounted by mapping the sampling means  $S_d$  in those accounting for diagram in Eq. (3.19). This consists in

$$S_d \rightarrow S_d + \mu - (\nu + \mu)S_d. \quad (3.42)$$

The result of considering all the noises and errors is given by the right panel of Fig. 3.1.

# Chapter 4

## Quantum Error Correction

### 4.1 Quantum Error Correction

Several techniques have been developed to correct errors due to the presence of noise. This is not only a considered issue in the quantum information context, but also in the classical one. In both cases, the key ingredient is the redundancy.

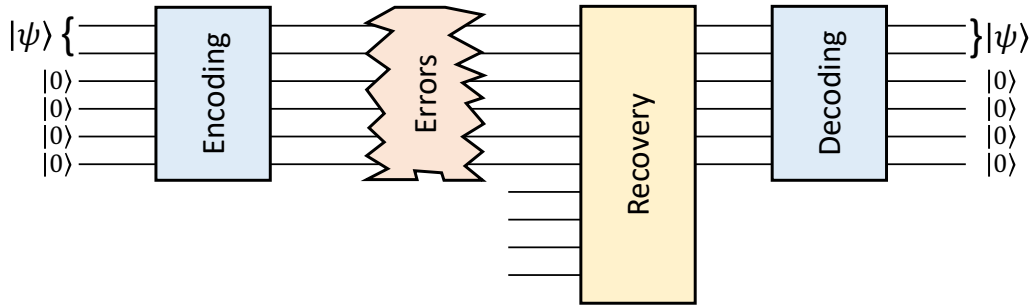


Fig. 4.1: Schematic representation of the Quantum Error Correcting approach.

#### 4.1.1 Classical error correction

Consider the following example, that will make clear the usefulness of redundancies. We have Alice that wants to send a single bit information to Bob. The communication channel is not perfect: a bit-flip error noise can act on the bit with the following probabilities:

$$\text{Alice sends the bit} = \begin{array}{c} 0 \\ \xrightarrow{\epsilon} \\ 1 \end{array} \quad \begin{array}{c} \xrightarrow{(1-\epsilon)} \\ \diagup \quad \diagdown \\ 0 \\ \xrightarrow{\epsilon} \\ 1 \end{array} \quad \text{is the bit the Bob receives.} \quad (4.1)$$

With this scheme, the protocol has a probability of failing that is

$$P_{\text{fail}} = \epsilon, \quad (4.2)$$

which is equal to the probability  $\epsilon$  of the bit being flipped. The idea of error correction is to suitably modify the protocol so one can recover the wanted information, with a failing probability being

$$P_{\text{fail}} < \epsilon. \quad (4.3)$$

Specifically, what Alice does is to send the bit string 000 in place of only the single bit 0. This operation is called encoding, and in this specific case, one encodes the classical information in the following way

$$\begin{aligned} 0 &\rightarrow 000, \\ 1 &\rightarrow 111. \end{aligned} \quad (4.4)$$

Then, Bob receives three bits and needs to decode the information. This is performed via a majority voting. For example, let us assume the second bit is flipped while the other remain untouched: Bob receives 010, and the majority voting gives

$$010 \rightarrow 0. \quad (4.5)$$

This is a decoding of the classical information. Considering all the possible three bits strings  $(A, B, C)$  that Bob can receive if Alice sends 000, with the corresponding probabilities  $p(A, B, C)$ , we have

	$(A, B, C)$	$p(A, B, C)$	decoded bit	
Alice encodes 0 in 000 → Bob receives	$(0, 0, 0)$	$(1 - \epsilon)^3$	0	At most 1 error Majority voting works 2 or more errors Majority voting fails
	$(0, 0, 1)$	$\epsilon(1 - \epsilon)^2$	0	
	$(0, 1, 0)$	$\epsilon(1 - \epsilon)^2$	0	
	$(1, 0, 0)$	$\epsilon(1 - \epsilon)^2$	0	
	$(0, 1, 1)$	$\epsilon^2(1 - \epsilon)$	1	
	$(1, 0, 1)$	$\epsilon^2(1 - \epsilon)$	1	
	$(1, 1, 0)$	$\epsilon^2(1 - \epsilon)$	1	
	$(1, 1, 1)$	$\epsilon^3$	1	

The probability that the protocol fails is given by the sum of the probabilities of the failing cases:

$$P_{\text{fail}} = 3 \times \epsilon^2(1 - \epsilon) + \epsilon^3 = 3\epsilon^2 - 2\epsilon^3, \quad (4.7)$$

which is reported in Fig. 4.2.

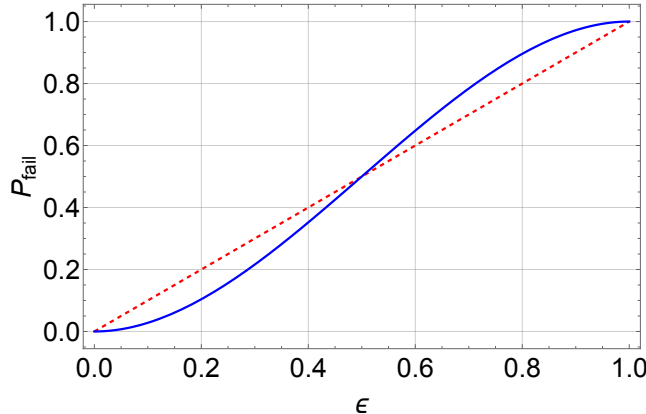


Fig. 4.2: Probability of failing  $P_{\text{fail}}$  for the single bit channel (dashed red line) and the three-bit classical correcting code (blue line).

Specifically, for  $0 \leq \epsilon < 1/2$ , we have that Eq. (4.3) is satisfied. This means that by using this protocol one has less probability to fail ( $p_{\text{fail}}$ ) rather than using a single bit ( $\epsilon$ ). Therefore, the redundancy is a good approach to reduce errors, as long as Eq. (4.3) is satisfied.

### 4.1.2 Quantum information context

The direct application of redundancy in the quantum information context encounters some important, although not insurmountable, difficulties.

- The no-cloning theorem (see Sec. 1.1) does not allow to create copies of an unknown quantum state. This means that Alice cannot generate  $|\psi\rangle|\psi\rangle|\psi\rangle$  to protect an unknown state  $|\psi\rangle$ .
- The second difficulty comes in how the classical error correcting code operates: one measures the state of the bit and applies a correcting operation accordingly. In the quantum case, the measurement operation would destroy the coherence of the state and thus the information encoded in the state. To be more quantitative, take the generic state  $|\psi\rangle = \alpha|0\rangle + \beta|1\rangle$ . After the measurement, the state collapses in  $|0\rangle$  or in  $|1\rangle$  with the respective probabilities. However, one cannot reconstruct the coherence of the state after its collapse.
- In classical information, the only possible error is a bit-flip:  $0 \rightarrow 1$  and  $1 \rightarrow 0$ . Conversely, in quantum information the class of possible noises is far wider. For example, the phase-flip maps  $\alpha|0\rangle + \beta|1\rangle \rightarrow \alpha|0\rangle - \beta|1\rangle$ , and this does not have a classical counterpart. Moreover, in the quantum context, one can also have infinitesimal errors that can accumulate as the depth of the algorithm increases. An example can be  $\alpha|0\rangle + \beta|1\rangle \rightarrow \alpha|0\rangle + \hat{R}^x(\epsilon)\beta|1\rangle$ , where  $\hat{R}^x(\epsilon)$  is a rotation of an infinitesimal angle  $\epsilon$  around the  $x$  axis.

### 4.1.3 The 3-qubit bit-flip code

The first Quantum Error Correction (QEC) code we see is that correcting bit-flip errors. This is the counterpart of that seen in the classical information context.

Suppose Alice wants to send the generic state  $|\psi\rangle = \alpha|0\rangle + \beta|1\rangle$  to Bob via a bit-flip noisy channel. We assume that the noise acts independently on each of the qubits that Alice sends. This is an important assumption for the QEC codes we will see here. We assume that the noise leaves the qubit untouched with a probability  $(1 - \epsilon)$ , while it applies  $\hat{\sigma}_x$  with a probability  $\epsilon$ . Indeed,  $\hat{\sigma}_x|0\rangle = |1\rangle$  and  $\hat{\sigma}_x|1\rangle = |0\rangle$ . This is essentially the quantum version of what shown in Eq. (4.1).

To protect the information from bit-flip errors, Alice employs the following encoding:

$$\begin{aligned} |0\rangle &\rightarrow |0_L\rangle = |0\rangle|0\rangle|0\rangle, \\ |1\rangle &\rightarrow |1_L\rangle = |1\rangle|1\rangle|1\rangle, \end{aligned} \tag{4.8}$$

where  $|0\rangle$  and  $|1\rangle$  are physical qubits, while  $|0_L\rangle$  and  $|1_L\rangle$  are logical qubits. Then, the generic state  $|\psi\rangle$  is encoded in

$$|\psi\rangle = \alpha|0\rangle + \beta|1\rangle \rightarrow \alpha|0_L\rangle + \beta|1_L\rangle = \alpha|000\rangle + \beta|111\rangle, \tag{4.9}$$

with the notation  $|q_1q_2q_3\rangle = |q_1\rangle|q_2\rangle|q_3\rangle$ . This encoding can be implemented via the following circuit



Indeed, we have

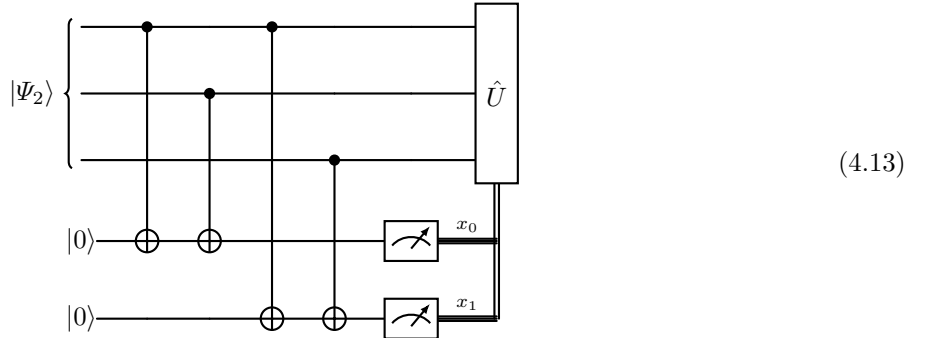
$$|\psi 00\rangle = \alpha |000\rangle + \beta |100\rangle \xrightarrow{CNOT \otimes \hat{\mathbb{I}}} \alpha |000\rangle + \beta |110\rangle \xrightarrow{\hat{\mathbb{I}} \otimes CNOT} \alpha |000\rangle + \beta |111\rangle = |\Psi_1\rangle. \quad (4.11)$$

We underline that the entangled state  $|\Psi_1\rangle$  is not equal to  $|\psi\rangle|\psi\rangle|\psi\rangle$ , so the no-cloning theorem is not violated.

Now, the state  $|\Psi_1\rangle$  is sent to Bob via the noisy channel. Bob receives one of the following states  $|\Psi_2\rangle$  with the respective probabilities  $p(|\Psi_2\rangle)$ :

	$ \Psi_2\rangle$	$p( \Psi_2\rangle)$
Alice encodes $ \psi\rangle$ in $ \Psi_1\rangle \rightarrow$ Bob receives	$\alpha  000\rangle + \beta  111\rangle$	$(1-\epsilon)^3$
	$\alpha  001\rangle + \beta  110\rangle$	$\epsilon(1-\epsilon)^2$
	$\alpha  010\rangle + \beta  101\rangle$	$\epsilon(1-\epsilon)^2$ At most 1 error
	$\alpha  100\rangle + \beta  011\rangle$	$\epsilon(1-\epsilon)^2$
	$\alpha  011\rangle + \beta  100\rangle$	$\epsilon^2(1-\epsilon)$
	$\alpha  101\rangle + \beta  010\rangle$	$\epsilon^2(1-\epsilon)$
	$\alpha  110\rangle + \beta  001\rangle$	$\epsilon^2(1-\epsilon)$ 2 or more errors
	$\alpha  111\rangle + \beta  000\rangle$	$\epsilon^3$

Let us suppose that Bob receives the state  $|\Psi_2\rangle = \alpha |100\rangle + \beta |011\rangle$ . To correct the bit-flip, Bob would be tempted to perform a simultaneous measurement of the spin of the three qubits, i.e.  $\hat{\sigma}_z^{(1)}\hat{\sigma}_z^{(2)}\hat{\sigma}_z^{(3)}$ . Such an operation would give as an outcome 100 with probability  $|\alpha|^2$  and 011 with probability  $|\beta|^2$ . Then, by applying a majority voting, Bob would understand that the first qubit is flipped. However, the coherence of the state is lost. Indeed, the measurement of the spin of the qubits collapses the state. To solve the problem, one needs to perform the so-called error syndrome. In particular, Bob employs two ancillary qubits that are prepared in the  $|0\rangle$  state and coupled to the qubits carrying the encoded state. The circuit implementing the correction then is



To be quantitative, starting from  $|\Psi_2\rangle = \alpha |100\rangle + \beta |011\rangle$ , we have

$$\begin{aligned}
 |\Psi_2\rangle |00\rangle &= \alpha |10000\rangle + \beta |01100\rangle \xrightarrow{CNOT_{1,4}} \alpha |10010\rangle + \beta |01100\rangle, \\
 &\xrightarrow{CNOT_{2,4}} \alpha |10010\rangle + \beta |01110\rangle, \\
 &\xrightarrow{CNOT_{1,5}} \alpha |10011\rangle + \beta |01110\rangle, \\
 &\xrightarrow{CNOT_{3,4}} \alpha |10010\rangle + \beta |01111\rangle, \\
 &= (\alpha |100\rangle + \beta |011\rangle) |11\rangle.
 \end{aligned} \quad (4.14)$$

Fundamentally, the last two qubits are not entangled with the first three. Thus, the measurement on the last two qubits does not impose the collapse of the first three. After such a measurement, Bob has the outcomes  $x_0 = 1$  and  $x_1 = 1$ . In particular,  $x_0 = 1$  indicates that one among the first and the second qubit has flipped. Similarly,  $x_1 = 1$  indicates that one among the first and the third qubit has flipped. Then, Bob knows, under the assumption of single qubit errors, that the first qubit has flipped and can apply  $\hat{U} = \hat{\sigma}_x^{(1)}$  to flip it back.

In general, Bob will apply the following unitary operations to correct the errors:

$x_0$	$x_1$	$\hat{U}$
0	0	$\hat{\mathbb{1}}$
0	1	$\hat{\sigma}_x^{(3)}$
1	0	$\hat{\sigma}_x^{(2)}$
1	1	$\hat{\sigma}_x^{(1)}$

(4.15)

After having applied the correction, Bob gets the state  $|\Psi_3\rangle$  with the following probabilities

$ \Psi_2\rangle$	$ \Psi_3\rangle$	$p( \Psi_3\rangle)$
$\alpha 000\rangle + \beta 111\rangle$	$\alpha 000\rangle + \beta 111\rangle$	$(1-\epsilon)^3$
$\alpha 001\rangle + \beta 110\rangle$	$\alpha 000\rangle + \beta 111\rangle$	$\epsilon(1-\epsilon)^2$
$\alpha 010\rangle + \beta 101\rangle$	$\alpha 000\rangle + \beta 111\rangle$	$\epsilon(1-\epsilon)^2$
$\alpha 100\rangle + \beta 011\rangle$	$\alpha 000\rangle + \beta 111\rangle$	$\epsilon(1-\epsilon)^2$
$\alpha 011\rangle + \beta 100\rangle$	$\alpha 111\rangle + \beta 000\rangle$	$\epsilon^2(1-\epsilon)$
$\alpha 101\rangle + \beta 010\rangle$	$\alpha 111\rangle + \beta 000\rangle$	$\epsilon^2(1-\epsilon)$
$\alpha 110\rangle + \beta 001\rangle$	$\alpha 111\rangle + \beta 000\rangle$	$\epsilon^2(1-\epsilon)$
$\alpha 111\rangle + \beta 000\rangle$	$\alpha 111\rangle + \beta 000\rangle$	$\epsilon^3$

(4.16)

Finally, Bob applies the following decoding circuit



which is the inverse of the circuit in Eq. (4.10). The final state  $|\phi\rangle$  is

$$\begin{aligned} |\phi\rangle &= \alpha|0\rangle + \beta|1\rangle = |\psi\rangle, & \text{with probability } p = (1-\epsilon)^3 + 3\epsilon(1-\epsilon)^2, \\ |\phi\rangle &= \alpha|1\rangle + \beta|0\rangle = \hat{\sigma}_x|\psi\rangle, & \text{with probability } p = 3\epsilon^2(1-\epsilon) + \epsilon^3. \end{aligned} \quad (4.18)$$

Thus, the failing probability of this QEC code is

$$P_{\text{fail}} = 3\epsilon^2 - 2\epsilon^3, \quad (4.19)$$

which is the same as in the classical correcting algorithm seen previously and it is plotted in Fig. 4.2. Notably, Bob does not learn anything about the weights  $\alpha$  and  $\beta$  thought this QEC code. The coherence of the state remains intact.

#### 4.1.4 The 3-qubit phase-flip code

Let us consider the case of the phase-flip noise, where the following error generates with a probability  $\epsilon$ :

$$\begin{aligned} |0\rangle &\rightarrow \hat{\sigma}_z|0\rangle = |0\rangle, \\ |1\rangle &\rightarrow \hat{\sigma}_z|1\rangle = -|1\rangle. \end{aligned} \quad (4.20)$$

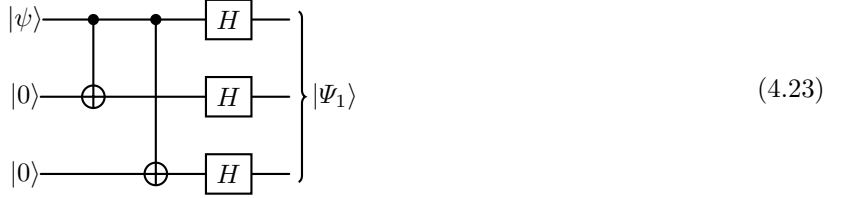
Consequently, one has

$$|\psi\rangle = \alpha|0\rangle + \beta|1\rangle \rightarrow \alpha|0\rangle - \beta|1\rangle. \quad (4.21)$$

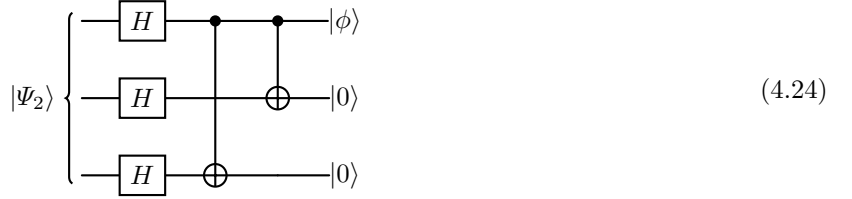
Notably, this noise does not have a classical counterpart. Since the error is imprinted in the relative phase between  $|0\rangle$  and  $|1\rangle$ , the bit-flip QEC code developed in Sec. 4.1.3 does not correct this type of errors. However, a phase-flip error in the computational basis  $\{|0\rangle, |1\rangle\}$  corresponds to a bit-flip error in the  $\{|+\rangle, |-\rangle\}$  basis. Indeed,

$$\begin{aligned}\hat{\sigma}_z |+\rangle &= |-\rangle, \\ \hat{\sigma}_z |-\rangle &= |+\rangle.\end{aligned}\quad (4.22)$$

Then, by simply adding a Hadamard gate, one changes basis and thus is able to employ the bit-flip QEC code to correct phase-flip errors. This is done both in the encoding and the decoding parts of the code. The encoding circuit is then



while the deencoding becomes



The remaining parts of the code remain identical.

#### 4.1.5 The 9-qubit Shor code

We saw how the 3-qubit bit-flip and phase flip QEC codes can correct respectively bit-flip and phase flip errors. Here, we show that concatenating these two codes, one can protect for generic single qubit errors. Indeed, consider the situation of a single qubit initially prepared in the state  $|\psi\rangle$ . Suppose it is coupled to the surrounding environment, whose state is initially  $|e\rangle$ , and that the latter entangles with the system. Such a transformation is described as

$$|\psi\rangle|e\rangle \rightarrow c_0 \hat{1} |\psi\rangle|e_0\rangle + c_1 \hat{\sigma}_x |\psi\rangle|e_1\rangle + c_2 \hat{\sigma}_y |\psi\rangle|e_2\rangle + c_3 \hat{\sigma}_z |\psi\rangle|e_3\rangle, \quad (4.25)$$

where  $c_i$  are suitable constants, and  $|e_i\rangle$  are states of the environment. Then, the state of the system is transformed via the application of the four Pauli operators. Here,  $\hat{\sigma}_0 = \hat{1}$  does not imply any change in the state, so no error needs to be corrected. The errors due to  $\hat{\sigma}_x$  and  $\hat{\sigma}_z$  are respectively corrected via bit-flip and phase-flip QEC codes. It remains that due to  $\hat{\sigma}_y$ . However, one can notice that, since the Pauli matrices form a Lie algebra, one can express  $\hat{\sigma}_y$  in terms of  $\hat{\sigma}_x$  and  $\hat{\sigma}_z$ . Namely,  $\hat{\sigma}_y = i\hat{\sigma}_x\hat{\sigma}_z$ . Then, one needs only to correct two consecutive errors (phase-flip and then bit-flip) to correct a bit-phase flip. The following QEC code is sufficient to perform such a correction.

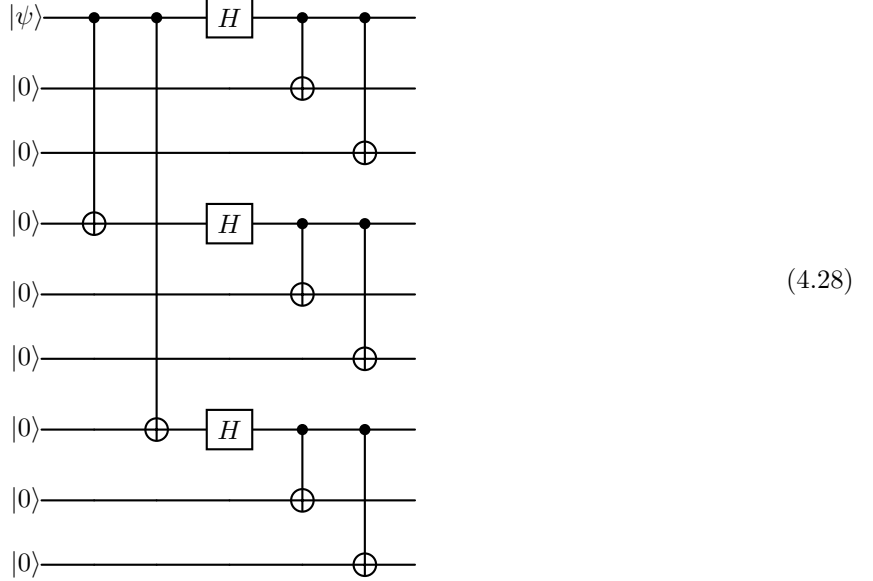
The encoding of the 9-qubit Shor code is given by

$$\begin{aligned}|0\rangle \rightarrow |0_L\rangle &= \frac{1}{\sqrt{8}} (|000\rangle + |111\rangle)(|000\rangle + |111\rangle)(|000\rangle + |111\rangle), \\ |1\rangle \rightarrow |1_L\rangle &= \frac{1}{\sqrt{8}} (|000\rangle - |111\rangle)(|000\rangle - |111\rangle)(|000\rangle - |111\rangle).\end{aligned}\quad (4.26)$$

This implies the following encoding for a generic state  $|\psi\rangle$

$$|\psi\rangle \rightarrow \frac{\alpha}{\sqrt{8}} (|000\rangle + |111\rangle) (|000\rangle + |111\rangle) (|000\rangle + |111\rangle) + \frac{\beta}{\sqrt{8}} (|000\rangle - |111\rangle) (|000\rangle - |111\rangle) (|000\rangle - |111\rangle). \quad (4.27)$$

The encoding is implemented via the following circuit



The action of the first two CNOT gates and three Hadamard in Eq. (4.28) is to map the qubits 1, 4 and 7 as follows:

$$\begin{aligned} |\psi00\rangle &= \alpha |000\rangle + \beta |100\rangle, \\ &\rightarrow \alpha |000\rangle + \beta |110\rangle, \\ &\rightarrow \alpha |000\rangle + \beta |111\rangle, \\ &\rightarrow \alpha |+++> + \beta |--->. \end{aligned} \quad (4.29)$$

Namely, they perform the encoding for the phase-flip QEC code:

$$\begin{aligned} |0\rangle &\rightarrow |+++>, \\ |1\rangle &\rightarrow |--->. \end{aligned} \quad (4.30)$$

Then, every  $|+\rangle$  and  $|-\rangle$  state in these qubits is further encoded with the last CNOT gates. Specifically, one has

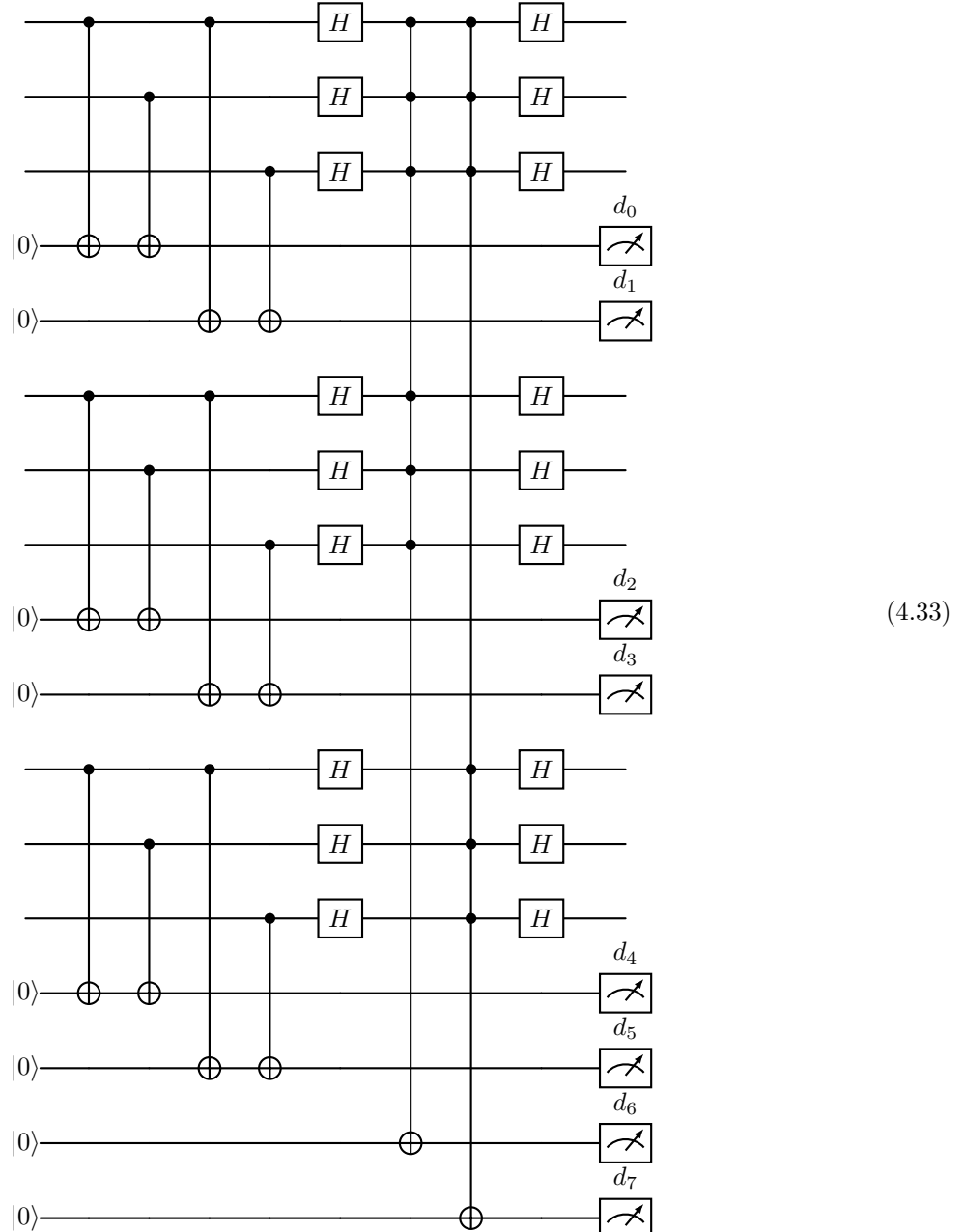
$$\begin{aligned} |+00\rangle &= \frac{1}{\sqrt{2}} (|000\rangle + |100\rangle), \\ &\rightarrow \frac{1}{\sqrt{2}} (|000\rangle + |110\rangle), \\ &\rightarrow \frac{1}{\sqrt{2}} (|000\rangle + |111\rangle), \end{aligned} \quad (4.31)$$

and

$$\begin{aligned}
 | -00 \rangle &= \frac{1}{\sqrt{2}} (| 000 \rangle - | 100 \rangle), \\
 &\rightarrow \frac{1}{\sqrt{2}} (| 000 \rangle - | 110 \rangle), \\
 &\rightarrow \frac{1}{\sqrt{2}} (| 000 \rangle - | 111 \rangle).
 \end{aligned} \tag{4.32}$$

These effectively perform the encoding for the bit-flip QEC code. Such an encoding combines the phase-flip and the bit-flip encoding.

To extract the error syndrome, one employs a collective measurement, similarly as for the bit-flip. In particular, 8 ancillary qubits are employed to construct the following circuit



Here, the outcomes  $(d_0, d_1)$ ,  $(d_2, d_3)$  and  $(d_4, d_5)$  respectively indicate bit-flip errors within the first, second and third block of three physical qubits. Specifically, for the first block, one employs exactly what described in Sec. 4.1.3.

The outcomes  $(d_6, d_7)$  are instead used to detect phase-flip errors of the logical state encoded with the three blocks. The collective measurements to do this are

$$\begin{aligned}\hat{\sigma}_x^{(1)}\hat{\sigma}_x^{(2)}\hat{\sigma}_x^{(3)}\hat{\sigma}_x^{(4)}\hat{\sigma}_x^{(5)}\hat{\sigma}_x^{(6)}, \\ \hat{\sigma}_x^{(1)}\hat{\sigma}_x^{(2)}\hat{\sigma}_x^{(3)}\hat{\sigma}_x^{(7)}\hat{\sigma}_x^{(8)}\hat{\sigma}_x^{(9)},\end{aligned}\quad (4.34)$$

which provide  $d_6$  and  $d_7$  respectively. If one gets, for example,  $(d_6 = -1, d_7 = -1)$ , then a phase flip occurred in the first block.

#### 4.1.6 On the redundancy and threshold

As we saw, a fundamental step in the QEC codes is the redundancy of the state. Notably, there is no need in having exactly 3 copies. It can be extended to any  $k$  copies, as long as  $k > 1$  is an odd number. What one wants is that the probability  $P_{\text{fail}}$  that the QEC code fails is smaller than the probability  $\epsilon$  of an error occurring on a single physical qubit:  $P_{\text{fail}} < \epsilon$ .

Consider the case of  $k$  physical qubits encoding a single logical qubit. Given the probability  $\epsilon$  of having an error on one of these qubits, that of having  $j$  qubits with errors is given by

$$p(j) = \epsilon^j (1 - \epsilon)^{k-j}, \quad (4.35)$$

and there are

$$\binom{k}{j} = \frac{k!}{(k-j)!j!}, \quad (4.36)$$

different possible combinations. Then,  $P_{\text{fail}}$  is given by the sum over these when the faulty qubits are at least half of the total. This is

$$P_{\text{fail}} = \sum_{j=\frac{(k+1)}{2}}^k \binom{k}{j} \epsilon^j (1 - \epsilon)^{k-j}. \quad (4.37)$$

Namely, for  $k = 3$ , one has

$$P_{\text{fail}} = \sum_{j=\frac{(3+1)}{2}}^3 \binom{3}{j} \epsilon^j (1 - \epsilon)^{3-j} = 3\epsilon^2(1 - \epsilon) + \epsilon^3. \quad (4.38)$$

The behaviour of  $P_{\text{fail}}$  for different values of  $k$  is shown in Fig. 4.3.

However, one can consider an alternative approach. Instead of encoding a logical qubit just once in a large number of physical qubits, one can concatenate encodings. One encodes the logical qubit in different levels, where each level employs a small number of qubits. To be more explicit, the following is the encoding of a single physical qubit in a 2 level encoding with three qubits each:

$$|0\rangle \xrightarrow{\text{first encoding}} |000\rangle \xrightarrow{\text{second encoding}} |000\rangle |000\rangle |000\rangle, \quad (4.39)$$

and similarly for  $|1\rangle$ . Now, with this encoding, the actual physical qubit is that in the highest level of encoding, and this is that directly suffering from the noise. Suppose there is a probability  $\epsilon$  that an error occurs on this physical qubit. Then, at the level 1, the probability of failing, for example for the bit-flip QEC code, is

$$P_{\text{fail},1} = 3\epsilon^2 - 2\epsilon^3. \quad (4.40)$$

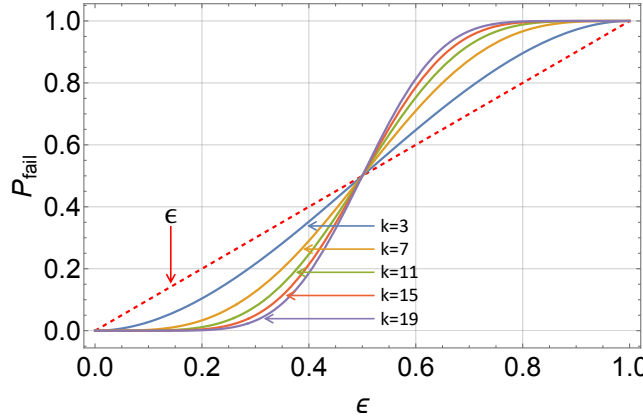


Fig. 4.3: Probability of failing  $P_{\text{fail}}$  for the single bit channel (dashed red line) with respect to a redundant encoding with  $k$  physical qubits (continuous lines).

This quantity is the probability that the noise corrupts a qubit at the level 1. Thus, when computing the probability of failing for the qubit at level 0, the actual logical qubit,  $P_{\text{fail},1}$  needs to be interpreted as the probability  $\epsilon_1$  that an error occurs on the qubit at the level 1. Then, at level 0, one has that the failing probability is

$$\begin{aligned} P_{\text{fail},0} &= 3P_{\text{fail},1}^2 - 2P_{\text{fail},1}^3, \\ &= 3[3\epsilon^2 - 2\epsilon^3]^2 - 2[3\epsilon^2 - 2\epsilon^3]^3, \\ &= 27\epsilon^4 - 36\epsilon^5 - 42\epsilon^6 + 108\epsilon^7 - 72\epsilon^8 + 16\epsilon^9. \end{aligned} \quad (4.41)$$

The question is then which is the best encoding. Figure 4.4 compares the failing probabilities  $P_{\text{fail}}$  for a single level encoding with 9 physical qubits (blue line), where Eq. (4.37) gives

$$P_{\text{fail}} = 126\epsilon^5 - 420\epsilon^6 + 540\epsilon^7 - 315\epsilon^8 + 70\epsilon^9, \quad (4.42)$$

and that for a 2 level encoding each with 3 qubits (red line). This is a fair comparison, as both the approaches are employing the same number of physical qubits, i.e.  $n = 9$ .

To keep the discussion more general, suppose  $p$  is the probability of failing for a qubit with no encoding (this is what we called  $\epsilon$  until now). Then, the failing probability is

$$P_{\text{fail}}^{(0)} = p. \quad (4.43)$$

Suppose that after one encoding the failing probability is

$$P_{\text{fail}}^{(1)} = cp^2, \quad (4.44)$$

where  $c$  is some suitable constant. In the case of the 3-qubit encoding, one had

$$P_{\text{fail}} = 3p^2 - 2p^3 \sim 3p^2, \quad (4.45)$$

for small values of  $p$ . After 2 encodings, one has

$$P_{\text{fail}}^{(2)} = c(cp^2)^2 = \frac{1}{c}(cp)^{2^2}. \quad (4.46)$$

After  $k$  encodings, one has

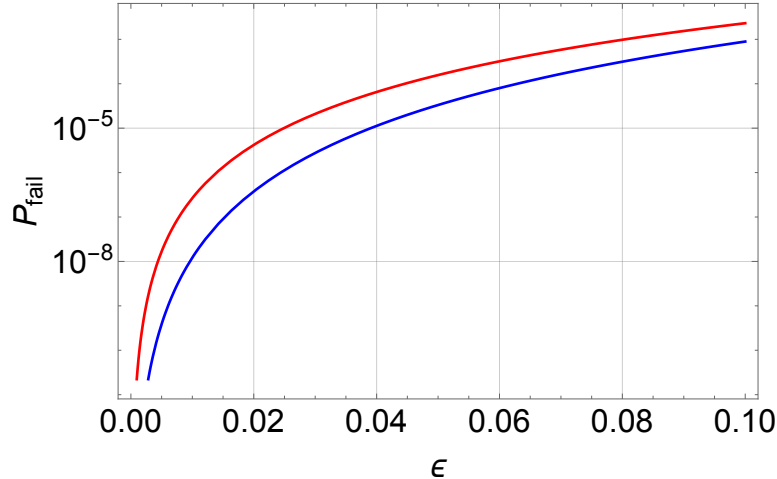


Fig. 4.4: Comparison of the failing probabilities  $P_{\text{fail}}$  for a single level encoding with 9 physical qubits (blue line) and that for a 2 level encoding each with 3 qubits (red line).

$$P_{\text{fail}}^{(k)} = p_{\text{th}} \left( \frac{p}{p_{\text{th}}} \right)^{2^k}, \quad (4.47)$$

where we defined the threshold probability as

$$p_{\text{th}} = \frac{1}{c}. \quad (4.48)$$

Such a probability depends on varius parameters, among which the QEC code used, the physical components, the experimental implementation of the QEC protocol etc.

The threshold probability  $p_{\text{th}}$  is fundamental due to the following theorem.

**Theorem 4.1 (Threshold theorem).** *If a threshold probability  $p_{\text{th}}$  exists, then it is always possible to correct errors at a faster than they are created. It is sufficient to increase the level  $k$  of encoding.*

*Proof.* The proof is trivial. As long as the the occurrence of an error on the physical qubit  $p = \epsilon$  is smaller than the threshold probability  $p_{\text{th}}$ , then the ratio

$$\frac{p}{p_{\text{th}}} < 1, \quad (4.49)$$

and thus the quantity

$$\left( \frac{p}{p_{\text{th}}} \right)^{2^k}, \quad (4.50)$$

can be made suitably small by simply increasing  $k$ .

The beauty of the threshold theorem is its simplicity. However, it also highlights a non-trivial problem, which is the necessity of employing a very large number of physical qubits. It naturally follows the question: How many physical qubits are necessary to quantum error correcting a faulty circuit?

Suppose we have  $N$  components (this is the number of qubits times the number of gates). Suppose for each of these components one needs  $R$  physical qubit accounting for QEC at the 1 level of encoding. Then, after  $k$  levels of encoding there is a total of  $NR^k$  qubits. Suppose we want that the entire circuit works with a failing probability  $P_{\text{fail, circuit}} < \epsilon$ , where  $\epsilon$  is a given probability. Then, per component, we have

$$P_{\text{fail}} = p_{\text{th}} \left( \frac{p}{p_{\text{th}}} \right)^{2^k} < \frac{\epsilon}{N}. \quad (4.51)$$

The question is then how many levels  $k$  of encoding are necessary? Or equivalently, how many physical qubits  $R^k$  per components are required? From the previous expression we obtain

$$2^k \sim \frac{\log_2 \left( \frac{Np_{\text{th}}}{\epsilon} \right)}{\log_2 \left( \frac{p_{\text{th}}}{p} \right)}, \quad (4.52)$$

which implies

$$R^k \sim \left( \frac{\log_2 \left( \frac{Np_{\text{th}}}{\epsilon} \right)}{\log_2 \left( \frac{p_{\text{th}}}{p} \right)} \right)^{\log_2 R}. \quad (4.53)$$

Thus, the size of the full circuit scales as

$$NR^k \sim \text{poly} \left( \log \frac{Np_{\text{th}}}{\epsilon} \right). \quad (4.54)$$

This is the quantitative result of the threshold theorem.

#### 4.1.7 More layers of encoding or only more qubits

Until now, we worked under the assumption of having only noises that act independently on the physical qubits. Let us suppose now a different kind of noise map, that correlates the noise on different qubits. Specifically, we consider a Kraus map acting on  $N$  qubits, that reads

$$\mathcal{T}[\hat{\rho}] = \frac{1}{N(N-1)} \sum_{i \neq j}^N \left[ (1-p)\hat{\rho} + p\hat{\sigma}_x^{(i)}\hat{\sigma}_x^{(j)}\hat{\rho}\hat{\sigma}_x^{(j)}\hat{\sigma}_x^{(i)} \right], \quad (4.55)$$

where there is a probability  $p$  that the noise acts on the qubits and the prefactor is required to properly normalise the state.

First of all, let us introduce a graphical notation. Suppose we have three physical qubits, and the noise has acted on the first and second. Then, we denote this with the following scheme

$$\begin{array}{c} \text{Before the noise} \quad \overline{\quad} \\ \text{After the noise} \quad \overline{\quad} \quad \overline{\quad} \end{array} \quad (4.56)$$

Now, suppose we are performing the encoding with  $N = 3$  qubits and  $k = 1$  layer of encoding. If there are no errors — this happens with probability  $(1-p)$  — then physical qubits are

$$\overline{\quad} \quad \text{and correspond to a logical qubit} \quad \overline{\quad} \quad (4.57)$$

which is untouched by the noise. If there is one error, which corresponds to two qubits being affected with a probability  $p$ , then the physical qubits are in one of the following three states

$$\begin{array}{ccccc} \overline{\quad} \quad \overline{\quad} & \overline{\quad} \quad \overline{\quad} & \overline{\quad} \quad \overline{\quad} & \longrightarrow & -X- \\ \overline{\quad} \quad X & \overline{\quad} \quad X & \overline{\quad} \quad X & & \end{array} \quad (4.58)$$

that correspond to a logical qubit that is affected to the noise. Here, we denote decodings with horizontal arrows. Thus, the protocol fails. These states contribute to the failing probability:

$$P_{\text{fail}} \sim 3p, \quad (4.59)$$

where the factor 3 is given by the number of equivalent states at the physical level, namely those represented graphically in the left side of Eq. (4.58).

If there are two errors, which is a process involving a probability  $p^2$  and four qubits, one has the following 9 states:

$$(4.60)$$

which correspond to

$$(4.61)$$

as the application of an bit-flip error twice on the same qubit correspond to not having an error, i.e.  $\hat{\sigma}_x^2 = \hat{1}$ . In such a case, only some combination are faulty, while in others the errors have cancelled. Here, we denote equivalence with vertical arrows. These states will contribute to  $P_{\text{fail}}$  with  $+6p^2$ . Thus, one gets

$$P_{\text{fail}} = 3p + 6p^2 + \dots \sim 3p, \quad (4.62)$$

where the  $\dots$  indicate higher order errors. Nevertheless, is the lowest order term in  $p$  that is the most significant, under the hypothesis of small error probabilities.

Consider now a double encoding  $k = 2$  with a total of  $N = 3^2 = 9$  qubits. In case of no errors, prob =  $(1 - p)$ , we have

layer 2	layer 1	layer 0
$\overline{\phantom{x}}$	$\rightarrow \overline{\phantom{x}}$	
$\overline{\phantom{x}}$	$\rightarrow \overline{\phantom{x}}$	$\rightarrow \overline{\phantom{x}}$
$\overline{\phantom{x}}$	$\rightarrow \overline{\phantom{x}}$	

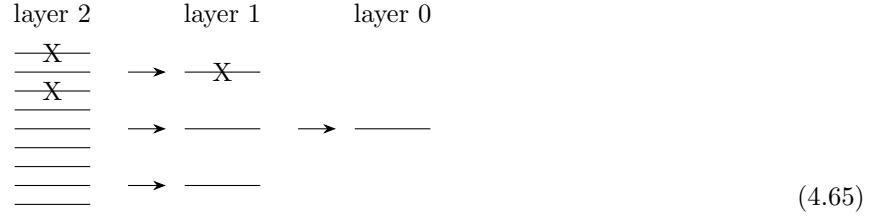
$$(4.63)$$

which do not contribute to  $P_{\text{fail}}$ . If there is one error, prob =  $p$ , we have  $\binom{9}{1} = 36$  states. Some states display two affected physical qubits in different layer-1 logical qubit,

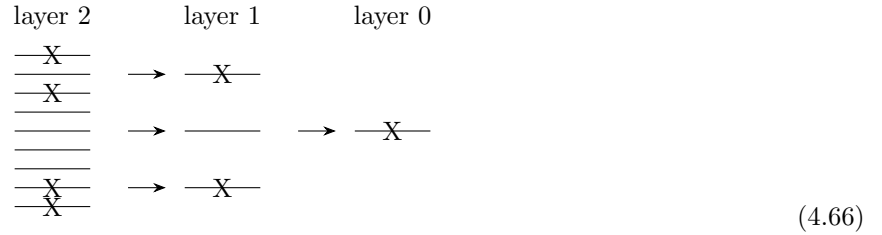
layer 2	layer 1	layer 0
$\overline{X}$	$\rightarrow \overline{\phantom{x}}$	
$\overline{\phantom{x}}$	$\rightarrow \overline{\phantom{x}}$	
$\overline{X}$	$\rightarrow \overline{\phantom{x}}$	$\rightarrow \overline{\phantom{x}}$
$\overline{\phantom{x}}$	$\rightarrow \overline{\phantom{x}}$	

$$(4.64)$$

Some have two physical qubits in the same layer-1 logical qubit. Thus, the corresponding layer-1 logical qubit fails, but the layer-0 logical qubit is still protected



This is the worst-case scenario with one error. If there are two errors,  $\text{prob} = p^2$ , the states that are relevant are those that have 2 layer-1 logical qubits affected. Namely, they reproduce the same graph as that in Eq. (4.58). For example, of the form



At the layer-1, this correspond to a probability being  $3p$ . For each of the layer-1 affected logical qubits, one needs 2 layer-2 affected physical qubits, with associated a probability  $3p$ . Thus, one has

$$P_{\text{fail}} = (3p)^2 + \dots \sim 9p^2. \quad (4.67)$$

With generic  $k$  layers of encoding, one has

$$P_{\text{fail}} = (3p)^k + \dots, \quad (4.68)$$

which is graphically represented in Fig. 4.5, where the lines are listed at increasing values of  $k$  and condense towards the value of  $p_{\text{th}} = 1/3$ .

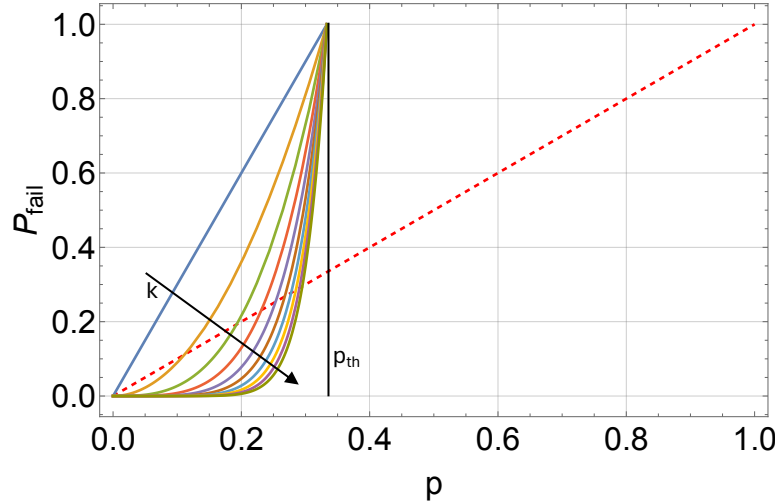
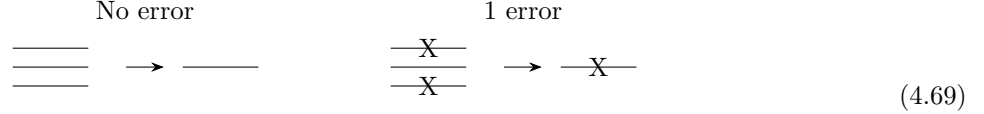


Fig. 4.5: Comparison of the failing probabilities  $P_{\text{fail}}$  for different  $k$  layers of encoding with 3 qubits each. The arrow indicates the direction of increasing values of  $k$ , while the vertical black line indicates the threshold probability  $p_{\text{th}}$ .

Let us now consider the alternative. Instead of taking a large number of layers of encoding with just a few qubits per layer, we consider a large number of qubits on a single encoding layer.

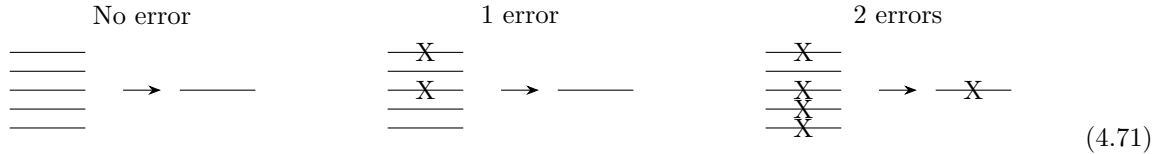
For  $N = 3$ , a single error, i.e. having two physical qubits affected, is sufficient to make the encoding fail:



where there are three different combinations (see Eq. (4.58)) that count. Thus, we have

$$P_{\text{fail}} \sim 3p \quad (4.70)$$

For  $N = 5$ , one requires two errors, with four qubits affected, to make the encoding fail. Indeed,

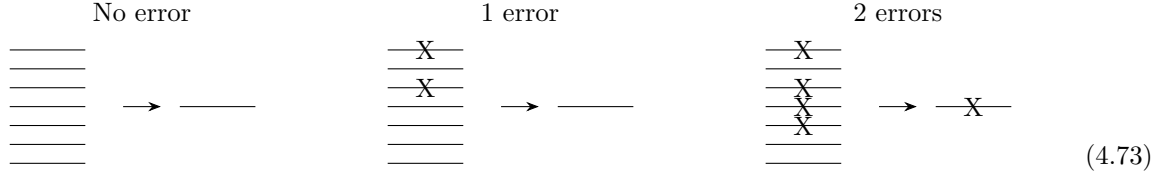


In such a case, the failing probability is given by

$$P_{\text{fail}} = \frac{1}{2} \binom{5}{2} \binom{3}{2} p^2 + \dots \sim 15p^2, \quad (4.72)$$

where the first binomial chooses 2 qubits to affect among the available 5, the second binomial chooses 2 qubits among the remaining 3. The factor one-half accounts for the symmetry between the first error and the second one, i.e. between the first couple of affected qubits and the second one.

Also for  $N = 7$ , one requires 2 errors, i.e. four affected qubits. Indeed



In such a case, we get

$$P_{\text{fail}} = \frac{1}{2} \binom{7}{2} \binom{5}{2} p^2 + \dots \sim 105p^2. \quad (4.74)$$

Figure 4.6 compares failing probabilities of the encodings with different values of  $N$ . As one can see the knee of the curves moves towards zero, meaning that the threshold does not exist.

Thus, for the error defined in Eq. (4.55), employing several layers of encoding can allow for a fault-tolerant quantum computing, while employing only a single layer encoding with more qubits has strong limits.

## 4.2 Stabiliser formalism

The stabiliser formalism exploits the fact that there exist operations, namely stabilisers, that can be used to detect errors without changing the state of the logical qubit. While the single stabiliser can only tell if there

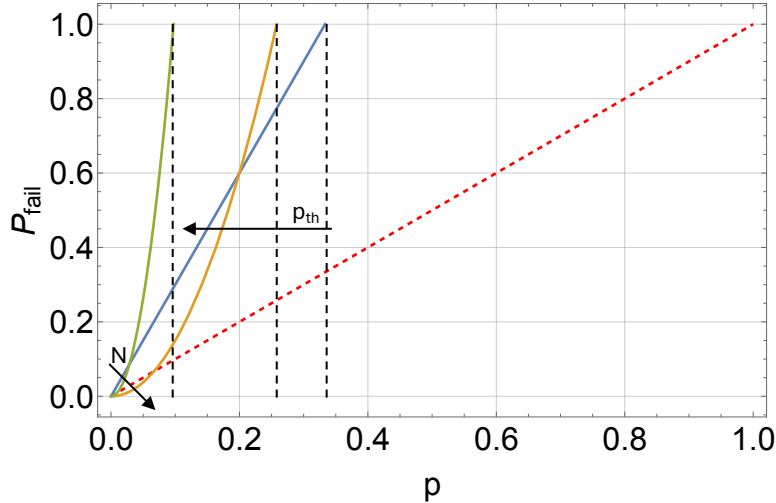


Fig. 4.6: Comparison of the failing probabilities  $P_{\text{fail}}$  for different values  $N$  of the qubits with a single layer of encoding. The arrow indicates the direction of increasing values of  $N$ , while the vertical black dashed lines indicate how the curves cannot define a threshold probability.

was an error, without establishing which error, a specific set of stabilisers can identify the specific errors that occurred, and thus providing the information to correct it.

#### 4.2.1 Inverting quantum channels

The following scheme summarises the QEC philosophy. Given a qubit, this is encoded in a logical qubit made of a set of physical qubits. The interaction with the surrounding environment (or other faulty components of the physical circuit) leads to errors in the state. The action of these errors can be described in terms of a CPTP map. The QEC code applies a recovery CPTP map, which — up to a certain probability — gives back the same initial state, as there were no errors, cf. Fig. 4.7.



Fig. 4.7: Schematic representation of the QEC scheme, where a recovery CPTP map is applied to recover the information as there were no errors.

The question is: when is this possible?

Consider two CPTP maps  $\mathcal{E}$  and  $\mathcal{R}$ , which describe respectively the occurrence of environmental errors and the recovery map. Their action is

$$\mathcal{B}(\mathbb{H}) \xrightarrow{\mathcal{E}} \mathcal{B}(\mathbb{H}') \xrightarrow{\mathcal{R}} \mathcal{B}(\mathbb{H}''), \quad (4.75)$$

where  $\mathcal{B}(\mathbb{H})$  is the space of all the linear operators acting on  $\mathbb{H}$ . We want to have no effects of the errors, i.e.  $\mathcal{R} \circ \mathcal{E} = \text{id}$ .

Now, we show that the following two statements are equivalent:

- 1) Given a CPTP map  $\mathcal{E}$ , it exists another CPTP map  $\mathcal{R}$  such that  $\mathcal{R} \circ \mathcal{E} = \text{id}$ .
- 2) For any Kraus representation of  $\mathcal{E}$ , which is defined through the set of Kraus operators  $\hat{E}_i$ , then one has that

$$\hat{E}_i^\dagger \hat{E}_j = \mu_{ij} \hat{\mathbb{1}}, \quad (4.76)$$

where  $\mu_{ij} \in \mathbb{C}$  are the coefficients of the density matrix of the environment imposing the map  $\mathcal{E}$ . Namely,

$$\hat{\mu} = \sum_{ij} \mu_{ij} |e_i\rangle \langle e_j|. \quad (4.77)$$

First, we prove that 1) implies 2). Consider  $|\psi\rangle \in \mathbb{H}$ , to which we apply the map  $\mathcal{E}$ . This gives

$$|\psi\rangle \xrightarrow{\mathcal{E}} \sum_j \hat{E}_j |\psi\rangle |e_j\rangle, \quad (4.78)$$

where  $|e_j\rangle$  is the state of the environment with which the system is entangling. Now, we apply the map  $\mathcal{R}$ :

$$\xrightarrow{\mathcal{R}} \sum_{jk} \hat{R}_k \hat{E}_j |\psi\rangle |e_j\rangle |a_k\rangle, \quad (4.79)$$

where  $|a_k\rangle$  is the state of an ancilla, whose interaction defines the map  $\mathcal{R}$ . Since we want that the map  $\mathcal{R}$  works as a recovery map for the map  $\mathcal{E}$ , we have to impose that

$$\sum_{jk} \hat{R}_k \hat{E}_j |\psi\rangle |e_j\rangle |a_k\rangle = |\psi\rangle \otimes (\dots), \quad (4.80)$$

where  $(\dots)$  is a suitable state of the environment and the ancilla. In this way, the entanglement between the system and the environment is transferred to the environment and the ancilla, with no correlation to the state of the system. This is possible only if

$$\hat{R}_k \hat{E}_j = \alpha_{kj} \hat{\mathbb{1}}. \quad (4.81)$$

In such a case, one has that  $(\dots) = \sum_{jk} \alpha_{kj} |e_j\rangle |a_k\rangle$  and

$$\begin{aligned} \hat{E}_i^\dagger \hat{E}_j &= \sum_k \hat{E}_i^\dagger \hat{R}_k^\dagger \hat{R}_k \hat{E}_j, \\ &= \sum_k \alpha_{ki}^* \alpha_{kj} \hat{\mathbb{1}}, \end{aligned} \quad (4.82)$$

where we used that

$$\sum_k \hat{R}_k^\dagger \hat{R}_k = \hat{\mathbb{1}}. \quad (4.83)$$

Then, we can define

$$\mu_{ij} = \sum_k \alpha_{ki}^* \alpha_{kj}. \quad (4.84)$$

Notably, we have that  $\mu_{ji}^* = \mu_{ij}$ , indeed

$$\mu_{ji}^* \hat{\mathbb{1}} = (\mu_{ij} \hat{\mathbb{1}})^\dagger = (\hat{E}_i^\dagger \hat{E}_j)^\dagger = \hat{E}_j^\dagger \hat{E}_i = \mu_{ij} \hat{\mathbb{1}}. \quad (4.85)$$

Moreover, we have that

$$\sum_i \mu_{ii} \hat{\mathbb{1}} = \sum_i \hat{E}_i^\dagger \hat{E}_i = \hat{\mathbb{1}}, \quad (4.86)$$

and that

$$\mu_{ii}\hat{\mathbb{1}} = \hat{E}_i^\dagger \hat{E}_i, \quad (4.87)$$

is a positive operator, which implies that  $\mu_{ii} > 0$ . Thus,  $\{\mu_{ij}\}_{ij}$  have all the properties to be the coefficients of a density matrix, and this proves that 1) implies 2).

We now prove that 2) implies 1). We start from

$$\hat{E}_i^\dagger \hat{E}_j = \mu_{ij}\hat{\mathbb{1}}, \quad (4.88)$$

and we diagonalise  $\mu_{ij}$ . This implies a change the Kraus operators according to  $\hat{E}_i \rightarrow \hat{F}_i$  such that

$$\hat{F}_i^\dagger \hat{F}_j = \delta_{ij} p_i \hat{\mathbb{1}}, \quad (4.89)$$

where  $p_i > 0$  by definition. We then introduce the isometries  $\hat{V}_i$  that are related to  $\hat{F}_i$  via

$$\hat{F}_i = \sqrt{p_i} \hat{V}_i. \quad (4.90)$$

Then, as represented in Fig. 4.8, the map  $\mathcal{E}$  is mapping  $\mathbb{H}$  to different subspaces  $\mathbb{H}'_i$  of  $\mathbb{H}'$ . Each of these

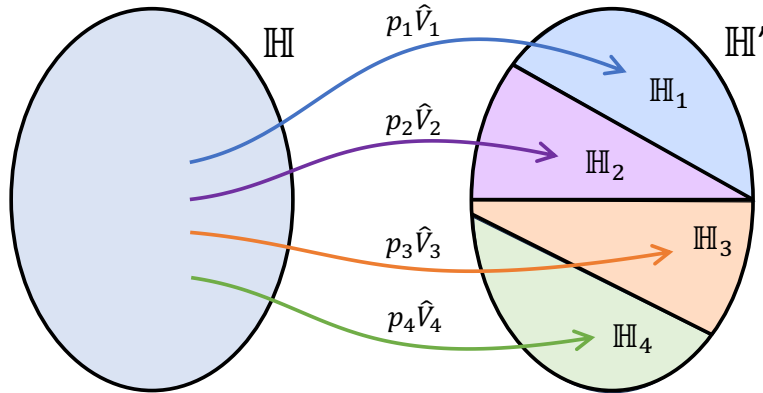


Fig. 4.8: Graphical representation of the mapping between  $\mathbb{H}$  and  $\mathbb{H}'$ .

mapping is performed with a probability  $p_i$  by the operator  $\hat{V}_i \propto \hat{F}_i$ . Notably, since we diagonalised  $\mu_{ij}$ , the different operators  $\hat{V}_i$  are orthogonal, and thus are also the subspaces  $\mathbb{H}'_i$ . Now, given this set of isometries, we can construct the recovery Kraus operators as

$$\hat{R}_i = \hat{V}_i^\dagger, \quad (4.91)$$

which will act only on the corresponding subspace  $\mathbb{H}'_i$ , leaving the rest of Hilbert space  $\mathbb{H}'$  untouched: indeed, for  $i \neq j$  we have  $\hat{V}_i^\dagger \hat{V}_j \propto \hat{V}_i^\dagger \hat{V}_j = 0$ . Finally, we compose the maps  $\mathcal{E}$  and  $\mathcal{R}$ :

$$\begin{aligned} \hat{\rho} &\xrightarrow{\mathcal{E}} \mathcal{E}(\hat{\rho}) = \sum_i p_i \hat{V}_i \hat{\rho} \hat{V}_i^\dagger, \\ &\xrightarrow{\mathcal{R}} \mathcal{R}(\mathcal{E}(\hat{\rho})) = \sum_j \hat{V}_j^\dagger \left( \sum_i p_i \hat{V}_i \hat{\rho} \hat{V}_i^\dagger \right) \hat{V}_j, \\ &= \sum_{ij} p_i \hat{V}_j^\dagger \hat{V}_i \hat{\rho} \hat{V}_i^\dagger \hat{V}_j, \\ &= \sum_i p_i \hat{\rho} = \hat{\rho}, \end{aligned} \quad (4.92)$$

where we used that  $\hat{V}_j^\dagger \hat{V}_i = \delta_{ij} \hat{1}$ .

#### 4.2.2 Correctable errors

The generic scheme for QEC is the following. We are given  $k$  qubits in an unknown state  $|\psi\rangle \in \mathbb{H}$ . We encode  $|\psi\rangle$  in a larger number  $n > k$  of qubits. These  $n$  qubits are subject to errors, which are described in terms of a Kraus map  $\mathcal{E}$  with the Kraus operators being  $\hat{E}_i$  or equivalently  $\hat{V}_i$ , see Eq. (4.90). The recovery protocol employs some extra  $n'$  ancillary qubits to apply the QEC, which inverts the error Kraus map under certain conditions.

After the encoding, the relevant state will be  $|\psi'\rangle \in \mathbb{H}_C$ , which is a subspace of  $\mathbb{H}'$  and it is called code space. In particular, the entire Hilbert space  $\mathbb{H}'$  is the union of the code space  $\mathbb{H}_C$  with the  $\otimes_i \mathbb{H}'_i$ . Here, the basis of each  $\mathbb{H}'_i$  is obtained by applying the corresponding  $\hat{V}_i$  to the basis of  $\mathbb{H}_C$ . Under this perspective, one can say that also the basis of  $\mathbb{H}_C$  is generated in the same way, where the corresponding error operator is  $\hat{V}_C = \hat{1}$ . Now, since the subspace  $\mathbb{H}'_i$  so constructed is orthogonal to  $\mathbb{H}_C$ , then the error can be recovered. What is needed is a error syndrome measurement that identifies the subspace  $\mathbb{H}'_i$  in which the state  $|\psi'\rangle$  has been mapped. Given such a measurement, one can apply the corresponding Kraus recovery operator. This is graphically represented in Fig. 4.9

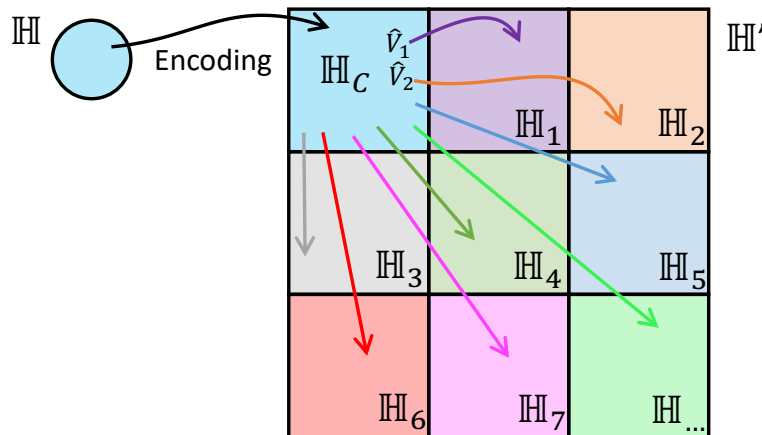


Fig. 4.9: Graphical representation of the division of the Hilbert space  $\mathbb{H}'$  in the code space  $\mathbb{H}$  and error spaces  $\mathbb{H}_i$ , which are linked by the operators  $\hat{V}_i$ .

One can invert the error map if the corresponding operators  $\hat{E}_i$  satisfy

$$\hat{P} \hat{E}_i^\dagger \hat{E}_j \hat{P} = \mu_{ij} \hat{P}, \quad (4.93)$$

where  $\hat{P}$  is a projector on the code space  $\mathbb{H}_C$ .

Notably,  $\hat{P}$  acts as an identity operator if restricted on  $\mathbb{H}_C$ . This also implies that there exists a special set of Kraus operators, which allow to rewrite the error map, and thus also the recovery map, as a mixture of isometries. These are induced by a set of unitary operators  $\hat{U}_i$  on the code space:

$$\hat{V}_i = \hat{U}_i \hat{P}, \quad (4.94)$$

such that

$$\hat{P} \hat{U}_i^\dagger \hat{U}_j \hat{P} = \delta_{ij} \hat{P}. \quad (4.95)$$

Then, one can map the state  $\hat{V}_i |\psi'\rangle$  back to  $\mathbb{H}_C$  by selecting the corresponding recovery Kraus operator  $\hat{R}_i = \hat{V}_i^\dagger$ .

An important note is the following. Let be  $\mathcal{R}$  the recovery map for  $\mathcal{E}$ . Then, one has

$$\begin{aligned}\mathcal{E}(\hat{\rho}) &= \sum_i \hat{E}_i \hat{\rho} \hat{E}_i^\dagger, \\ \mathcal{R}(\hat{\rho}) &= \sum_k \hat{R}_k \hat{\rho} \hat{R}_k^\dagger,\end{aligned}\tag{4.96}$$

such that  $\hat{R}_k \hat{E}_i = \alpha_{ki} \hat{1}$ . We define the map  $\mathcal{D}$  as

$$\mathcal{D}(\hat{\rho}) = \sum_i \hat{D}_i \hat{\rho} \hat{D}_i^\dagger,\tag{4.97}$$

with  $\hat{D}_i$  appertaining to the span of  $\{\hat{E}_i\}_i$ , i.e.  $\hat{D}_i = \sum_j c_{ij} \hat{E}_j$ . Then, the map  $\mathcal{D}$  can be recovered with the same recovery map  $\mathcal{R}$ .

Consider the case of  $n$  qubits. We want to construct the recovery map for errors due to the application of the Pauli operators. These are  $\{\hat{1}, \hat{\sigma}_x, \hat{\sigma}_y, \hat{\sigma}_z\}^{\otimes n}$ , and they form the basis of  $\mathcal{B}(\mathbb{H}^{\otimes n})$ . The operator  $\hat{1}$  is the identity, so is not associated to any error. The operator  $\hat{\sigma}_y = i\hat{\sigma}_x\hat{\sigma}_z$ . So, one needs to construct the recovery map  $\mathcal{R}$  that corrects only errors due to  $\hat{\sigma}_x$  and  $\hat{\sigma}_z$ . Now, for every Pauli operator different from the identity, we have two important properties:  $\text{Tr}[\hat{\sigma}_i] = 0$  and  $\hat{\sigma}_i^2 = \hat{1}$ . They imply that their eigenvalues are  $\pm 1$ . Thus, one can divide the full Hilbert space  $\mathbb{H}' = \mathbb{H}$ , with  $\dim(\mathbb{H}) = 2^n$ , in two subspaces (of the same dimension), which are associated to the corresponding eigenvalues, see Fig. 4.10. Namely, given  $\hat{\sigma}_i$  we have  $\mathbb{H}_{\sigma_i=1}$  and  $\mathbb{H}_{\sigma_i=-1}$ , with  $\dim(\mathbb{H}_i) = 2^{n-1}$ , whose union gives  $\mathbb{H}'$ . Suppose the code space  $\mathbb{H}_C$  is defined in terms of the operators  $\hat{E}_1$  and  $\hat{E}_2$  as it follows:  $\forall |\psi\rangle \in \mathbb{H}_C$ , one has

$$\hat{E}_1 |\psi\rangle = +1 |\psi\rangle, \quad \text{and} \quad \hat{E}_2 |\psi\rangle = +1 |\psi\rangle.\tag{4.98}$$

Any other combination identifies an error subspace  $\mathbb{H}'_i$ .

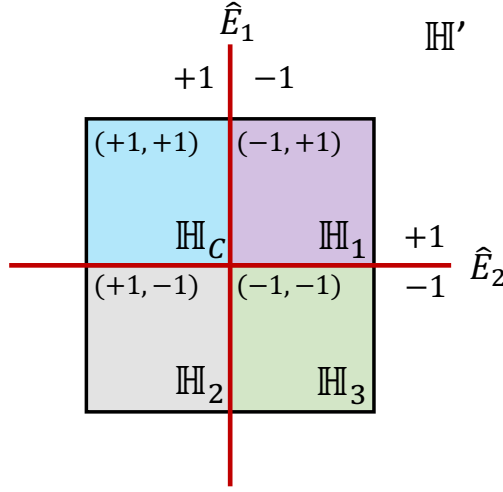


Fig. 4.10: Division of the Hilbert space  $\mathbb{H}'$  with respect to the subspaces defined by the eigenvalues of  $\hat{E}_1$  and  $\hat{E}_2$ .

More in general, given the operators in  $\mathcal{B}(\mathbb{H})$ , they are part of one of the following families:

- They specify the subspaces we are going to divide  $\mathbb{H}'$ .

- They are responsible for errors. So they describe how a state moves from  $\mathbb{H}_C$  to  $\mathbb{H}'_i$ .
- They are responsible for logical operations within the individual subspaces  $\mathbb{H}_C$  and  $\mathbb{H}_i$ .

### 4.2.3 Stabilisers

For  $n$  qubits, one has  $4 \times 4^n$  Pauli operators. The first factor 4 accounts for the four relevant phases  $\{+1, -1, +i, -i\}$ , while the rest count the operators being the basis of the operators acting on a  $2^n$  dimensional space. We define as stabilisers the elements of an abelian subgroup which is responsible of the division of  $\mathbb{H}'$  in subspaces. Namely, there will be one code space  $\mathbb{H}_C$  and the other are the error spaces.

**Example 4.1**

Consider the case of  $n = 3$ . The stabilisers are

$$(Stabilisers for n = 3) = \{\hat{1}\hat{1}\hat{1}, \hat{\sigma}_z\hat{\sigma}_z\hat{1}, \hat{1}\hat{\sigma}_z\hat{\sigma}_z, \hat{\sigma}_z\hat{1}\hat{\sigma}_z\}. \quad (4.99)$$

Consider  $\hat{\sigma}_z\hat{\sigma}_z\hat{1}$ . It determines the parity of the first and the second qubit. Thus, it divides the Hilbert space  $\mathbb{H}'$  in two parts, one associated to its  $+1$  eigenvalue and to its  $-1$  eigenvalue:

$$\begin{array}{c|c} +1 & -1 \\ \hline |000\rangle & |100\rangle \\ |111\rangle & |011\rangle \\ |001\rangle & |010\rangle \\ |110\rangle & |101\rangle \end{array} \quad (4.100)$$

A similar division can be done considering the operator  $\hat{1}\hat{\sigma}_z\hat{\sigma}_z$ , for which we have

$$\begin{array}{c|c} +1 & -1 \\ \hline |000\rangle & |001\rangle \\ |111\rangle & |110\rangle \\ |100\rangle & |010\rangle \\ |011\rangle & |101\rangle \end{array} \quad (4.101)$$

We notice that there are no other possible partitions of  $\mathbb{H}'$ . Indeed, the last non-trivial stabiliser is  $\hat{\sigma}_z\hat{1}\hat{\sigma}_z$  can be expressed as the product of the other two:

$$\hat{\sigma}_z\hat{1}\hat{\sigma}_z = (\hat{\sigma}_z\hat{1}\hat{\sigma}_z)(\hat{\sigma}_z\hat{\sigma}_z\hat{1}). \quad (4.102)$$

To be specific, the operators  $\hat{\sigma}_z\hat{1}\hat{\sigma}_z$  and  $\hat{\sigma}_z\hat{\sigma}_z\hat{1}$  are the generators of the abelian subgroup of the stabilisers.

Now, we can define the code space  $\mathbb{H}_C$  as that associated to the  $+1$  eigenvalues for all the stabilisers. Namely, this is the subspace of  $\mathbb{H}'$  which is spanned by the  $+1$  eigenstates of all the generators of the abelian subgroup:

$$\mathbb{H}_C = \text{span}(|000\rangle, |111\rangle). \quad (4.103)$$

The partitioning of  $\mathbb{H}'$  is represented graphically in Fig. 4.11.

Now, consider  $\hat{E}_i$  being one of the  $4 \times 4^n$  Pauli operators not being one of the stabilisers  $S_k$ . Now, since it is constructed as the product of single qubit Pauli operators,  $\hat{E}_i$  can only commute or anticommute with the stabilisers  $S_k$ .

- Assume that it commutes:  $[\hat{E}_i, \hat{S}_k] = 0$ . Then, we have that for any  $|\psi\rangle \in \mathbb{H}_C$ , it holds

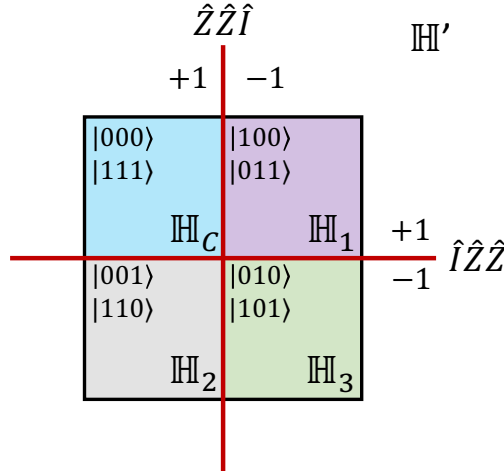


Fig. 4.11: Division of the Hilbert space  $\mathbb{H}'$  with respect to the subspaces defined by the eigenvalues of  $\hat{\sigma}_z \hat{\sigma}_z \hat{1}$  and  $\hat{1} \hat{\sigma}_z \hat{\sigma}_z$ .

$$\hat{S}_k \hat{E}_i |\psi\rangle = \hat{E}_i \hat{S}_k |\psi\rangle = \hat{E}_i |\psi\rangle, \quad (4.104)$$

where the last equality follows from the fact that  $S_k$  is a stabiliser and thus acts as an identity on  $\mathbb{H}_C$ . Then, if  $\hat{E}_i$  commutes stabiliser  $\hat{S}_k$ , it is associated to the eigenvalue +1 of the latter. Indeed, the state  $|\phi_i\rangle = \hat{E}_i |\psi\rangle$  is associated to the +1 eigenvalue of  $\hat{S}_k$ .

- Conversely, if it anticommutes:  $\{\hat{E}_i, \hat{S}_k\} = 0$ , then

$$\hat{S}_k \hat{E}_i |\psi\rangle = -\hat{E}_i \hat{S}_k |\psi\rangle = -\hat{E}_i |\psi\rangle. \quad (4.105)$$

In such a case, one says that  $\hat{E}_i$  is associated to the -1 eigenvalue of  $S_k$ .

#### Example 4.2

In the case of  $n = 3$  one has that the operators  $\hat{\sigma}_x \hat{1} \hat{1}$  and  $\hat{\sigma}_x \hat{\sigma}_x \hat{\sigma}_x$  are associated to the eigenvalues of  $\hat{\sigma}_z \hat{\sigma}_z \hat{1}$  and  $\hat{1} \hat{\sigma}_z \hat{\sigma}_z$  as

$$\begin{array}{c|cc} & \left| \hat{\sigma}_z \hat{\sigma}_z \hat{1} \right| \hat{1} \hat{\sigma}_z \hat{\sigma}_z \\ \hline \hat{\sigma}_x \hat{1} \hat{1} & -1 & +1 \\ \hat{\sigma}_x \hat{\sigma}_x \hat{\sigma}_x & +1 & +1 \end{array} \quad (4.106)$$

Now,  $\hat{\sigma}_x \hat{\sigma}_x \hat{\sigma}_x$  commutes with both the (generators of the subgroup of) stabilisers. Thus, it means that if

$$|\psi\rangle \in \mathbb{H}_C, \quad \text{then} \quad \hat{\sigma}_x \hat{\sigma}_x \hat{\sigma}_x |\psi\rangle \in \mathbb{H}_C. \quad (4.107)$$

Namely, it is a normaliser (see below) and it acts as a logical  $\hat{\sigma}_x$ .

Conversely,  $\hat{\sigma}_x \hat{1} \hat{1}$  anticommutes with  $\hat{\sigma}_z \hat{\sigma}_z \hat{1}$ . This means that given a state

$$|\psi\rangle \in \mathbb{H}_C, \quad \text{then} \quad \hat{\sigma}_x \hat{1} \hat{1} |\psi\rangle \in \mathbb{H}'_1 \cup \mathbb{H}'_3, \quad (4.108)$$

where  $\mathbb{H}'_1$  and  $\mathbb{H}'_3$  are respectively associated to the eigenvalues (-1, +1) and (-1, -1) of  $(\hat{\sigma}_z \hat{\sigma}_z \hat{1}, \hat{1} \hat{\sigma}_z \hat{\sigma}_z)$ . However, since  $\hat{\sigma}_x \hat{1} \hat{1}$  commutes with  $\hat{1} \hat{\sigma}_z \hat{\sigma}_z$ , then  $\hat{\sigma}_x \hat{1} \hat{1} |\psi\rangle \in \mathbb{H}'_1$ .

Namely, the operator  $\hat{\sigma}_x \hat{1} \hat{1}$  is one of the  $\hat{V}_i$  errors that maps the states from the code space to the corresponding  $\mathbb{H}'_i$ .

If we have  $k$  qubits that are encoded in  $n$  qubits, with  $n > k$ , then we need  $(n - k)$  generators from the stabilisers to define the partitions. By starting with  $\dim(\mathbb{H}') = 2^n$ , since each generator divides the Hilbert space in two parts, we have  $2^{n-k}$  different subspaces of dimension  $2^k$ .

#### 4.2.4 Normalisers and Centralisers

There are Pauli operators that commute with all the elements of the stabilisers, but do not appartain to the stabilisers subgroup. These are the normalisers  $\hat{N}_k$ . They respect the partition of  $\mathbb{H}$ , meaning that they do not map states from the code space  $\mathbb{H}_C$  to an error space  $\mathbb{H}'_i$ , and act non-trivially in the code space. They are defined via

$$\hat{N}_k \hat{S}_i \hat{N}_k^\dagger = \hat{S}_j, \quad (4.109)$$

where  $\hat{S}_i$  are the stabilisers. If  $i = j$  they are called centralisers, while for  $i \neq j$  they are normalisers. In the particular case of the Pauli algebra, meaning that all the operators are generated by the product of Pauli operators, one has that the normalisers are centralisers. Indeed,

$$\hat{N}_k \hat{S}_i \hat{N}_k^\dagger = \pm \hat{N}_k \hat{N}_k^\dagger \hat{S}_i = \pm \hat{S}_i, \quad (4.110)$$

since Pauli operators can only commute or anticommute. However, given the stabilisers  $\hat{S}_i$ , the operator  $-\hat{S}_i$  does not stabilise the code space. Thus, the  $-$  sign cannot be accepted and one gets

$$\hat{N}_k \hat{S}_i \hat{N}_k^\dagger = \hat{S}_i = \hat{S}_j. \quad (4.111)$$

Thus, they are all centralisers.

**Example 4.3**

Consider the case of  $n = 3$ . The operator  $\hat{\sigma}_x \hat{\sigma}_x \hat{\sigma}_x$  acts as follows:

$$\begin{aligned} |000\rangle &\xrightarrow{\hat{\sigma}_x} |111\rangle, \\ |111\rangle &\xrightarrow{\hat{\sigma}_x} |000\rangle. \end{aligned} \quad (4.112)$$

Thus, it acts as a logical  $\hat{\sigma}_x$ . The same happens for  $\hat{\sigma}_x \hat{\sigma}_x \hat{\sigma}_x \hat{S}_k$  for any stabiliser  $\hat{S}_k$ . Indeed, for  $|\psi\rangle \in \mathbb{H}_C$ , we have that

$$\hat{\sigma}_x \hat{\sigma}_x \hat{\sigma}_x \hat{S}_k |\psi\rangle = \hat{\sigma}_x \hat{\sigma}_x \hat{\sigma}_x |\psi\rangle, \quad (4.113)$$

since  $\hat{S}_k$  acts as a logical identity on  $\mathbb{H}_C$ . Suppose we take the stabiliser  $\hat{S}_k = \hat{\sigma}_z \hat{\sigma}_z \hat{\mathbb{1}}$ , then

$$(\hat{\sigma}_x \hat{\sigma}_x \hat{\sigma}_x)(\hat{\sigma}_z \hat{\sigma}_z \hat{\mathbb{1}}) = -\hat{\sigma}_y \hat{\sigma}_y \hat{\sigma}_x, \quad (4.114)$$

which also acts as a logical  $\hat{\sigma}_x$ .

The normalisers contain  $\hat{\sigma}_x \hat{\sigma}_x \hat{\sigma}_x$ ,  $-\hat{\sigma}_y \hat{\sigma}_y \hat{\sigma}_y$ ,  $\hat{\sigma}_z \hat{\sigma}_z \hat{\sigma}_z$ , and all the products of these with all the stabilisers  $\hat{S}_k$ , which act as a logical identity.

Physical operation	Logical operation	
$\hat{1}\hat{1}\hat{1}$	$\hat{1}$	
$\hat{\sigma}_z\hat{\sigma}_z\hat{1}$	$\hat{1}$	
$\hat{\sigma}_z\hat{1}\hat{\sigma}_z$	$\hat{1}$	
$\hat{1}\hat{\sigma}_z\hat{\sigma}_z$	$\hat{1}$	
$\hat{\sigma}_x\hat{\sigma}_x\hat{\sigma}_x$	$\hat{\sigma}_x$	(4.115)
$\hat{\sigma}_x\hat{\sigma}_x\hat{\sigma}_x\hat{S}_k$	$\hat{\sigma}_x$	
$-\hat{\sigma}_y\hat{\sigma}_y\hat{\sigma}_y$	$\hat{\sigma}_y$	
$-\hat{\sigma}_y\hat{\sigma}_y\hat{\sigma}_y\hat{S}_k$	$\hat{\sigma}_y$	
$\hat{\sigma}_z\hat{\sigma}_z\hat{\sigma}_z$	$\hat{\sigma}_z$	
$\hat{\sigma}_z\hat{\sigma}_z\hat{\sigma}_z\hat{S}_k$	$\hat{\sigma}_z$	

#### 4.2.5 Stabiliser code

Consider the three qubits encoding a single logical qubit. The stabilisers are:

$$\hat{1}\hat{1}\hat{1}, \quad \hat{\sigma}_z\hat{\sigma}_z\hat{1}, \quad \hat{\sigma}_z\hat{1}\hat{\sigma}_z, \quad \hat{1}\hat{\sigma}_z\hat{\sigma}_z. \quad (4.116)$$

Among the possible errors, there are some that are more and less likely to occur. Under the assumption of errors that act independently on the qubits, the error  $\hat{1}\hat{\sigma}_x\hat{1}$  is more likely to occur than  $\hat{\sigma}_x\hat{\sigma}_x\hat{\sigma}_x$ . The first has weight 1 (only one operator different from the identity), while the second has weight 3.

Now, the question is which are the errors that can be corrected, and eventually how they can be corrected. As we already saw, the errors where only one of the qubits is modified can be corrected (see bit-flip, phase-flip and 9-qubit Shor QEC codes). These can be corrected via the application of the recovery operator  $\hat{R}_k = \hat{V}_k^\dagger$ , so that

$$\hat{R}_k \hat{V}_k = \hat{V}_k^\dagger \hat{V}_k = \hat{1}. \quad (4.117)$$

However, the operator  $\hat{R}_k$  can correct for a much wider class of operators. Indeed, given a state  $|\psi\rangle \in \mathbb{H}_C$  and a stabiliser  $\hat{S}_i$ , one has

$$\hat{R}_k(\hat{V}_k \hat{S}_i) |\psi\rangle = \hat{R}_k \hat{V}_k |\psi\rangle = |\psi\rangle. \quad (4.118)$$

Thus,  $\hat{R}_k$  can correct also errors of the form of a correctable error multiplied by a stabiliser, i.e.  $\hat{V}_k \hat{S}_i$ .

Conversely, an error in the class of normalisers which is not a stabiliser is a non-correctable error. Indeed, it acts non-trivially on the code space.

### 4.3 Surface code

The surface code is a QEC code that is related to topology. The idea is that a logical qubit is encoded in  $L \times L$  physical qubits as in the layout presented in Fig. 4.12. The array they construct has to be considered with periodic boundary conditions. The  $L^2$  qubits are divided in two classes:

- Half of the physical qubits are used as data qubits: they store quantum states  $|\psi_L\rangle$  that will be used for computation. They are represented with open circles  $\circ$ .
- Half of the physical qubits are called measurement qubits and they are employed as error detecting qubits. They are represented with full circles  $\bullet$ . There are two type of measurement qubits:
  - Measure Z or Z-syndrome qubits, which are represented in green,
  - Measure X or X-syndrome qubits, which are represented in yellow.

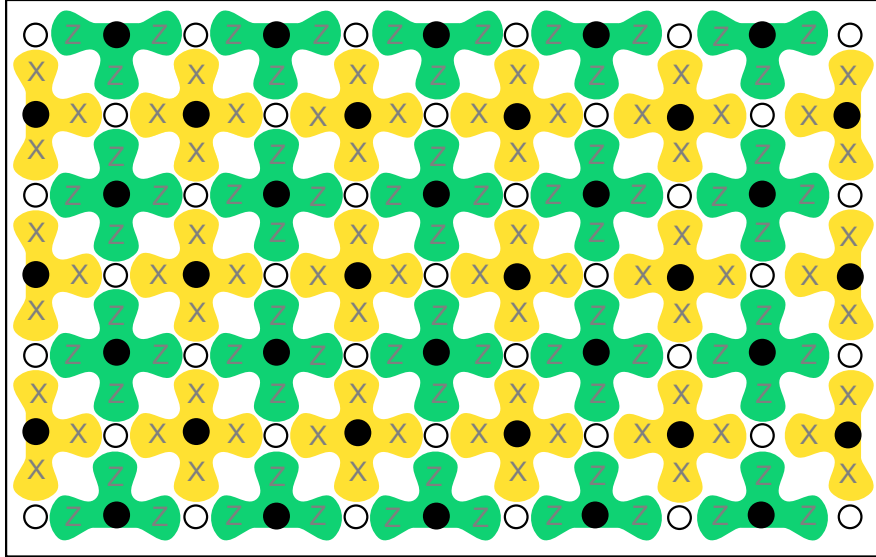


Fig. 4.12: Graphical representation of the  $L^2$  physical qubits (full and open circles) in the array generating the surface code through their interaction (green and yellow connections).

Each data qubit is coupled to two X-syndrome and two Z-syndrome qubits. Each measurement qubit is coupled to four data qubits. These couplings are described as follows. For the green block, i.e. the Z-syndrome, we have

$$\begin{array}{c}
 \textcircled{a} \\
 \textcircled{b} \quad \textcircled{c} \\
 \textcircled{d}
 \end{array}
 \text{ (green)} = |\psi_{abcd}\rangle \left\{ \begin{array}{c} \dots \\ \dots \\ \dots \\ \dots \\ |0_\bullet\rangle \xrightarrow{\oplus} \xrightarrow{\oplus} \xrightarrow{\oplus} \xrightarrow{\oplus} \xrightarrow{\text{Measure}} \end{array} \right. \quad (4.119)$$

where  $|0_\bullet\rangle$  indicates that the qubit  $\bullet$  has been initialised in  $|0\rangle$ . Similarly, for the yellow block one has

$$\begin{array}{c}
 \textcircled{a} \\
 \textcircled{b} \quad \textcircled{c} \\
 \textcircled{d}
 \end{array}
 \text{ (yellow)} = |\psi_{abcd}\rangle \left\{ \begin{array}{c} \dots \\ \oplus \\ \dots \\ \oplus \\ \dots \\ \oplus \\ \dots \\ |0_\bullet\rangle \xrightarrow{H} \xrightarrow{\cdot} \xrightarrow{\cdot} \xrightarrow{H} \xrightarrow{\text{Measure}} \end{array} \right. \quad (4.120)$$

In such a way, the measurement qubits are coupled to the data qubits. These circuits are run in cycles, between one logical operation and the following one, so to keep track of the errors that occur in between.

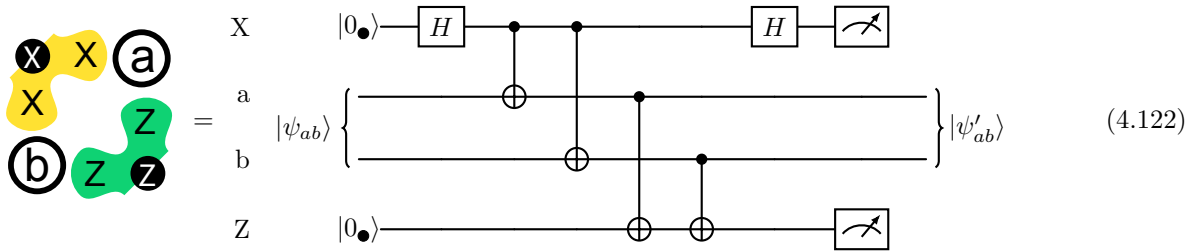
To understand the logic of the surface code, let us focus on the case where one has only four physical qubits: 2 are data qubits and 2 are measurement qubits (one in X and one in Z). The generators of the stabilisers are

the operators  $\hat{X}_a \hat{X}_b$  and  $\hat{Z}_a \hat{Z}_b$ . Here, we employ the notation  $\hat{Z}_i$  to identify the  $\hat{\sigma}_z^{(i)}$  Pauli operator acting on the  $i$ -th physical qubit. One can easily show that these operators commute, i.e.  $[\hat{X}_a \hat{X}_b, \hat{Z}_a \hat{Z}_b] = 0$ , although they do not at the level of single qubit, i.e.  $[\hat{X}_i, \hat{Z}_i] \neq 0$ . Thus, they have common eigenstates, which identify the division of the Hilbert space  $\mathbb{H}'$  in the code and error subspaces (for the sake of simplicity, we will drop all the normalisation constants):

$ \psi\rangle$	$ \hat{X}_a \hat{X}_b  \hat{Z}_a \hat{Z}_b$	
$ 00\rangle +  11\rangle$	+1	+1
$ 00\rangle -  11\rangle$	-1	+1
$ 01\rangle +  10\rangle$	+1	-1
$ 01\rangle -  10\rangle$	-1	-1

(4.121)

The circuit that applies these two stabilisers is



where the first qubit is the X-syndrome and the last is the Z-syndrome. Considering the generic state  $|\psi_{ab}\rangle$  for the qubits  $a$  and  $b$  being

$$|\psi_{ab}\rangle = A|00\rangle + B|01\rangle + C|10\rangle + D|11\rangle, \quad (4.123)$$

one can input this state in the circuit in Eq. (4.122) and, before the measurements, obtains that the total state reads

$$\begin{aligned} |\Psi_{XabZ}\rangle &= (A+D)|0\rangle(|00\rangle + |11\rangle)|0\rangle \\ &\quad + (A-D)|1\rangle(|00\rangle - |11\rangle)|0\rangle \\ &\quad + (B+C)|0\rangle(|01\rangle + |10\rangle)|1\rangle \\ &\quad + (B-C)|1\rangle(|01\rangle - |10\rangle)|1\rangle. \end{aligned} \quad (4.124)$$

It follows that, after the measurement of the X and Z-syndrome qubits, one obtains — depending on the outcomes  $\{M_X, M_Z\}$  — the following states with the corresponding probabilities  $P_{|\psi'_{ab}\rangle}$ :

$\{M_X, M_Z\}$	$ \psi'_{ab}\rangle$	$P_{ \psi'_{ab}\rangle}$
$\{+1, +1\}$	$ 00\rangle +  11\rangle$	$ A+D ^2$
$\{-1, +1\}$	$ 00\rangle -  11\rangle$	$ A-D ^2$
$\{+1, -1\}$	$ 01\rangle +  10\rangle$	$ B+C ^2$
$\{-1, -1\}$	$ 01\rangle -  10\rangle$	$ B-C ^2$

(4.125)

After the collapse on one of these common eigenstates of  $\hat{X}_a \hat{X}_b$  and  $\hat{Z}_a \hat{Z}_b$ , subsequent applications of the circuit in Eq. (4.122) will provide always — in the assumption of no noise — the same state.

#### Example 4.4

Consider the state in Eq. (4.124) and suppose the first cycle (which acts effectively as an encoding) provides the measurements  $\{M_X = -1, M_Z = -1\}$  and  $|\psi'_{ab}\rangle = |01\rangle - |10\rangle$ . Now,  $|\psi'_{ab}\rangle$  is equal to  $|\psi_{ab}\rangle$  in Eq. (4.123) when setting  $A = D = 0$  and  $B = -C = 1$ . The corresponding output state at the end of the second cycle before the measurement will be  $|\Psi_{XabZ}\rangle = |1\rangle(|01\rangle - |10\rangle)|1\rangle$ . This has two important implications: 1) the

state  $|\psi'_{ab}\rangle$  remains untouched by the circuit, which is the implementation of the stabilisers:  $\hat{S}_2\hat{S}_1|\psi'_{ab}\rangle = |\psi'_{ab}\rangle$ ; 2) also the output of the measurement  $\{M_X = -1, M_Z = -1\}$  remains the same.

This example shows that, without measuring directly  $|\psi'_{ab}\rangle$ , one can use the output of the measurements to infer the state of the data qubits. Turning the argument upside-down, an error occurring in the data qubits will be identified by the change in the outcomes of the measurements.

We notice that, in the case of 2 data qubits and 2 measurement qubits, one has

- 4 degrees of freedom where to encode a logical state: there are 2 physical qubits having 2 dimensions. The total Hilbert space  $\mathbb{H}'$  has  $2 \times 2$  dimensions.
- 4 constraints from the stabilisers: we have 2 stabilisers and each divides  $\mathbb{H}'$  in 2 subspaces.

Then, there are no free degrees of freedom where one can perform logical operations. In order to do that, one needs to impose the length of the array of physical qubits  $L$  being an odd number  $> 1$ . In such a way, one has 2 free degrees of freedom that can be employed. The minimal array is that having  $L = 3$  with 5 data qubits and 4 measurement qubits. Such an array is shown in Fig. 4.13. The circuit corresponding to the stabilisers

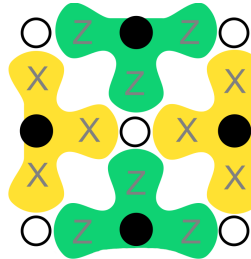
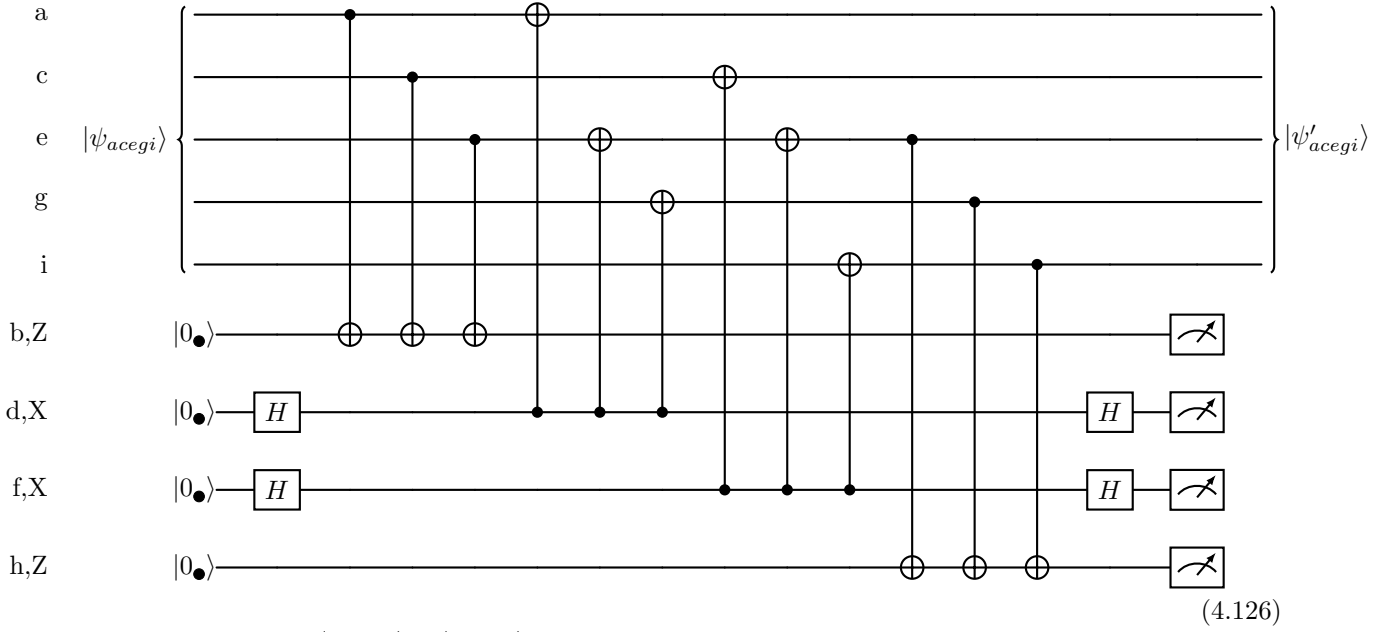


Fig. 4.13: Graphical representation of the surface code with 5 data qubits and 4 measurement qubits.

application is given by



Suppose we input the state  $|\psi_{acegi}\rangle = |00000\rangle$ . Then, the action of this circuit before the measurement is given by

$$\begin{aligned}
& (|00000\rangle + |10110\rangle + |01101\rangle + |11011\rangle) |0000\rangle \\
|00000, 0000\rangle \xrightarrow{\text{circuit in Eq. (4.126)}} & +(|00000\rangle - |10110\rangle + |01101\rangle - |11011\rangle) |0100\rangle \\
& +(|00000\rangle - |10110\rangle - |01101\rangle + |11011\rangle) |0010\rangle \\
& +(|00000\rangle - |10110\rangle - |01101\rangle + |11011\rangle) |0110\rangle,
\end{aligned} \tag{4.127}$$

where we expressed the states in the form  $|\psi_{acegi}, \phi_{bdfh}\rangle$ . Suppose the measurement results in  $\{M_b, M_d, M_f, M_h\} = \{+1, +1, -1, +1\}$ , which corresponds to the measurement state  $|\phi_{bdfh}\rangle = |0010\rangle$ . Then, the data state is given by

$$|\text{data}\rangle = |\psi'_{acegi}\rangle = |00000\rangle - |10110\rangle - |01101\rangle + |11011\rangle, \tag{4.128}$$

which remains untouched by subsequent applications of the circuit in Eq. (4.126). This is an easy but lengthy computation if performed in terms of states. However, it becomes trivial and immediate if considering that the circuit corresponds to the application of the stabilisers  $\hat{S}_4\hat{S}_3\hat{S}_2\hat{S}_1$  on the state  $|\text{data}\rangle$ , which has been already stabilised by the same circuit. Thus,  $\hat{S}_4\hat{S}_3\hat{S}_2\hat{S}_1|\text{data}\rangle = |\text{data}\rangle$ .

### 4.3.1 Detecting errors

There are several kinds of errors that can be detected with surface code. For the sake of simplicity, we consider the case of the array with 5 data and 4 measurement qubits, and that the logical state is encoded in  $|\text{data}\rangle$  shown in Eq. (4.128). The latter corresponds to the measurement state  $|0010\rangle$ , i.e. to the measurement outcomes  $\{M_b, M_d, M_f, M_h\} = \{+1, +1, -1, +1\}$ . We construct the table of outcomes with respect to the number of cycles that are performed. In the case of no errors and no logical operations, such table reads

# cycles	$M_b$	$M_d$	$M_f$	$M_h$
1	+1	+1	-1	+1
2	+1	+1	-1	+1
3	+1	+1	-1	+1
4	+1	+1	-1	+1
5	+1	+1	-1	+1
:	:	:	:	:

(4.129)

We now introduce errors, that will appear exactly at the third cycle. There are also other relevant errors, but we only focuses on the following two kinds.

- 1) Errors on the measurement or on the syndrome qubits;

These are the errors due to the erroneous output of a measurement  $M_i$ , or errors that are applied to the syndrome qubit. The latter will appear as the former. Suppose we have an error on the measurement of the  $f$  qubit. Then, the above table becomes

# cycles	$M_b$	$M_d$	$M_f$	$M_h$
1	+1	+1	-1	+1
2	+1	+1	-1	+1
3	+1	+1	+1	+1
4	+1	+1	-1	+1
5	+1	+1	-1	+1
:	:	:	:	:

(4.130)

where we highlighted the difference between the two tables. The error is only momentaneous. Later applications of the cycle will erase the action of these kind of errors. Indeed, if the error is due to the random erroneous measurement outcome, then the following cycle will (most probably) provide the exact outcome.

This will not be the case if there is a systematic error in the measurement process, which cannot be corrected. Conversely, if the error is caused by the application of an external action on the measurement qubit (say the surrounding environment acts with  $\hat{Z}$  on the  $f$  qubit), then the error vanishes in the next cycle since the qubit's state is initialised at the beginning of each cycle.

- 2) Errors on the data qubits. These are the errors on the data qubits that can be, for example, due to the surrounding environment, and that can corrupt the information encoded in the data state. It becomes then fundamental to being able to detect and account for such errors for the sake of computation.

Suppose we have a phase-flip error on the  $e$  qubit. The state is then transformed as

$$|\psi'_{acegi}\rangle \xrightarrow{\text{phase-flip error on qubit } e} \hat{Z}_e |\psi'_{acegi}\rangle. \quad (4.131)$$

Then, the Z-syndrome qubits will be unable to detect it. However, X-syndrome qubits  $d$  and  $f$  will detect the error: their coupling to the data qubit  $e$  imposes the action of  $\hat{X}_e$ , which do not commute with  $\hat{Z}_e$ . Then, what happens is that the state of the X-syndrome qubits will flip. By supposing that the error occurs at the third cycle. Then, the table of outcomes becomes

# cycles	$M_b$	$M_d$	$M_f$	$M_h$
1	+1	+1	-1	+1
2	+1	+1	-1	+1
3	+1	-1	+1	+1
4	+1	-1	+1	+1
5	+1	-1	+1	+1
:	:	:	:	:

(4.132)

Importantly, the outcomes  $M_d$  and  $M_f$  change sign for any subsequent cycle (if no other errors or logical operations take place). This is how one can distinguish an error on the measurement and on the data qubits. The best way to account for this error is to employ a classical control software that will changes the sign of every subsequent measurement of that data qubit's two adjacent X-syndrome qubits.

When one has an array of larger dimensions, then the situation is more complicated. For example, one might have that several data errors that form paths on the array. If this happens, the errors will be highlighted only by two syndrome qubits at the ends of the error path. An example is shown in Fig. 4.14, where the X-syndrome qubits  $a$  and  $f$  indicate that an error occurred. However, there is no indication about which path between  $a$  and  $f$  the Z-errors are covering.

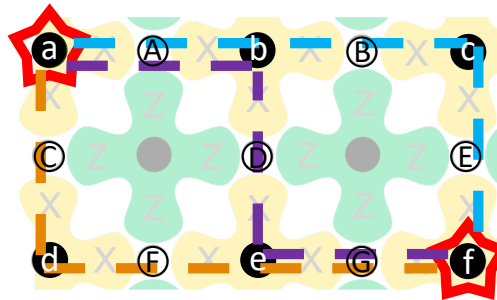


Fig. 4.14: Graphical representation of  $Z$  noises detected by the measurement qubits  $a$  and  $f$ . Different paths (blue, purple and orange) can produce this error syndrome.

This could be one among  $ABE$  (blue path),  $ADG$  (purple path) or  $CFG$  (orange path). When accounting via classical control software for the errors, one needs to select one of these paths. The question is what happens if one selects the wrong path? The beauty of the surface code kicks in: as long as the error path and the selected one form a closed loop, the error is well accounted. This is shown with the following argument. Suppose the error path is  $ABE$ , which is produced by  $\hat{Z}_A \hat{Z}_B \hat{Z}_E$ , and we select the path  $CFG$  to be corrected, whose correction is given by  $\hat{Z}_C \hat{Z}_F \hat{Z}_G$ . This is however not a problem, indeed we have that

$$(\hat{Z}_A \hat{Z}_B \hat{Z}_E) = (\hat{Z}_C \hat{Z}_F \hat{Z}_G) \hat{S}_e \hat{S}_d, \quad (4.133)$$

where we defined the stabilisers

$$\hat{S}_e = \hat{Z}_B \hat{Z}_E \hat{Z}_D \hat{Z}_G, \quad \text{and} \quad \hat{S}_d = \hat{Z}_A \hat{Z}_C \hat{Z}_D \hat{Z}_F. \quad (4.134)$$

Therefore, the two errors are related by two stabilisers. This means, that recovery operator  $\hat{R}_k$  that corrects  $\hat{Z}_A \hat{Z}_B \hat{Z}_E$  can correct also for  $\hat{Z}_C \hat{Z}_F \hat{Z}_G$ . This has been discussed in Sec. 4.2.5. Thus, every time we can form closed loops, the error can be accounted properly. These are harmless errors.

Conversely, consider now the case shown in Fig. 4.15. Here the error path (shown in orange) crosses the boundary of the array, and due to the periodic boundary conditions only two syndrome qubits highlight the error path. In such a case, one would still be tempted to connect directly the syndrome qubits with a path fully in the array (shown in purple). However, such a correction is not the proper one. Indeed, the two paths would form a logical operation. To visualise harmless and harmful paths, one maps the array on a torus. If the

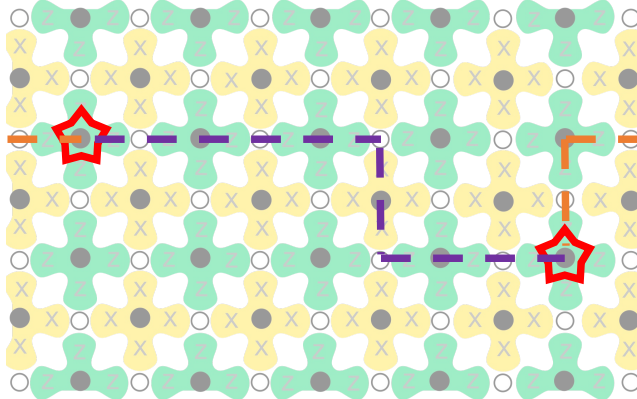


Fig. 4.15: Graphical representation of an error path that crosses the boundary of the array (orange path). If corrected with the purple path, it leads to a logical operation, thus not correcting for the error.

path can be closed, then it is harmless. If the path cannot be closed, then it is harmful. Figure 4.16 shows the mapping between the array and the torus, and highlights the harmless and harmful paths.

#### 4.4 Fault-tolerant computation

Let us suppose we want to implement the following logical circuit



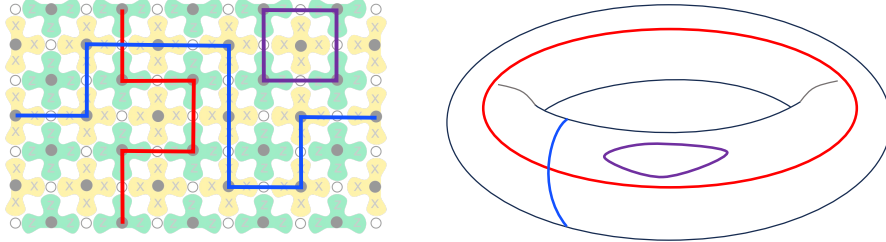


Fig. 4.16: Graphical representation of the mapping of the array on a torus surface. The red path corresponds to a logical  $X$ , while the blue path to a logical  $Z$  operation. These are harmful error. The purple path is an error that can be corrected.

so that if an error occurs it can be successfully corrected via a QEC code. The error can essentially occur in any of the components of the circuit. Namely,

- in the state preparation,
- in the logic quantum gates,
- in the measurement,
- in the simple transition of the quantum information along the quantum wires.

To combat the effect of the noise, one encodes the logical qubits in blocks of physical ones, using QEC codes. However, one needs also to replace the logical operations with encoded gates. Performing QEC periodically on the encoded states prevents the accumulation of errors in the state. However, it is not sufficient to prevent the build-up of errors, even if QEC is applied after each encoded gate.

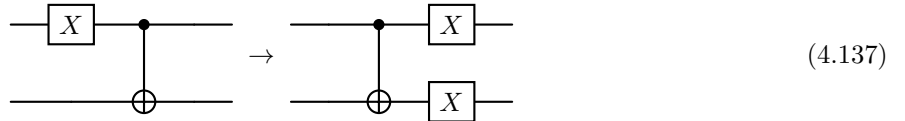
There are two main reasons:

- 1) The encoded gates can cause the propagation of errors.

Let us consider a specific example, where two qubits are connected by a CNOT gate and a  $X$  error occurs on the control qubit before the CNOT. Then, the error propagates also to the target qubit. This can be easily computed by considering that the CNOT is implemented by the unitary operator  $\hat{U}_{\text{CNOT}}$ . Then, one has

$$\hat{U}_{\text{CNOT}} \hat{\sigma}_x^{(1)} = \hat{U}_{\text{CNOT}} \hat{\sigma}_x^{(1)} \hat{U}_{\text{CNOT}}^\dagger \hat{U}_{\text{CNOT}} = \hat{\sigma}_x^{(1)} \hat{\sigma}_x^{(2)} \hat{U}_{\text{CNOT}}, \quad (4.136)$$

which can be graphically represented with



Then, one needs to design the encoded gates carefully, so that errors do not propagate on the entire block, but are limited to some physical qubits. In such a case the QEC code can remove these errors.

Performing encoded gates in such a way is a fault-tolerant (FT) procedure.

- 2) Also QEC can introduce errors.

An example is that graphically represented in Fig. 4.15, where an error is not correctly recovered.

To showcase the FT procedure, we introduce the Steane code.

#### 4.4.1 Steane code or 7-qubit code

The Steane code is a stabiliser code employing 7 data qubit and 6 syndrome qubits for each logical qubit. The total Hilbert space  $\mathbb{H}'$  has 128 dimensions that are divided in 64 subspaces of two dimensions. The graphical representation is given in Fig. 4.17. The generators of the stabilisers are

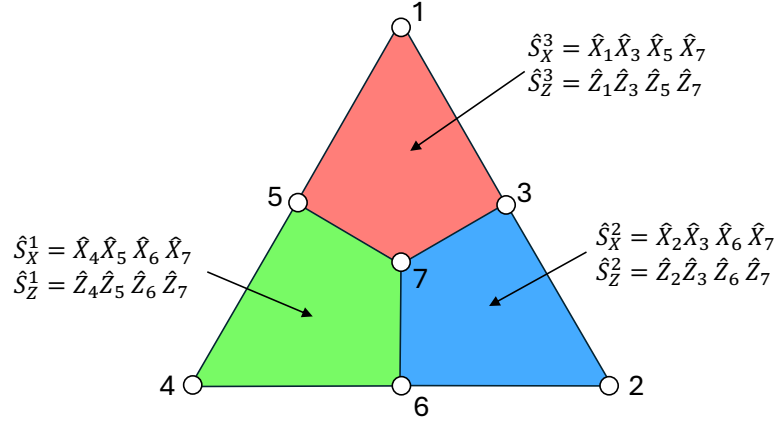


Fig. 4.17: Graphical representation of the Steane code with the data qubit represented as open circles and the corresponding stabilisers.

$$\{\hat{S}_k\}_{k=1}^6 = \begin{Bmatrix} \hat{1} & \hat{1} & \hat{1} & \hat{X} & \hat{X} & \hat{X} & \hat{X}, \\ \hat{1} & \hat{X} & \hat{X} & \hat{1} & \hat{1} & \hat{X} & \hat{X}, \\ \hat{X} & \hat{1} & \hat{X} & \hat{1} & \hat{X} & \hat{1} & \hat{X}, \\ \hat{1} & \hat{1} & \hat{1} & \hat{Z} & \hat{Z} & \hat{Z} & \hat{Z}, \\ \hat{1} & \hat{Z} & \hat{Z} & \hat{1} & \hat{1} & \hat{Z} & \hat{Z}, \\ \hat{Z} & \hat{1} & \hat{Z} & \hat{1} & \hat{Z} & \hat{1} & \hat{Z} \end{Bmatrix} = \begin{Bmatrix} \hat{X}_4 \hat{X}_5 \hat{X}_6 \hat{X}_7, \\ \hat{X}_2 \hat{X}_3 \hat{X}_6 \hat{X}_7, \\ \hat{X}_1 \hat{X}_3 \hat{X}_5 \hat{X}_7, \\ \hat{Z}_4 \hat{Z}_5 \hat{Z}_6 \hat{Z}_7, \\ \hat{Z}_2 \hat{Z}_3 \hat{Z}_6 \hat{Z}_7, \\ \hat{Z}_1 \hat{Z}_3 \hat{Z}_5 \hat{Z}_7, \end{Bmatrix}. \quad (4.138)$$

With the Steane code, any single-qubit error can be correctly recovered as it send the code space  $\mathbb{H}_C$  in one of the other subspaces  $\mathbb{H}_i$ . Specifically, the code space  $\mathbb{H}_C$  is given by the span of two logical states  $\{|0_L\rangle, |1_L\rangle\}$ . These are encoded as

$$\begin{aligned} |0_L\rangle &= \frac{1}{\sqrt{8}} [|0000000\rangle + |1010101\rangle + |0110011\rangle + |1100110\rangle + |0001111\rangle + |1011010\rangle + |0111100\rangle + |1101001\rangle], \\ |1_L\rangle &= \frac{1}{\sqrt{8}} [|1111111\rangle + |0101010\rangle + |1001100\rangle + |0011001\rangle + |1110000\rangle + |0100101\rangle + |1000011\rangle + |0010110\rangle]. \end{aligned} \quad (4.139)$$

The logical operations are given by the normalisers. In the Pauli group, we have the logical X-gate and the logical Z-gate. These are constructed by applying the corresponding single qubit operators to each physical qubit. Namely,

$$\begin{aligned} \hat{X}_L &= \hat{X}_1 \hat{X}_2 \hat{X}_3 \hat{X}_4 \hat{X}_5 \hat{X}_6 \hat{X}_7, \\ \hat{Z}_L &= \hat{Z}_1 \hat{Z}_2 \hat{Z}_3 \hat{Z}_4 \hat{Z}_5 \hat{Z}_6 \hat{Z}_7. \end{aligned} \quad (4.140)$$

These operations are allowed, as there are still two free degrees of freedom. There are also other logical operations that one can construct. These are normalisers that do not appartain to the Pauli group. An example is the Hadamard gate, which can be also implemented as the application of single qubit Hadamards:

$$\hat{H}_L = \hat{H}_1 \hat{H}_2 \hat{H}_3 \hat{H}_4 \hat{H}_5 \hat{H}_6 \hat{H}_7. \quad (4.141)$$

At this point, one would naively extrapolate that any logical operation can be constructed via the application of the corresponding gate on the single data qubits where the logical state is encoded. However, this is not the case. An example is the phase gate  $\hat{S}$ , whose representation in the computation basis reads

$$S = \begin{pmatrix} 1 & 0 \\ 0 & i \end{pmatrix}. \quad (4.142)$$

The corresponding logical gate is constructed as

$$\hat{S}_L = \hat{S}_1^\dagger \hat{S}_2^\dagger \hat{S}_3^\dagger \hat{S}_4^\dagger \hat{S}_5^\dagger \hat{S}_6^\dagger \hat{S}_7^\dagger. \quad (4.143)$$

Indeed, when applied to the logical computational basis we find

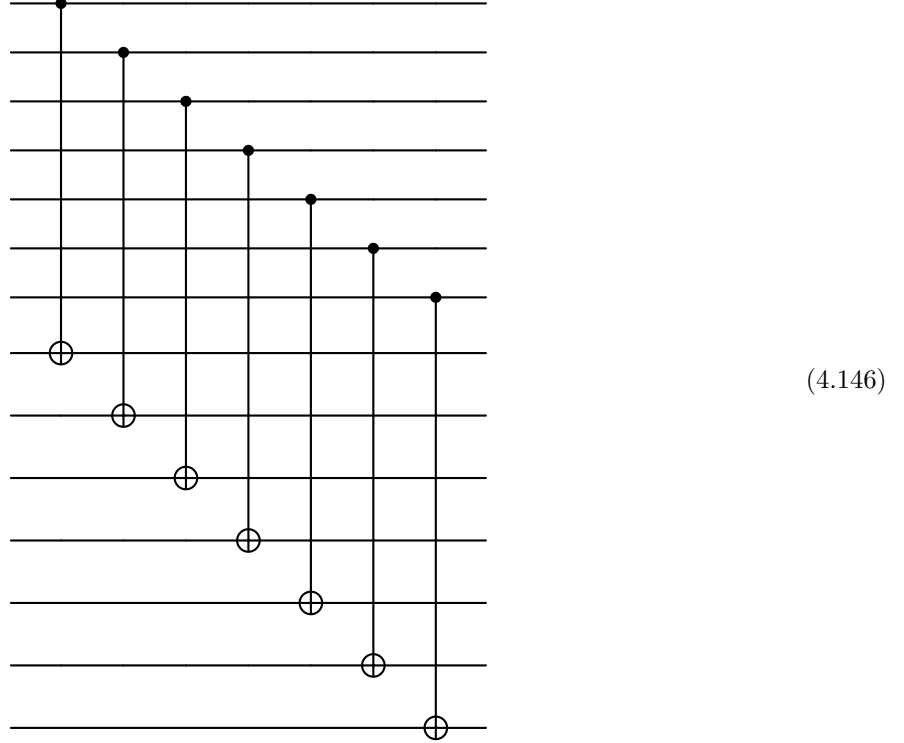
$$\begin{aligned} \hat{S}_L |0_L\rangle &= |0_L\rangle, \\ \hat{S}_L |1_L\rangle &= i |1_L\rangle. \end{aligned} \quad (4.144)$$

Conversely, if one would have defined a  $\hat{S}'_L$  as just simply applying the S-gate to each physical qubit, one would have obtained

$$\begin{aligned} \hat{S}'_L |0_L\rangle &= |0_L\rangle, \\ \hat{S}'_L |1_L\rangle &= -i |1_L\rangle. \end{aligned} \quad (4.145)$$

Thus, the construction of logical gates needs to be done with care and it depends on the QEC code that one is employing.

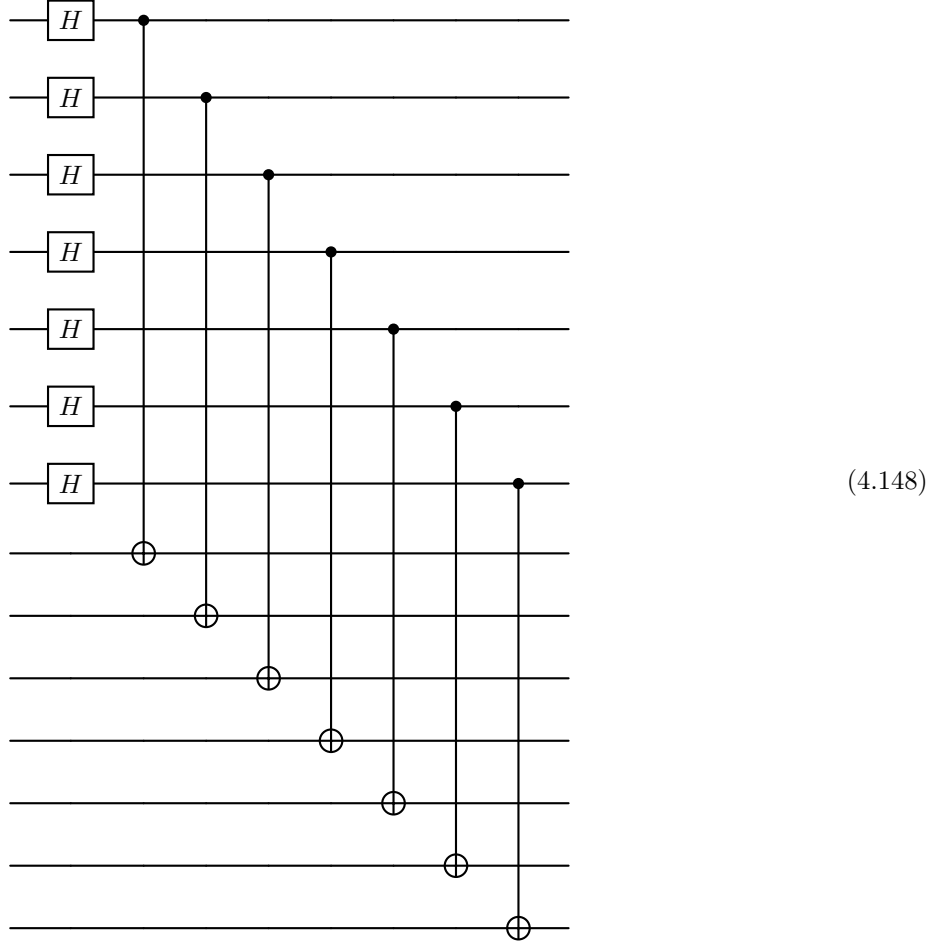
Let us consider the case of a CNOT gate. Here, we have two logical qubits, each corresponding to 7 data and 6 syndrome qubits. One can see that the logical CNOT gate can be implemented pairwise as described by the following circuit



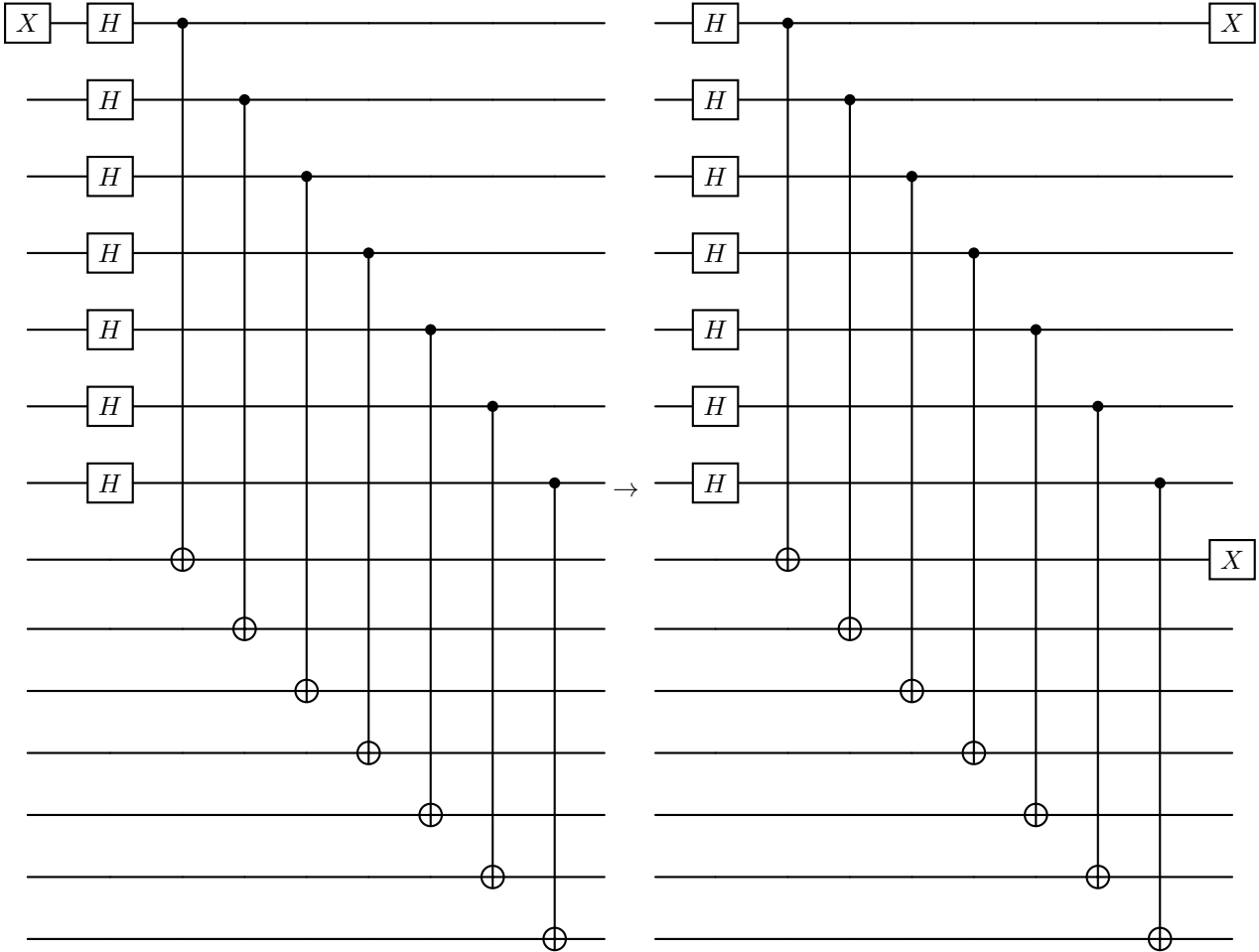
It follows that one can implement the logical circuit



as



This way of implementing logical gates is called transversal construction. This is a really easy and straightforward construction, but most importantly allows to confine errors, as they are unable to propagate. Let us take as an example the circuit in Eq. (4.148) and suppose we have initially a X error on the first qubit of the first block. In such a case, the error propagates accordingly to



(4.149)

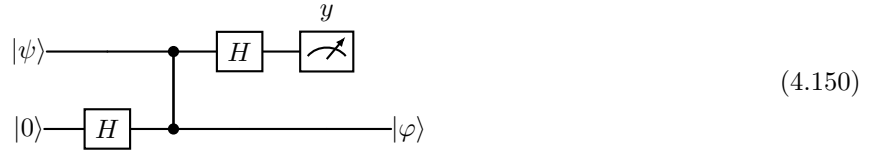
Thus, the error has been copied to the first qubit of the second block, but all the other qubits are not affected. The Steane code can correct for such an error. This holds true for any transverse construction.

Till now, we have covered the case for the normalisers  $\{\hat{X}_L, \hat{Z}_L, \hat{H}_L, \hat{S}_L, \text{CNOT}_L\}$ , which is the so-called Clifford group. Notably, the Gottesman-Knill theorem indicates that operations performed using only elements of this group can be simulated classically. Thus, one cannot have a real quantum advantage over a classical computer. Moreover, the Clifford group is not universal, meaning that the composition of elements of this group is not sufficient to implement any arbitrary gate. This is essentially the argument of the Solovay-Kitaev theorem. One needs to extend the Clifford group with the addition of at least an extra gate not appertaining to the group. This can be the T-gate or the Toffoli gate.

Unfortunately, one does not know how to implement through unitary operations the T-gate in a transversal way using the Steane code. This is a code-related problem. One could consider a different QEC code and implement the T-gate, but they will have problems with another gate, e.g. the Hadarmard gate. The Eastin-Knill theorem indicates that it is not possible to construct a fault-tolerant universal set with unitary operations.

Notably, the latter theorem applies only to unitary operations. One can still have the entire universal set by substituting the problematic gate with an effective implementation. Below, we focus on the derivation of an effective T-gate for the Steane code.

Consider the following circuit

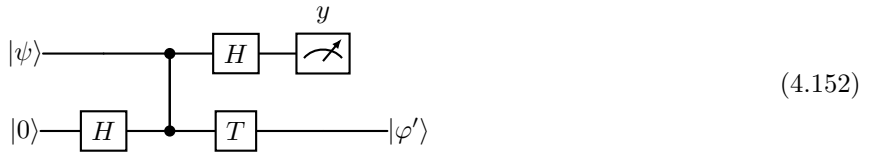


where one obtains that the state  $|\varphi\rangle$  is given by

$$|\varphi\rangle = \hat{X}^y \hat{H} |\psi\rangle, \quad (4.151)$$

with  $y = 0, 1$ . Notably, the three operations performed here, the two Hadamards and the control-Z gates, are all fault-tolerant.

Suppose we slightly modify the circuit by adding a T-gate on the second qubit as follows



where the representation of the T-gate on the computational basis reads

$$T = \begin{pmatrix} 1 & 0 \\ 0 & e^{-i\frac{\pi}{4}} \end{pmatrix} \quad (4.153)$$

and the final state of the second qubit now is

$$|\varphi'\rangle = \hat{T} \hat{X}^y \hat{H} |\psi\rangle. \quad (4.154)$$

Since, a part from a total phase, the T-gate can be written as

$$\hat{T} = e^{i\frac{\pi}{8}\hat{Z}}, \quad (4.155)$$

one obtains

$$|\varphi'\rangle = \hat{X}^y \hat{T}^{(1-2y)} \hat{H} |\psi\rangle. \quad (4.156)$$

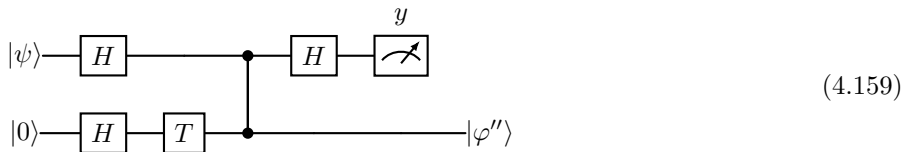
But,  $\hat{T}^{(1-2y)}$  can be expressed as

$$\hat{T}^{(1-2y)} = \hat{T} e^{-i\frac{\pi y}{4}\hat{Z}} = e^{-i\frac{\pi y}{4}} \hat{S}^y \hat{T}, \quad (4.157)$$

where we can safely omit the phase in the last expression. Thus, we get

$$|\varphi'\rangle = \hat{X}^y \hat{S}^y \hat{T} \hat{H} |\psi\rangle = (\hat{X} \hat{S})^y \hat{T} \hat{H} |\psi\rangle. \quad (4.158)$$

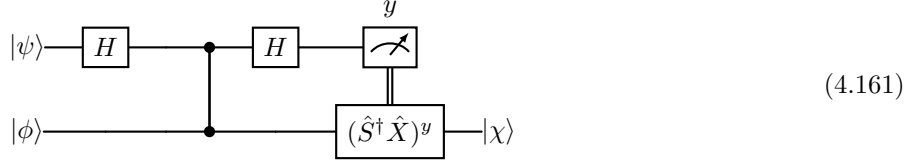
Here, the last equality holds since the value of  $y$  can be only 0 or 1. Moreover, we also find that the T-gate commutes with the control-Z, since it commutes with  $\hat{Z}$ . Thus, by adding an extra Hadamard gate on the first qubit, we obtain



where

$$|\varphi''\rangle = (\hat{X}\hat{S})^y \hat{T} |\psi\rangle. \quad (4.160)$$

Specifically, the latter implies the following one



where

$$\begin{aligned} |\chi\rangle &= \hat{T} |\psi\rangle, \\ |\phi\rangle &= \hat{T} \hat{H} |0\rangle. \end{aligned} \quad (4.162)$$

This means that, if one is able to prepare the second qubit in the state  $|\phi\rangle$ , then they also can apply the T-gate to an arbitrary state  $|\psi\rangle$  that was initially embedded in the first qubit. This is an effective application of the T-gate. Clearly, it requires the preparation of  $|\phi\rangle$ . Specifically, this is given by

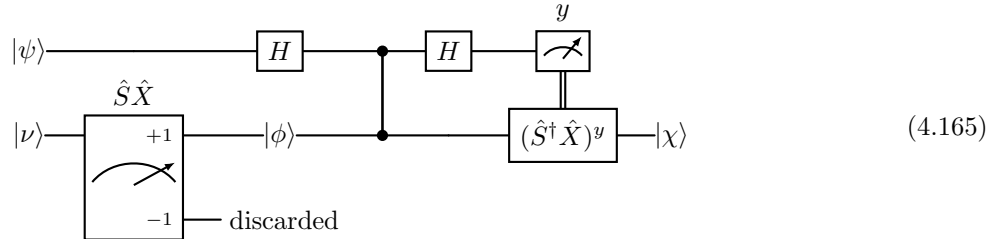
$$|\phi\rangle = \hat{T} \hat{H} |0\rangle = e^{-i\frac{\pi}{8}\hat{Z}} |+\rangle. \quad (4.163)$$

Now, the state  $|+\rangle$  is eigenstate of  $\hat{X}$  with eigenvalue  $(+1)$ , and in the same way  $|\phi\rangle$  is eigenstate of the operator

$$e^{-i\frac{\pi}{8}\hat{Z}} \hat{X} e^{i\frac{\pi}{8}\hat{Z}} = e^{-i\frac{\pi}{4}\hat{Z}} \hat{X} = \hat{S} \hat{X}, \quad (4.164)$$

with the eigenvalue  $(+1)$ . Here, the last two equalities follow from the commutation of  $\hat{T}$  and  $\hat{X}$  and the definition of the S-gate. Thus,  $|\phi\rangle$  is eigenstate of  $\hat{S} \hat{X}$  with eigenvalue  $(+1)$ . Similarly, the orthogonal state  $|\phi_{\perp}\rangle$  is associated to the eigenvalue  $(-1)$ . Now, this implies that given an arbitrary state  $|\nu\rangle$  by measuring the operator  $\hat{S} \hat{X}$ , the state will collapse in  $|\phi\rangle$  or  $|\phi_{\perp}\rangle$  with corresponding outcomes respectively given by  $(+1)$  and  $(-1)$ .

The complete circuit thus becomes



and effectively applies the T-gate to an arbitrary state  $|\psi\rangle$ . If the measurement is also FT (this can be proven, but it will not be tackled here), then one has that the entire circuit is FT.

# Chapter 5

## Dynamical Decoupling and Quantum Error Mitigation

The greatest problem in the development of quantum computers are the presence of errors and noises. QEC works in theory: the threshold theorem guarantees it. However, it requires a number of physical qubits ( $\sim 10^3$  to  $\sim 10^6$ ) that is often beyond what possible with the current technology. In this chapter, we introduce two possible routes to tackle the problem. These are the Dynamical Decoupling and the Quantum Error Mitigation.

### 5.1 Dynamical Decoupling

The dynamical decoupling (DD) approach leverage on averaging out the unwanted effects of the surrounding environment by applying a control on the system.

To introduce the idea, we focus on the specific model of a qubit coupled to a thermal bath of harmonic oscillators, with  $\hat{b}_k$  being the annihilation operator of the  $k$  oscillator. The total Hamiltonian reads

$$\hat{H}_0 = \hat{H}_S + \hat{H}_B + \hat{H}_{SB} = \frac{1}{2}\hbar\omega_0\hat{\sigma}_z + \sum_k \hbar\omega_k \hat{b}_k^\dagger \hat{b}_k + \sum_k \hbar\hat{\sigma}_z(g_k \hat{b}_k^\dagger + g_k^* \hat{b}_k), \quad (5.1)$$

where the first and second contributions are the free Hamiltonian of the qubit system and thermal bath respectively, while the last term describes their interaction being weighted by the constants  $g_k$ . Eventually, one focuses on the dynamics of the qubit alone. Thus, the state of interest is the reduced density matrix, which is obtained via

$$\hat{\rho}_S(t) = \text{Tr}^{(B)} \left[ e^{-i\hat{H}_0 t/\hbar} \hat{\rho}_T(0) e^{i\hat{H}_0 t/\hbar} \right], \quad (5.2)$$

where  $\hat{\rho}_T(0)$  is the total state at time  $t = 0$ . The latter can be decomposed on the computational basis  $\{ |0\rangle, |1\rangle \}$  as

$$\hat{\rho}_S(t) = \sum_{i,j=0,1} \rho_{ij}(t) |i\rangle \langle j|. \quad (5.3)$$

Now, given the total Hamiltonian  $\hat{H}_0$ , one finds that the populations  $\rho_{ii}$  are conserved. Indeed,  $[\hat{\sigma}_z, \hat{H}_0] = 0$  and thus the model describes a purely decohering mechanism, where no energy exchange between the system and the bath is present. Specifically, one can focus on the dynamics of the coherences  $\rho_{01}(t)$  alone, and we do it in the interaction picture. Thus, we have that the total state is given by

$$\hat{\rho}_T^{(I)}(t) = e^{i(\hat{H}_S + \hat{H}_B)t/\hbar} \hat{\rho}_T(0) e^{-i(\hat{H}_S + \hat{H}_B)t/\hbar}, \quad (5.4)$$

with the effective Hamiltonian reading

$$\hat{H}_0^{(I)}(t) = \hbar\hat{\sigma}_z \sum_k \left( g_k \hat{b}_k^\dagger e^{i\omega_k t} + g_k^* \hat{b}_k e^{-i\omega_k t} \right). \quad (5.5)$$

Correspondingly, the unitary operator determining the time evolution in the interaction picture from time  $t_0$  to  $t$  is

$$\hat{U}^{(I)}(t_0, t) = T \exp \left\{ -\frac{i}{\hbar} \int_{t_0}^t ds \hat{H}_0^{(I)}(s) \right\}, \quad (5.6)$$

where  $T$  indicates the time-ordering operator. The corresponding Dyson expansion, which is effectively a Taylor expansion accounting also for the time-ordering, reads

$$\hat{U}^{(I)}(t_0, t) = \hat{1} - \frac{i}{\hbar} \int_{t_0}^t dt_1 \hat{H}_0^{(I)}(t_1) - \frac{1}{\hbar^2} \int_{t_0}^t dt_2 \int_{t_0}^{t_2} dt_1 \hat{H}_0^{(I)}(t_2) \hat{H}_0^{(I)}(t_1) + \dots \quad (5.7)$$

Let us focus on the second order term, which can be rewritten in term of the integral from  $t_0$  to  $t$  for both variables as

$$\int_{t_0}^t dt_2 \int_{t_0}^{t_2} dt_1 \hat{H}_0^{(I)}(t_2) \hat{H}_0^{(I)}(t_1) = \int_{t_0}^t dt_2 \int_{t_0}^t dt_1 \hat{H}_0^{(I)}(t_2) \hat{H}_0^{(I)}(t_1) - \int_{t_0}^t dt_2 \int_{t_2}^t dt_1 \hat{H}_0^{(I)}(t_2) \hat{H}_0^{(I)}(t_1). \quad (5.8)$$

The last term corresponds to the integral over the area highlighted by the blue lines in Fig. 5.1: for each value of  $t_2 \in [t_0, t]$ , the  $t_1$  integral runs from  $t_2$  to  $t$ . Equivalently, this area can be described by the red lines: for each value of  $t_1 \in [t_0, t]$ , one performs the  $t_2$  integral from  $t_0$  to  $t_1$ .

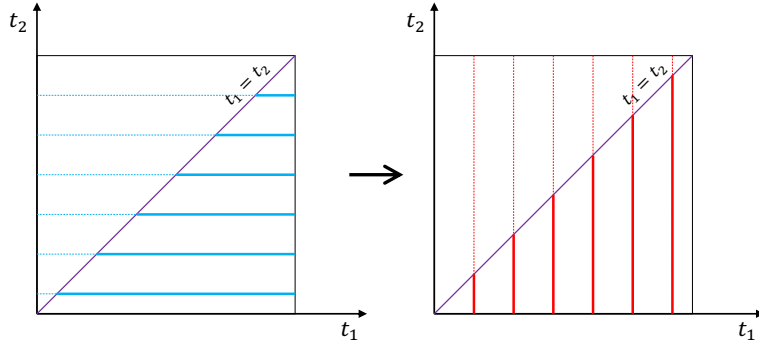


Fig. 5.1: Representation of different but equivalent ways of performing the integral in Eq. (5.9).

Mathematically, this implies that the following equality holds

$$\int_{t_0}^t dt_2 \int_{t_2}^t dt_1 \hat{H}_0^{(I)}(t_2) \hat{H}_0^{(I)}(t_1) = \int_{t_0}^t dt_1 \int_{t_0}^{t_1} dt_2 \hat{H}_0^{(I)}(t_2) \hat{H}_0^{(I)}(t_1). \quad (5.9)$$

Moreover, we can recast the right-hand-side of the latter equation as

$$\begin{aligned} \int_{t_0}^t dt_1 \int_{t_0}^{t_1} dt_2 \hat{H}_0^{(I)}(t_2) \hat{H}_0^{(I)}(t_1) &= \int_{t_0}^t dt_1 \int_{t_0}^{t_1} dt_2 [\hat{H}_0^{(I)}(t_2), \hat{H}_0^{(I)}(t_1)] + \int_{t_0}^t dt_1 \int_{t_0}^{t_1} dt_2 \hat{H}_0^{(I)}(t_1) \hat{H}_0^{(I)}(t_2), \\ &= \int_{t_0}^t dt_1 \int_{t_0}^{t_1} dt_2 [\hat{H}_0^{(I)}(t_2), \hat{H}_0^{(I)}(t_1)] + \int_{t_0}^t dt_2 \int_{t_0}^{t_2} dt_1 \hat{H}_0^{(I)}(t_2) \hat{H}_0^{(I)}(t_1), \end{aligned} \quad (5.10)$$

where we swapped the variables  $t_1 \leftrightarrow t_2$  in the second term. Namely, such second term is identical to that in the left-hand-side of Eq. (5.8). Here, the non-equal time Hamiltonians do not commute, but give

$$\begin{aligned} \left[ \hat{H}_0^{(I)}(t_2), \hat{H}_0^{(I)}(t_1) \right] &= \hbar^2 \hat{\sigma}_z^2 \sum_{kk'} \left( g_k g_{k'}^* e^{i\omega_k t_2 - i\omega_{k'} t_1} [\hat{b}_k^\dagger, \hat{b}_{k'}] + g_k^* g_{k'} e^{-i\omega_k t_2 + i\omega_{k'} t_1} [\hat{b}_k, \hat{b}_{k'}^\dagger] \right), \\ &= -2i\hbar^2 \sum_k |g_k|^2 \sin[\omega_k(t_2 - t_1)], \end{aligned} \quad (5.11)$$

which is an imaginary number. Now, by merging the last four equations, we find

$$\begin{aligned} \int_{t_0}^t dt_2 \int_{t_0}^{t_2} dt_1 \hat{H}_0^{(I)}(t_2) \hat{H}_0^{(I)}(t_1) &= \frac{1}{2} \int_{t_0}^t dt_2 \int_{t_0}^t dt_1 \hat{H}_0^{(I)}(t_2) \hat{H}_0^{(I)}(t_1) - \frac{1}{2} \int_{t_0}^t dt_1 \int_{t_0}^{t_1} dt_2 \left[ \hat{H}_0^{(I)}(t_2), \hat{H}_0^{(I)}(t_1) \right], \\ &= \frac{1}{2} \left( \int_{t_0}^t dt_1 \hat{H}_0^{(I)}(t_1) \right)^2 + i\hbar^2 \int_{t_0}^t dt_1 \int_{t_0}^{t_1} dt_2 \sum_k |g_k|^2 \sin[\omega_k(t_2 - t_1)]. \end{aligned} \quad (5.12)$$

This allows to recast the Dyson expansion as

$$\hat{U}^{(I)}(t_0, t) = \hat{\mathbb{1}} - \frac{i}{\hbar} \int_{t_0}^t dt_1 \hat{H}_0^{(I)}(t_1) + \frac{1}{2} \left( -\frac{i}{\hbar} \int_{t_0}^t dt_1 \hat{H}_0^{(I)}(t_1) \right)^2 - i\phi(t_0, t) + \dots, \quad (5.13)$$

where

$$\phi(t_0, t) = \frac{1}{2} \int_{t_0}^t dt_1 \int_{t_0}^{t_1} dt_2 \sum_k |g_k|^2 \sin[\omega_k(t_2 - t_1)]. \quad (5.14)$$

By summing all the terms, one gets

$$\hat{U}^{(I)}(t_0, t) = e^{-i\varphi(t_0, t)} \exp \left\{ -\frac{i}{\hbar} \int_{t_0}^t ds \hat{H}_0^{(I)}(s) \right\}, \quad (5.15)$$

where one has an extra global phase, which is however unimportant since

$$\hat{U}^{(I)}(t_0, t) \hat{\rho} \left[ \hat{U}^{(I)}(t_0, t) \right]^\dagger = \exp \left\{ -\frac{i}{\hbar} \int_{t_0}^t ds \hat{H}_0^{(I)}(s) \right\} \hat{\rho} \exp \left\{ \frac{i}{\hbar} \int_{t_0}^t ds \hat{H}_0^{(I)}(s) \right\}, \quad (5.16)$$

and there is not time-ordering operator.

Specifically, one can perform explicitly the time integral in the exponential of  $\hat{U}^{(I)}(t_0, t)$ , which reads

$$-\frac{i}{\hbar} \int_{t_0}^t ds \hat{H}_0^{(I)}(s) = \frac{1}{2} \hat{\sigma}_z \sum_k \left( \hat{b}_k^\dagger e^{i\omega_k t_0} \xi_k(t - t_0) - \hat{b}_k e^{-i\omega_k t_0} \xi_k^*(t - t_0) \right), \quad (5.17)$$

where

$$\xi_k(t - t_0) = \frac{2g_k}{\omega_k} (1 - e^{i\omega_k(t - t_0)}). \quad (5.18)$$

Now, the quantity of interest is the coherence, which in the interaction picture is given by

$$\rho_{01}^{(I)}(t) = \langle 0 | \hat{\rho}_S^{(I)}(t) | 1 \rangle = \langle 0 | \text{Tr}^{(B)} \left[ \hat{U}^{(I)}(t_0, t) \hat{\rho}_T(t_0) \left( \hat{U}^{(I)}(t_0, t) \right)^\dagger \right] | 1 \rangle, \quad (5.19)$$

and it can be computed analytically under the following assumptions:

1) The total initial state is separable, namely

$$\hat{\rho}_T(t_0) = \hat{\rho}_S(t_0) \otimes \hat{\rho}_B(t_0); \quad (5.20)$$

2) The initial state of the bath is a thermal state of the form

$$\hat{\rho}_B(t_0) = \prod_k (1 - e^{-\beta \hbar \omega_k}) \exp \left( -\beta \hbar \omega_k \hat{b}_k^\dagger \hat{b}_k \right), \quad (5.21)$$

with  $\beta = (k_B T)^{-1}$  being the inverse temperature.

By going back to the Schrödinger picture, Eq. (5.19) reads

$$\begin{aligned} \rho_{01}(t) &= e^{-i\omega_0(t-t_0)} \rho_{01}^{(I)}(t), \\ &= e^{-i\omega_0(t-t_0)} \langle 0 | \text{Tr}^{(B)} \left[ \exp \left[ \frac{1}{2} \hat{\sigma}_z \sum_k \left( \hat{b}_k^\dagger e^{i\omega_k t_0} \xi_k(t-t_0) - \hat{b}_k e^{-i\omega_k t_0} \xi_k^*(t-t_0) \right) \right] \hat{\rho}_T(t_0) \right. \\ &\quad \times \left. \exp \left[ -\frac{1}{2} \hat{\sigma}_z \sum_k \left( \hat{b}_k^\dagger e^{i\omega_k t_0} \xi_k(t-t_0) - \hat{b}_k e^{-i\omega_k t_0} \xi_k^*(t-t_0) \right) \right] \right] |1\rangle. \end{aligned} \quad (5.22)$$

By applying with  $\hat{\sigma}_z$  on the  $\langle 0 |$  and  $|1\rangle$  states, we get

$$\rho_{01}(t) = e^{-i\omega_0(t-t_0)} \text{Tr}^{(B)} \left[ \exp \left[ \sum_k \left( c_k \hat{b}_k^\dagger - c_k^* \hat{b}_k \right) \right] \hat{\rho}_B(t_0) \right] \rho_{01}(t_0), \quad (5.23)$$

where we exploited the cyclicity of the partial trace with respect to the bath operators, the assumption of separability of the initial state, the definition of the initial coherence  $\rho_{01}(t_0) = \langle 0 | \hat{\rho}_S(t_0) | 1 \rangle$ , and defined

$$c_k = c_k(t_0, t) = e^{i\omega_k t_0} \xi_k(t-t_0). \quad (5.24)$$

In Eq. (5.23), one can recognise the displacement operator. Namely, the latter equation can be recasted as

$$\rho_{01}(t) = e^{-i\omega_0(t-t_0)} \text{Tr}^{(B)} \left[ \prod_k \hat{D}_k(c_k) \hat{\rho}_B(t_0) \right] \rho_{01}(t_0), \quad (5.25)$$

where

$$\hat{D}(\beta) = \exp(\beta \hat{b}_k^\dagger - \beta^* \hat{b}) \quad (5.26)$$

is the displacement operator.

**Recall 5.1 (Coherent states)**

Given the ground state  $|0\rangle$ , one can construct a coherent state via the application of a displacement operator to  $|0\rangle$ . Namely,

$$\hat{D}(\beta) |0\rangle = |\beta\rangle, \quad (5.27)$$

where  $\beta \in \mathbb{C}$ . The coherent states form an overcomplete basis of the Hilbert space  $\mathbb{H}$ , for which one has

$$\hat{\mathbb{1}} = \int \frac{d^2 z}{\pi} |z\rangle \langle z|, \quad (5.28)$$

where  $d^2 z = d(\Re z) d(\Im z)$ . The combination of two displacement operators is governed by

$$\hat{D}(\alpha) \hat{D}(\beta) = e^{\frac{1}{2}(\alpha\beta^* - \beta\alpha^*)} \hat{D}(\alpha + \beta). \quad (5.29)$$

Finally, one can express the coherent states in terms of the Fock basis  $\{|n\rangle\}$ , where

$$\langle n | z \rangle = \frac{z^n}{\sqrt{n!}} e^{-|z|^2/2}, \quad (5.30)$$

determines the weights between the two basis.

Let us then consider the partial trace over the  $k$ -th mode of the displacement operator and the thermal state, which explicitly reads

$$\begin{aligned} \text{Tr}^{(\text{B})} \left[ \hat{D}_k(c_k) \hat{\rho}_{\text{B}_k}(t_0) \right] &= (1 - e^{-\beta \hbar \omega_k}) \text{Tr}^{(\text{B})} \left[ \hat{D}_k(c_k) e^{-\beta \hbar \omega_k \hat{b}_k^\dagger \hat{b}_k} \right], \\ &= (1 - e^{-\beta \hbar \omega_k}) \int \frac{d^2 z}{\pi} \langle z | e^{-\beta \hbar \omega_k \hat{b}_k^\dagger \hat{b}_k} \hat{D}_k(c_k) | z \rangle, \end{aligned} \quad (5.31)$$

where we exploited the coherent basis to compute the partial trace and exploit its cyclicity. By applying the composition of displacement operators (namely, Eq. (5.29) merged with Eq. (5.27)), and introducing an identity in the Fock basis, i.e.  $\hat{1} = \sum_{n=0}^{+\infty} |n\rangle \langle n|$ , we get

$$\begin{aligned} \text{Tr}^{(\text{B})} \left[ \hat{D}_k(c_k) \hat{\rho}_{\text{B}_k}(t_0) \right] &= (1 - e^{-\beta \hbar \omega_k}) \int \frac{d^2 z}{\pi} \sum_n \langle z | n \rangle e^{-\beta \hbar \omega_k n} e^{\frac{1}{2}(c_k z^* - z c_k^*)} \langle n | z + c_k \rangle, \\ &= (1 - e^{-\beta \hbar \omega_k}) \int \frac{d^2 z}{\pi} \sum_n e^{-\beta \hbar \omega_k n} e^{\frac{1}{2}(c_k z^* - z c_k^*)} \frac{(z^*)^n}{\sqrt{n!}} e^{-|z|^2/2} \frac{(z + c_k)^n}{\sqrt{n!}} e^{-|z+c_k|^2/2}, \end{aligned} \quad (5.32)$$

where we applied Eq. (5.30). By putting together the exponentials, we obtain

$$\text{Tr}^{(\text{B})} \left[ \hat{D}_k(c_k) \hat{\rho}_{\text{B}_k}(t_0) \right] = (1 - e^{-\beta \hbar \omega_k}) \int \frac{d^2 z}{\pi} e^{-|z|^2} e^{-|c_k|^2/2} e^{-zc_k^*} S(z, c_k) \quad (5.33)$$

where

$$\begin{aligned} S(z, c_k) &= \sum_n e^{-\beta \hbar \omega_k n} \frac{(z^*)^n}{\sqrt{n!}} \frac{(z + c_k)^n}{\sqrt{n!}}, \\ &= \sum_n \frac{1}{n!} [e^{-\beta \hbar \omega_k (|z|^2 + c_k z^*)}]^n, \\ &= \exp [e^{-\beta \hbar \omega_k (|z|^2 + c_k z^*)}]. \end{aligned} \quad (5.34)$$

Thus,

$$\text{Tr}^{(\text{B})} \left[ \hat{D}_k(c_k) \hat{\rho}_{\text{B}_k}(t_0) \right] = (1 - e^{-\beta \hbar \omega_k}) \int \frac{d^2 z}{\pi} e^{-|z|^2 \alpha_k} e^{-|c_k|^2/2} e^{-zc_k^*} \exp[c_k z^* e^{-\beta \hbar \omega_k}], \quad (5.35)$$

where

$$\alpha_k = 1 - e^{-\beta \hbar \omega_k}, \quad (5.36)$$

is a positive quantity. Then, the Gaussian integral in Eq. (5.35) can be safely implemented and gives

$$\begin{aligned} \text{Tr}^{(\text{B})} \left[ \hat{D}_k(c_k) \hat{\rho}_{\text{B}_k}(t_0) \right] &= (1 - e^{-\beta \hbar \omega_k}) \frac{1}{\alpha_k} \exp \left[ -\frac{|c_k|^2}{\alpha_k} e^{-\beta \hbar \omega_k} \right] e^{-|c_k|^2/2}, \\ &= \exp \left[ -|c_k|^2 \left( \frac{1}{2} + \frac{e^{-\beta \hbar \omega_k}}{(1 - e^{-\beta \hbar \omega_k})} \right) \right], \\ &= \exp \left[ -\frac{|c_k|^2}{2} \coth \left( \frac{\beta \hbar \omega_k}{2} \right) \right]. \end{aligned} \quad (5.37)$$

Finally, by merging together the latter equation with Eq. (5.25), we obtain

$$\rho_{01}(t) = e^{-i\omega_0(t-t_0)} e^{-\Gamma(t_0,t)} \rho_{01}(t_0), \quad (5.38)$$

where we defined

$$\begin{aligned}
\Gamma(t_0, t) &= \sum_k \frac{|c_k|^2}{2} \coth\left(\frac{\beta\hbar\omega_k}{2}\right), \\
&= \sum_k \frac{|e^{i\omega_k t_0} \xi_k(t - t_0)|^2}{2} \coth\left(\frac{\beta\hbar\omega_k}{2}\right), \\
&= \sum_k \frac{|\frac{2g_k}{\omega_k}(1 - e^{i\omega_k(t-t_0)})|^2}{2} \coth\left(\frac{\beta\hbar\omega_k}{2}\right), \\
&= \sum_k \frac{4|g_k|^2}{\omega_k^2} (1 - \cos[\omega_k(t - t_0)]) \coth\left(\frac{\beta\hbar\omega_k}{2}\right)
\end{aligned} \tag{5.39}$$

where we simply substituted the definitions of  $c_k$  and  $\xi_k(t - t_0)$ . Now, by introducing the spectral density  $I(\omega)$  as

$$I(\omega) = \sum_k \delta(\omega - \omega_k) |g_k|^2, \tag{5.40}$$

which determines the strength of the coupling between the system and each bath's modes, we can rewrite  $\Gamma(t_0, t)$  as

$$\begin{aligned}
\Gamma(t_0, t) &= 4 \int_0^{+\infty} d\omega I(\omega) \coth\left(\frac{\beta\hbar\omega}{2}\right) \frac{(1 - \cos[\omega(t - t_0)])}{\omega^2}, \\
&= 4 \int_0^{+\infty} d\omega I(\omega) (2\bar{n}(\omega, T) + 1) \frac{(1 - \cos[\omega(t - t_0)])}{\omega^2},
\end{aligned} \tag{5.41}$$

where  $\bar{n}(\omega, T)$  is the mean number of excitations of the mode  $\omega$  at the temperature  $T = (k_B\beta)^{-1}$ . Notably,  $\Gamma(t_0, t)$  is positive. This can be seen explicitly from the first line of Eq. (5.39). This means, that — as expected — the interaction with the environment reduces the coherences [cf. Eq. (5.38)].

Suppose now that we want to perturb the system so the induce a spin-flip transition. Physically, since the interaction Hamiltonian  $\hat{H}_{\text{SB}}$  is proportional to  $\hat{\sigma}_z$ , then opposite contributions arise when the system is in  $|0\rangle$  and  $|1\rangle$ . Thus, by making the system change fast between  $|0\rangle$  and  $|1\rangle$ , one can average out the contributions from  $\hat{H}_{\text{SB}}$ , effectively decoupling the system from the environment.

Specifically, we will consider a modified Hamiltonian reading

$$\hat{H}_0 \rightarrow \hat{H}(t) = \hat{H}_0 + \hat{H}_{\text{P}}(t), \tag{5.42}$$

where the Hamiltonian perturbation  $\hat{H}_{\text{P}}(t)$  can be implemented via a monocromatic alternating magnetic field applied at the resonance. Its explicit form we consider is

$$\begin{aligned}
\hat{H}_{\text{P}}(t) &= \sum_{n=1}^{n_{\text{P}}} V^{(n)}(t) \left\{ \hat{\sigma}_x \cos[\omega_0(t - t_{\text{P}}^{(n)})] + \hat{\sigma}_y \sin[\omega_0(t - t_{\text{P}}^{(n)})] \right\}, \\
&= \sum_{n=1}^{n_{\text{P}}} V^{(n)}(t) \left( \hat{\sigma}_+ e^{i\omega_0(t - t_{\text{P}}^{(n)})} + \hat{\sigma}_- e^{-i\omega_0(t - t_{\text{P}}^{(n)})} \right),
\end{aligned} \tag{5.43}$$

with  $n_{\text{P}}$  being the number of pulses,  $t_{\text{P}}^{(n)}$  is the time at which the pulse is switched on every  $\Delta t$ , namely

$$t_{\text{P}}^{(n)} = t_0 + n\Delta t, \quad \text{with } n \in \{1, \dots, n_{\text{P}}\}. \tag{5.44}$$

Finally, the switch of the impulse is determined by  $V^{(n)}(t)$ , which is defined as

$$V^{(n)}(t) = \begin{cases} V, & \text{for } t \in [t_{\text{P}}^{(n)}, t_{\text{P}}^{(n)} + \tau_{\text{P}}], \\ 0, & \text{otherwise,} \end{cases} \tag{5.45}$$

where  $\tau_P$  is the duration time of the pulses.

The exact dynamics with respect to the modified Hamiltonian  $\hat{H}(t)$  cannot be solved. However, we can assume that during the pulses the contribution of  $\hat{H}_{\text{SB}}$  is negligible and we completely neglect it. Then, the dynamics becomes piecewise, alternating  $\hat{H}_{\text{SB}}$  to  $\hat{H}_P$ .

As for the unperturbed case, we tackle the problem in the interaction picture. Namely, the effective Hamiltonian becomes

$$\hat{H}^{(I)}(t) = \hat{H}_0^{(I)}(t) + \hat{H}_P^{(I)}(t), \quad (5.46)$$

where  $\hat{H}_0^{(I)}(t)$  is shown in (5.5) and

$$\begin{aligned} \hat{H}_P^{(I)}(t) &= \exp \left[ \frac{i}{\hbar} (\hat{H}_S + \hat{H}_B) \right] \hat{H}_P(t) \exp \left[ -\frac{i}{\hbar} (\hat{H}_S + \hat{H}_B) \right], \\ &= e^{i\omega_0 \hat{\sigma}_z t/2} \sum_{n=1}^{n_P} V^{(n)}(t) \left( \hat{\sigma}_+ e^{i\omega_0(t-t_P^{(n)})} + \hat{\sigma}_- e^{-i\omega_0(t-t_P^{(n)})} \right) e^{-i\omega_0 \hat{\sigma}_z t/2}. \end{aligned} \quad (5.47)$$

However, one has that

$$\begin{aligned} e^{i\omega_0 \hat{\sigma}_z t/2} \hat{\sigma}_- e^{-i\omega_0 \hat{\sigma}_z t/2} &= e^{i\omega_0 \hat{\sigma}_z t/2} |0\rangle \langle 1| e^{-i\omega_0 \hat{\sigma}_z t/2}, \\ &= e^{i\omega_0 t} |0\rangle \langle 1|, \\ &= e^{i\omega_0 t} \hat{\sigma}_-, \end{aligned} \quad (5.48)$$

and similarly

$$e^{i\omega_0 \hat{\sigma}_z t/2} \hat{\sigma}_+ e^{-i\omega_0 \hat{\sigma}_z t/2} = e^{-i\omega_0 t} \hat{\sigma}_+. \quad (5.49)$$

Then, we obtain

$$\begin{aligned} \hat{H}_P^{(I)}(t) &= \sum_{n=1}^{n_P} V^{(n)}(t) \left( \hat{\sigma}_+ e^{-i\omega_0 t_P^{(n)}} + \hat{\sigma}_- e^{i\omega_0 t_P^{(n)}} \right), \\ &= \sum_{n=1}^{n_P} V^{(n)}(t) e^{i\omega_0 \hat{\sigma}_z t_P^{(n)}/2} \hat{\sigma}_x e^{-i\omega_0 \hat{\sigma}_z t_P^{(n)}/2}, \end{aligned} \quad (5.50)$$

where we exploited that  $\hat{\sigma}_+ + \hat{\sigma}_- = \hat{\sigma}_x$ . Notably, the only time dependence is in  $V^{(n)}(t)$ , but it is only formal as one can see from Eq. (5.45). Then, when considering the corresponding unitary, we have

$$\begin{aligned} \hat{V}_n^{(I)}(\tau_P) &= \exp \left( -\frac{i}{\hbar} \int_{t_P^{(n)}}^{t_P^{(n)} + \tau_P} ds \hat{H}_P^{(I)}(s) \right), \\ &= \exp \left( -\frac{i}{\hbar} V e^{i\omega_0 \hat{\sigma}_z t_P^{(n)}/2} \hat{\sigma}_x e^{-i\omega_0 \hat{\sigma}_z t_P^{(n)}/2} \tau_P \right). \end{aligned} \quad (5.51)$$

By Taylor expanding

$$\begin{aligned} \hat{V}_n^{(I)}(\tau_P) &= \sum_k \frac{1}{k!} \left( -\frac{i}{\hbar} V e^{i\omega_0 \hat{\sigma}_z t_P^{(n)}/2} \hat{\sigma}_x e^{-i\omega_0 \hat{\sigma}_z t_P^{(n)}/2} \tau_P \right)^k, \\ &= e^{i\omega_0 \hat{\sigma}_z t_P^{(n)}/2} \sum_k \frac{1}{k!} \left( -\frac{i}{\hbar} V \hat{\sigma}_x \tau_P \right)^k e^{-i\omega_0 \hat{\sigma}_z t_P^{(n)}/2}, \\ &= e^{i\omega_0 \hat{\sigma}_z t_P^{(n)}/2} e^{-\frac{i}{\hbar} V \hat{\sigma}_x \tau_P} e^{-i\omega_0 \hat{\sigma}_z t_P^{(n)}/2}. \end{aligned} \quad (5.52)$$

We finally fix  $V$  and  $\tau_P$  so to have an actual bit-flip. This is provided by setting

$$\frac{V \tau_P}{\hbar} = \frac{\pi}{2}, \quad (5.53)$$

which gives

$$e^{-\frac{i}{\hbar}V\hat{\sigma}_x\tau_p} = e^{-i\frac{\pi}{2}\hat{\sigma}_x} = -i\hat{\sigma}_x. \quad (5.54)$$

Notably, we can consider the limit of the time pulses that go to zero, i.e.  $\tau_p \rightarrow 0$ , as long as  $V \rightarrow \infty$  and Eq. (5.53) holds. Since from here  $V$  does not appear explicitly, this will only simplify the calculations.

Then, we have that

$$\dot{\mathcal{V}}_n^{(1)}(\tau_p) = \dot{\mathcal{V}}_n^{(1)} = -ie^{i\omega_0\hat{\sigma}_z t_p^{(n)}/2} \hat{\sigma}_x e^{-i\omega_0\hat{\sigma}_z t_p^{(n)}/2}. \quad (5.55)$$

By considering that the following relation holds

$$e^{-i\omega_0\hat{\sigma}_z t/2} = \cos(\omega_0 t/2)\hat{1} - i \sin(\omega_0 t/2)\hat{\sigma}_z, \quad (5.56)$$

and the anticommutation relation  $\{\hat{\sigma}_x, \hat{\sigma}_z\} = 0$ , we have that

$$\hat{\sigma}_x e^{-i\omega_0\hat{\sigma}_z t/2} = e^{i\omega_0\hat{\sigma}_z t/2} \hat{\sigma}_x. \quad (5.57)$$

It follows that one can write the operator  $\dot{\mathcal{V}}_n^{(1)}$  in two equivalent ways:

$$\dot{\mathcal{V}}_n^{(1)} = -ie^{i\omega_0\hat{\sigma}_z t_p^{(n)}} \hat{\sigma}_x = -i\hat{\sigma}_x e^{-i\omega_0\hat{\sigma}_z t_p^{(n)}}. \quad (5.58)$$

Let us now consider the time evolution of the first entire cycle of spin-flips: this is from time  $t_0$  through time  $t_p^{(1)}$  when the spin flips the first time, to time  $t_p^{(2)}$  when the spin flips back to the original spin state. In particular, we define this latter time as  $t_1 = t_0 + 2\Delta t$ . The unitary dynamics from  $t_0$  to  $t_1$  is given by

$$\begin{aligned} \hat{U}_p^{(1)}(t_0, t_1) &= \hat{\mathcal{V}}_2^{(1)} \hat{U}^{(1)}(t_p^{(1)}, t_p^{(2)}) \hat{\mathcal{V}}_1^{(1)} \hat{U}^{(1)}(t_0, t_p^{(1)}), \\ &= \left[ \hat{\mathcal{V}}_2^{(1)} \hat{\mathcal{V}}_1^{(1)} \right] \left[ \left( \hat{\mathcal{V}}_1^{(1)} \right)^{-1} \hat{U}^{(1)}(t_p^{(1)}, t_p^{(2)}) \hat{\mathcal{V}}_1^{(1)} \right] \hat{U}^{(1)}(t_0, t_p^{(1)}), \end{aligned} \quad (5.59)$$

where

$$\hat{U}^{(1)}(t_\alpha, t_\beta) = \exp \left[ \frac{1}{2} \hat{\sigma}_z \sum_k \left( \hat{b}_k^\dagger e^{i\omega_k t_\alpha} \xi_k(t_\beta - t_\alpha) - \hat{b}_k e^{-i\omega_k t_\alpha} \xi_k^*(t_\beta - t_\alpha) \right) \right]. \quad (5.60)$$

The first square parenthesis in the last line of Eq. (5.59) is given by

$$\begin{aligned} \hat{\mathcal{V}}_2^{(1)} \hat{\mathcal{V}}_1^{(1)} &= \left( -ie^{i\omega_0\hat{\sigma}_z t_p^{(2)}} \hat{\sigma}_x \right) \left( -i\hat{\sigma}_x e^{-i\omega_0\hat{\sigma}_z t_p^{(1)}} \right), \\ &= -e^{i\omega_0\hat{\sigma}_z(t_p^{(2)} - t_p^{(1)})}. \end{aligned} \quad (5.61)$$

Similarly, the second square parenthesis in the last line of Eq. (5.59) can be rewritten as

$$\left( \hat{\mathcal{V}}_1^{(1)} \right)^{-1} \hat{U}^{(1)}(t_p^{(1)}, t_p^{(2)}) \hat{\mathcal{V}}_1^{(1)} = e^{i\omega_0\hat{\sigma}_z t_p^{(1)}} \hat{\sigma}_x \exp \left[ \frac{1}{2} \hat{\sigma}_z \hat{B}(t_p^{(1)}, t_p^{(2)}) \right] \hat{\sigma}_x e^{-i\omega_0\hat{\sigma}_z t_p^{(1)}} \quad (5.62)$$

where  $B(t_p^{(1)}, t_p^{(2)}) = \sum_k \left( \hat{b}_k^\dagger e^{i\omega_k t_p^{(1)}} \xi_k(\Delta t) - \hat{b}_k e^{-i\omega_k t_p^{(1)}} \xi_k^*(\Delta t) \right)$ . Here, we Taylor expand the central exponential, which gives

$$\exp \left[ \frac{1}{2} \hat{\sigma}_z \hat{B}(t_p^{(1)}, t_p^{(2)}) \right] = \sum_l \frac{1}{l!} \left( \frac{1}{2} \hat{\sigma}_z \hat{B}(t_p^{(1)}, t_p^{(2)}) \right)^l. \quad (5.63)$$

We divide the contributions to the sum in those with even and odd values of  $l$ . For even values, we have  $\hat{\sigma}_z^l = \hat{\sigma}_z^{2l}$ , where  $l = 2l'$ ; then  $\hat{\sigma}_z^l = \hat{1} = (-\hat{\sigma}_z)^l$ . For odd values of  $l$ , we have  $\hat{\sigma}_z^l = \hat{\sigma}_z^{2l'+1}$ , where  $l = 2l' + 1$ ; then  $\hat{\sigma}_z^l = \hat{\sigma}_z$ . But more specifically, we also have that  $\hat{\sigma}_x \hat{\sigma}_z^l \hat{\sigma}_x = \hat{\sigma}_x \hat{\sigma}_z \hat{\sigma}_x = -\hat{\sigma}_z = -\hat{\sigma}_z^l$ . Thus, it follows that

$$\left(\hat{\mathcal{V}}_1^{(1)}\right)^{-1} \hat{U}^{(1)}(t_{\text{P}}^{(1)}, t_{\text{P}}^{(2)}) \hat{\mathcal{V}}_1^{(1)} = \exp\left[-\frac{1}{2}\hat{\sigma}_z \hat{B}(t_{\text{P}}^{(1)}, t_{\text{P}}^{(2)})\right]. \quad (5.64)$$

Thus, we have that Eq. (5.59) reads

$$\hat{\mathcal{U}}_{\text{P}}^{(1)}(t_0, t_1) = -e^{i\omega_0 \hat{\sigma}_z(t_{\text{P}}^{(2)} - t_{\text{P}}^{(1)})} \exp\left[-\frac{1}{2}\hat{\sigma}_z \hat{B}(t_{\text{P}}^{(1)}, t_{\text{P}}^{(2)})\right] \exp\left[\frac{1}{2}\hat{\sigma}_z \hat{B}(t_0, t_{\text{P}}^{(1)})\right], \quad (5.65)$$

and can be recasted as

$$\hat{\mathcal{U}}_{\text{P}}^{(1)}(t_0, t_1) = \exp\left[i\omega_0 \hat{\sigma}_z(t_{\text{P}}^{(2)} - t_{\text{P}}^{(1)}) + \frac{1}{2}\hat{\sigma}_z \sum_k \left(\hat{b}_k^\dagger e^{i\omega_k t_0} \eta_k(\Delta t) - \hat{b}_k e^{-i\omega_k t_0} \eta_k^*(\Delta t)\right)\right], \quad (5.66)$$

where we neglected the overall unimportant phase and we defined

$$\eta_k(\Delta t) = \xi(\Delta t) (1 - e^{i\omega_k \Delta t}). \quad (5.67)$$

Now, the full evolution from time  $t_0$  to time  $t_N$  after  $N$  entire cycles of spin-flip is simply given by

$$\prod_{n=1}^N \hat{\mathcal{U}}_{\text{P}}^{(1)}(t_{n-1}, t_n) = \exp\left[i\omega_0 \hat{\sigma}_z(t_N - t_0) + \frac{1}{2}\hat{\sigma}_z \sum_k \left(\hat{b}_k^\dagger \sum_n e^{i\omega_k t_0} \eta_k(N, \Delta t) - \hat{b}_k \sum_n e^{-i\omega_k t_0} \eta_k^*(N, \Delta t)\right)\right], \quad (5.68)$$

where we introduced

$$\begin{aligned} \eta_k(N, \Delta t) &= e^{-i\omega_k t_0} \sum_n e^{i\omega_k t_{n-1}} \eta_k(\Delta t), \\ &= \eta_k(\Delta t) \sum_{n=1}^N e^{2i\omega_k \Delta t(n-1)}. \end{aligned} \quad (5.69)$$

Such an evolution is to be compared to that with no pulses on the same time period. This is given by Eq. (5.60) where one substitutes  $t_\alpha \rightarrow t_0$  and  $t_\beta \rightarrow t_N$ . Then, since  $t_N - t_0 = 2N\Delta t$ , we have

$$\hat{U}^{(1)}(t_0, t_N) = \exp\left[\frac{1}{2}\hat{\sigma}_z \sum_k \left(\hat{b}_k^\dagger e^{i\omega_k t_0} \xi_k(2N\Delta t) - \hat{b}_k e^{-i\omega_k t_0} \xi_k^*(2N\Delta t)\right)\right]. \quad (5.70)$$

Notably, the expressions in Eq. (5.68) and Eq. (5.70) have a similar structure, with the important difference being the factor  $\eta_k(N, \Delta t)$  substituted with  $\xi_k(2N\Delta t)$ . Thus, the decohering factor  $\Gamma(t_0, t_N)$  will take a suitably modified expression as that in Eq. (5.39), namely

$$\Gamma(t_0, t_N) = \sum_k \frac{|e^{i\omega_k t_0} \eta_k(N, \Delta t)|^2}{2} \coth\left(\frac{\beta\hbar\omega_k}{2}\right). \quad (5.71)$$

We now compare the difference between these two factors:

$$\eta_k(N, \Delta t) - \xi_k(2N\Delta t) = \eta_k(\Delta t) \sum_{n=1}^N e^{2i\omega_k \Delta t(n-1)} - \xi_k(2\Delta t) \sum_{n=1}^N e^{2i\omega_k \Delta t(n-1)}, \quad (5.72)$$

where we exploited the composition of the  $\xi_k$  terms. Then, by considering that

$$\begin{aligned}
\xi_k(\Delta t)(1 + e^{i\omega_k \Delta t}) &= \frac{2g_k}{\omega_k}(1 - e^{i\omega_k \Delta t})(1 + e^{i\omega_k \Delta t}), \\
&= \frac{2g_k}{\omega_k}(1 - e^{2i\omega_k \Delta t}), \\
&= \xi_k(2\Delta t),
\end{aligned} \tag{5.73}$$

and the definition of  $\eta_k(\Delta t)$  in Eq. (5.67), we obtain

$$\eta_k(N, \Delta t) - \xi_k(2N\Delta t) = -2\xi_k(\Delta t)e^{i\omega_k \Delta t} \sum_{n=1} e^{2i\omega_k \Delta t(n-1)}. \tag{5.74}$$

Equivalently, we have

$$\eta_k(N, \Delta t) = \xi_k(2N\Delta t)(1 - f_k(N, \Delta t)), \tag{5.75}$$

where

$$f_k(N, \Delta t) = 2 \frac{\xi_k(\Delta t)}{\xi_k(2N\Delta t)} e^{i\omega_k \Delta t} \sum_{n=1} e^{2i\omega_k \Delta t(n-1)}. \tag{5.76}$$

By exploiting the geometric series and the definition of  $\xi_k$ , we get

$$\begin{aligned}
f_k(N, \Delta t) &= 2 \frac{(1 - e^{i\omega_k \Delta t})}{(1 - e^{2i\omega_k N \Delta t})} e^{i\omega_k \Delta t} \frac{(1 - e^{2i\omega_k N \Delta t})}{(1 - e^{2i\omega_k \Delta t})}, \\
&= 2 \frac{(1 - e^{i\omega_k \Delta t})}{(1 - e^{2i\omega_k \Delta t})} e^{i\omega_k \Delta t}.
\end{aligned} \tag{5.77}$$

Finally, by taking the limit of dense pulses, i.e.  $\Delta t \rightarrow 0$ , we obtain

$$\lim_{\Delta t \rightarrow 0} f_k(N, \Delta t) = 1, \tag{5.78}$$

which means that under the same limit we have

$$\lim_{\Delta t \rightarrow 0} \eta_k(N, \Delta t) = 0. \tag{5.79}$$

As a consequence, the decoherence factor vanishes:  $\Gamma(t_0, t_N) \rightarrow 0$ . Namely, the decohering effect of the environment on the system is cancelled. Effectively, one has a (dynamical) decoupling of the system from its environment.

## 5.2 Quantum Error Mitigation

Quantum Error Mitigation (QEM) wants to translate the improvements of quantum hardware in those of quantum information and computation. Namely, it is an algorithmic scheme that reduces noise-induced bias in the expectation value of an observable of interest by post-processing outputs from an ensemble of circuit runs. To do this, it employs circuits at the same depth as the original unmitigated circuit or above. QEM applies post-processing directly from the hardware outputs. Thus, if the circuit size, being the product of the circuit depth times the number of qubits, becomes too large then QEM loses its usefulness.

A good QEM approach should employ a limited number of qubits, while still providing a guaranteed accuracy. This converts in a formal error bound, which indicates how well the QEM code works. Moreover, it should employ only a few (or better none) assumptions about the final state. For example, assuming that the final state is factorised is not a good assumption. Indeed, it would strongly limit the applicability of the corresponding QEM algorithm.

Before dwelling in two, among various, algorithms in the QEM context, we provide the general idea of the QEM approach. We defined the primary circuit as that process that would ideally produce the perfect output state  $\hat{\rho}_0$ . Due to the presence of noises, the primary circuit produces the noisy state  $\hat{\rho}$ . To account how a circuit works, we consider an observable of interests  $\hat{O}$  whose expectation value is the output information we seek. To compute this, we will run the circuit  $N_{\text{sample}}$  times, which is the number of circuit executions. Also in the noiseless case, a finite value of  $N_{\text{sample}}$  implies a finite inaccuracy of the estimated average. This is the so-called shot noise. However, in such a case, there will be no systematic shift, i.e. bias, in the expectation value of  $\hat{O}$  due to the noise. QEM aims to reduce such a bias. Often, this implies that the corresponding variace increases. Then, one needs to increase the number of circuit runs  $N > N_{\text{sample}}$  to compensate. The sampling overhead is the cost, in terms of number of repetitions, of the QEM method when compared to the noiseless circuit.

We underline that, conversely to QEC, in QEM there is no monitoring of the errors occurring during the run of the circuit.

### 5.2.1 Zero noise extrapolation

The Zero noise extrapolation (ZNE) method extracts the zero-noise expectations from a fitting of the circuit ran at different values of the noise. We define a time dependent Hamiltonian  $\hat{H}(t)$  that embeds action of the noiseless circuit. It can be written as

$$\hat{H}(t) = \sum_{\alpha} J_{\alpha}(t) \hat{P}_{\alpha}, \quad (5.80)$$

where  $J_{\alpha}(t)$  are some time dependent couplings that switch on and off the gates of the circuit, which are implemented by the corresponding  $N$ -qubit Pauli operators  $\hat{P}_{\alpha}$ . The full dynamics, including the action of the noise, is given by the following master equation

$$\frac{d\hat{\rho}_{\lambda}(t)}{dt} = -\frac{i}{\hbar} [\hat{H}(t), \hat{\rho}_{\lambda}(t)] + \lambda \mathcal{L}[\hat{\rho}_{\lambda}(t)], \quad (5.81)$$

where  $t \in [0, T]$ , with  $T$  being the time at which the circuit ends. We assume here that the noise coupling  $\lambda$  is small. Moreover, we assume that the noise dissipator  $\mathcal{L}$  is invariant under time rescaling and it is independent from  $\hat{J}_{\alpha}(t)$ .

Now, given the observable of interest  $\hat{A}$ , we compute the corresponding expectation value on the noisy circuit as  $E(\lambda) = \text{Tr} [\hat{A} \hat{\rho}_{\lambda}(T)]$ , where  $\hat{\rho}_{\lambda}(T)$  is the solution of Eq. (5.81). What we want to do is to estimate  $E(\lambda)$  for  $\lambda \rightarrow 0$ . Since one cannot reduce the value of  $\lambda$ , to construct a series of measurement from where extrapolate the estimate  $E(0)$ , we increase the value of  $\lambda$ . This can be done by considering the following rescaling. We dilate the time  $T$  at which the circuit is ran and, due to the time invariance of  $\mathcal{L}$ , this is equivalent to let the noise act more on the circuit. Then, one applies this idea with different values of  $\lambda$  and can perform a fit and deduce the value of  $E$  for  $\lambda \rightarrow 0$ . Practically, we perform the circuit  $N_{\text{cir}}$  times, at different values of the noise rate  $\lambda_j = c_j \lambda$ ,  $j = 0, \dots, N_{\text{cir}} - 1$  with  $c_0 = 1 < c_1 < \dots < c_{N_{\text{cir}}-1}$ . For each value of  $\lambda_j$ , we run the circuit with the following rescaled Hamiltonian

$$\hat{H}^{(j)}(t) = \sum_{\alpha} J_{\alpha}^{(j)}(t) \hat{P}_{\alpha}, \quad \text{where} \quad J_{\alpha}^{(j)}(t) = c_j^{-1} J_{\alpha}(c_j^{-1} t), \quad (5.82)$$

for a time  $T_j = c_j T$ . The rescaled dynamics gives

$$\frac{d\hat{\rho}_{\lambda}^{(j)}(t)}{dt} = -\frac{i}{\hbar} [\hat{H}^{(j)}(t), \hat{\rho}_{\lambda}^{(j)}(t)] + \lambda \mathcal{L}[\hat{\rho}_{\lambda}^{(j)}(t)]. \quad (5.83)$$

By merging the latter with Eq. (5.82), we obtain

$$\frac{d\hat{\rho}_\lambda^{(j)}(t)}{dt} = -\frac{i}{\hbar} \sum_{\alpha} c_j^{-1} J_\alpha(c_j^{-1} t) [\hat{P}_\alpha, \hat{\rho}_\lambda^{(j)}(t)] + \lambda \mathcal{L}[\hat{\rho}_\lambda^{(j)}(t)]. \quad (5.84)$$

By defining  $s = c_j^{-1}t$ , which runs in the interval  $s \in [0, T]$  since  $t \in [0, T_j]$ , we rewrite the above master equation as

$$\frac{d\hat{\rho}_\lambda^{(j)}(t)}{dt} = \frac{d\hat{\rho}_\lambda^{(j)}(c_j s)}{c_j ds} = -\frac{i}{\hbar} \sum_{\alpha} c_j^{-1} J_\alpha(s) [\hat{P}_\alpha, \hat{\rho}_\lambda^{(j)}(c_j s)] + \lambda \mathcal{L}[\hat{\rho}_\lambda^{(j)}(c_j s)]. \quad (5.85)$$

By multiplying the left and right hand side by  $c_j$  we obtain

$$\frac{d\hat{\rho}_\lambda^{(j)}(c_j s)}{ds} = -\frac{i}{\hbar} [\hat{H}(s), \hat{\rho}_\lambda^{(j)}(c_j s)] + c_j \lambda \mathcal{L}[\hat{\rho}_\lambda^{(j)}(c_j s)], \quad (5.86)$$

which is Eq. (5.81) with  $\lambda$  substituted with  $c_j \lambda$ . Its solution at time  $s = T$  is given by  $\hat{\rho}_{c_j \lambda}(T) = \hat{\rho}_\lambda^{(j)}(T_j)$ . Correspondingly, we compute the expectation value  $E(\lambda_j) = \text{Tr} [\hat{A} \hat{\rho}_\lambda^{(j)}(T_j)] = \text{Tr} [\hat{A} \hat{\rho}_{c_j \lambda}(T)]$ . Experimentally, for each  $c_j$ , one performs  $N_{\text{sample}}$  runs of the circuit and obtains an estimator  $\tilde{E}(\lambda_j)$ , which converges to the true value  $E(\lambda_j)$  only in the asymptotic limit  $N_{\text{sample}} \rightarrow \infty$ . Specifically, one has

$$\tilde{E}(\lambda_j) = E(\lambda_j) + \tilde{\delta}, \quad (5.87)$$

where  $\tilde{\delta}$  is a random variable with zero mean and variance  $\mathbb{E}[\tilde{\delta}^2] = \sigma_0^2/N_{\text{sample}}$ , with  $\sigma_0^2$  corresponding to the single-shot variance. Here,  $\mathbb{E}$  is to the mean over the sampling.

Now, the ZNE problem is to construct a good estimator  $\tilde{E}(0)$  for the expectation value  $E(\lambda = 0) = \text{Tr} [\hat{A} \hat{\rho}_0(T)]$  from the set of estimators  $\tilde{E}(\lambda_j)$ . Figure 5.2 represents the problem. To be a good estimator,

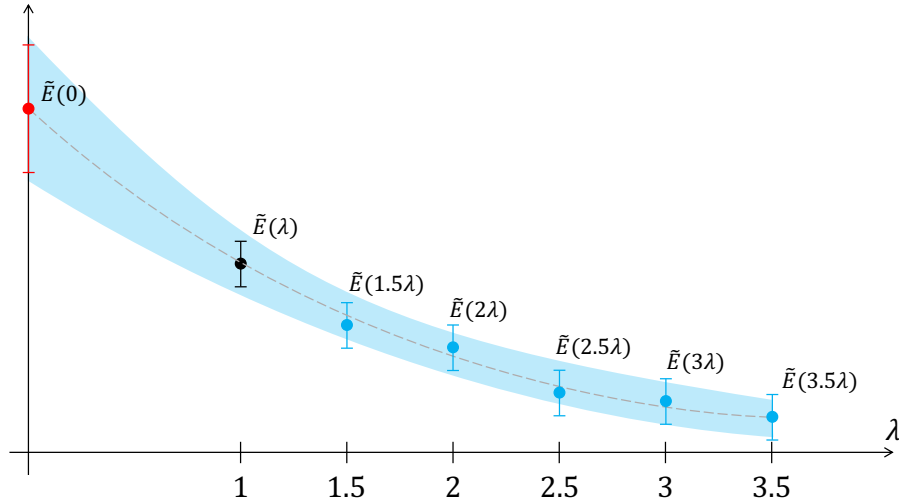


Fig. 5.2: Graphical representation of the Zero Error Extrapolation. Given the set of estimators  $\tilde{E}(\lambda)$  at different values of the noise (black and blue dots and error bars), one performs a fit assuming a specific model (gray dashed line) with corresponding confidence region (light blue region). In such a way, one extrapolates the value of  $\tilde{E}(0)$  with its corresponding error bar (red point and error bar).

we want that its bias

$$\text{Bias}(\tilde{E}(0)) = \mathbb{E}[\tilde{E}(0) - E(0)], \quad (5.88)$$

and its variance

$$\text{Var}(\tilde{E}(0)) = \mathbb{E}[\tilde{E}(0)^2] - \mathbb{E}[\tilde{E}(0)]^2, \quad (5.89)$$

are both small. We employ the mean squared error (MSE) as a figure of merit with respect to the true unknown parameter

$$\begin{aligned} \text{MSE}(\tilde{E}(0)) &= \mathbb{E}[(\tilde{E}(0) - E(0))^2], \\ &= \text{Var}(\tilde{E}(0)) + (\text{Bias}(\tilde{E}(0)))^2. \end{aligned} \quad (5.90)$$

If the expectation value  $E(\lambda)$  can be an arbitrary function of  $\lambda$  without any regularity assumption, then ZNE is impossible. However, from physical considerations, it is reasonable to have a model for it, for example we can assume a linear, a polynomial or an exponential dependence with respect to  $\lambda$ .

- 1 If we assume a linear dependence on  $\lambda$ , the corresponding linear model is given by

$$E_{\text{linear}}(\lambda) = a_0 + a_1 \lambda. \quad (5.91)$$

In such a case, a simple analytic solution exists, which is that of the ordinary least squared estimator of the intercept parameter. Namely, we have

$$\tilde{E}_{\text{linear}}(0) = \bar{E}(\lambda) - \frac{S_{\lambda E}}{S_{\lambda \lambda}} \bar{\lambda}, \quad (5.92)$$

where

$$\begin{aligned} \bar{\lambda} &= \frac{1}{N_{\text{cir}}} \sum_{j=0}^{N_{\text{cir}}-1} \lambda_j, \\ \bar{E}(\lambda) &= \frac{1}{N_{\text{cir}}} \sum_{j=0}^{N_{\text{cir}}-1} \tilde{E}(\lambda_j), \\ S_{\lambda E} &= \sum_{j=0}^{N_{\text{cir}}-1} (\lambda_j - \bar{\lambda})(\tilde{E}(\lambda_j) - \bar{E}(\lambda)), \\ S_{\lambda \lambda} &= \sum_{j=0}^{N_{\text{cir}}-1} (\lambda_j - \bar{\lambda})^2. \end{aligned} \quad (5.93)$$

With respect to the zero noise value  $E_{\text{linear}}(0)$ , the estimator  $\tilde{E}_{\text{linear}}(0)$  is unbiased. Its variance, under the assumption that the statistical uncertainty is the same for each  $\lambda_j$ , reads

$$\text{Var}(\tilde{E}_{\text{linear}}(0)) = \frac{\sigma_0^2}{N_{\text{sample}}} \left( \frac{1}{N_{\text{cir}}} + \frac{\bar{\lambda}^2}{S_{\lambda \lambda}} \right). \quad (5.94)$$

- 2 The Richardson's extrapolation is a special case of the polynomial extrapolation, which is limited at order  $N_{\text{cir}} - 1$ . The corresponding model is given by

$$E_{\text{Rich}}(\lambda) = a_0 + a_1 \lambda + \cdots + c_{N_{\text{cir}}-1} \lambda^{N_{\text{cir}}-1}. \quad (5.95)$$

This is the only case in which the fitted polynomial perfectly interpolates the  $N_{\text{cir}}$  data points such that, in the ideal limit of an infinite number of samples  $N_{\text{sample}} \rightarrow \infty$ , the error with respect to the true expectation value is by construction  $\mathcal{O}(N_{\text{cir}})$ . Using the Lagrange polynomial, the estimator can be expressed explicitly as

$$\tilde{E}_{\text{Rich}}(0) = \sum_{j=0}^{N_{\text{cir}}-1} \tilde{E}(\lambda_j) \gamma_j, \quad (5.96)$$

where

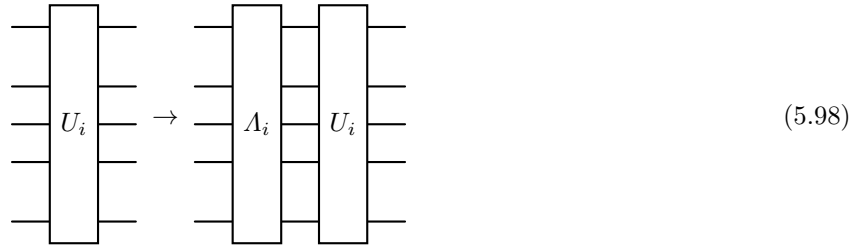
$$\gamma_j = \prod_{m \neq j} \frac{c_m}{c_j - c_m}. \quad (5.97)$$

The error of the estimator is  $\mathcal{O}(N_{\text{cir}})$  only in the asymptotic limit  $N_{\text{sample}} \rightarrow \infty$ . In other words,  $\mathcal{O}(N_{\text{cir}})$  corresponds to the bias term in Eq. (5.88). In a real scenario,  $N_{\text{sample}}$  is finite, and the variance term in Eq. (5.88) grows exponentially as we increase  $N_{\text{cir}}$ .

### 5.2.2 Probabilistic error cancellation

The Probabilistic error cancellation (PEC) method cancels the effects of the noise employing a map that acts as the inverse of the noise map under suitable average.

Suppose the ideal circuit is performed by a unitary CPTP map  $\mathcal{U}$  being the consecutive application of unitary gates:  $\hat{U}_{\text{circuit}} = \hat{U}_d \dots \hat{U}_1$ , where  $d$  is the depth of the circuit. One can represent the corresponding noisy circuit by substituting each unitary operation with its noisy counterpart, namely  $\hat{U}_i \hat{\rho} \hat{U}_i^\dagger \rightarrow \hat{U}_i \Lambda_i [\hat{\rho}] \hat{U}_i^\dagger$ , where  $\Lambda_i$  is a CPTP noisy map and  $\hat{\rho}$  is the  $N$ -qubit state. If we focus on a single gate  $\hat{U}_i$ , the two corresponding circuits are represented as

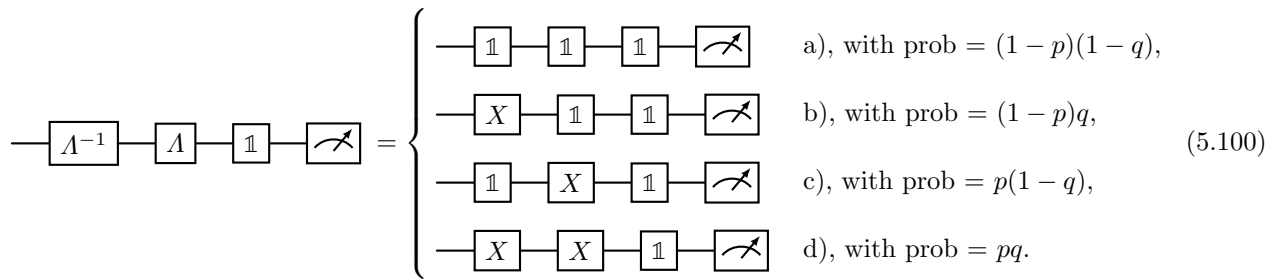


Now, the point is if we can invert the CPTP map  $\Lambda_i$  via the application of its inverse  $\Lambda_i^{-1}$ . In general, this is not possible. Indeed, typically,  $\Lambda_i^{-1}$  is not a CPTP map and thus such an inverse operation of the noise cannot be implemented. Nevertheless, such an operation can be implemented on average.

Consider the toy model of a single qubit, where the unitary noiseless operation is the identity:  $\hat{U} = \hat{1}$ , and the noise channel is the bit-flip with a probability  $p$ . Thus, the corresponding map is

$$\Lambda(\hat{\rho}) = (1 - p)\hat{1}\hat{\rho}\hat{1} + p\hat{\sigma}_x\hat{\rho}\hat{\sigma}_x. \quad (5.99)$$

This map corresponds to the unravelling with two components: with a probability  $p$  one applies an extra gate  $X$ , and with probability  $(1 - p)$  one does nothing, i.e. applies the gate  $\hat{1}$ . Notably, both these gates have an inverse. Indeed,  $\hat{1}^{-1} = \hat{1}$  and  $\hat{\sigma}_x^{-1} = \hat{\sigma}_x$ . Then, we construct the inverse noise map  $\Lambda^{-1}$  as having two components: with a probability  $q$  we apply an  $X$  gate, and with a probability  $(1 - q)$  we apply an  $\hat{1}$  gate. The corresponding total circuit can be then decomposed in the four components:



Now, we want to fix  $q$  such that, under the ensemble average, the circuit b) occurs with a probability being the opposite value of that of circuit c) occurring, and that the sum of the probabilities of having the circuit a) and d) gives 1. This implies the following system of equations

$$P_a P_d = (1-p)(1-q) + pq = 1, \quad \text{and} \quad P_b P_c = (1-p)q + p(1-q) = 0. \quad (5.101)$$

The solution is given by

$$q = \frac{-p}{1-2p}, \quad (5.102)$$

which is a quasi-probability, since it can take negative values, and it is shown in the left panel of Fig. 5.3. Now,

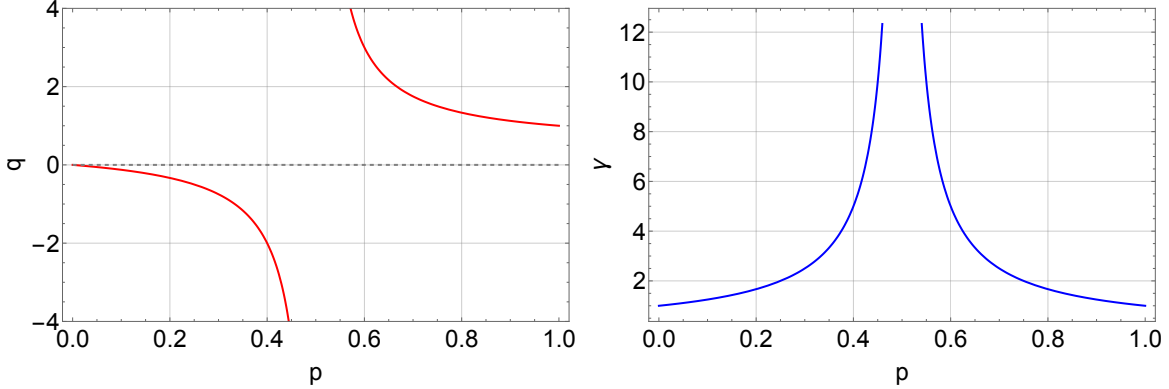


Fig. 5.3: Quasi-probability  $q$  (left panel) and renormalisation constant  $\gamma$  (right panel) as a function of the probability  $p$  of having an error.

the inverse noise map  $\Lambda^{-1}$  is given by

$$\begin{aligned} \Lambda^{-1}(\hat{\rho}) &= (1-q)\hat{1}\hat{\rho}\hat{1} + q\hat{\sigma}_x\hat{\rho}\hat{\sigma}_x, \\ &= \text{sgn}(1-q)|1-q|\hat{1}\hat{\rho}\hat{1} + \text{sgn}(q)|q|\hat{\sigma}_x\hat{\rho}\hat{\sigma}_x, \\ &= \gamma [S_1 P_1 \hat{1}\hat{\rho}\hat{1} + S_X P_X \hat{\sigma}_x\hat{\rho}\hat{\sigma}_x], \end{aligned} \quad (5.103)$$

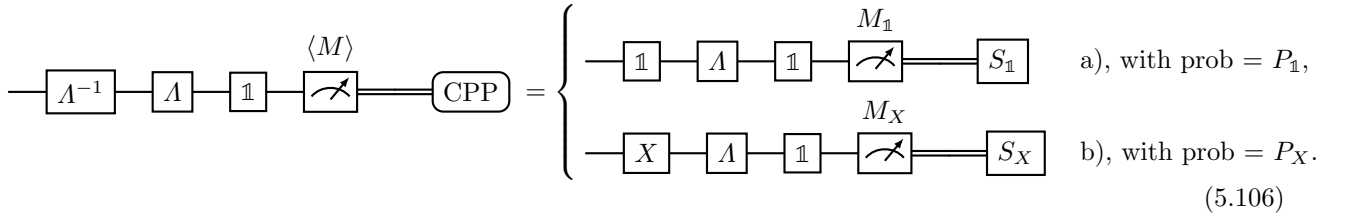
where in the first line we used  $x = \text{sgn}(x)|x|$ , with  $\text{sgn}$  indicating the sign function, and in the second line we introduced

$$\gamma = |1-q| + |q|, \quad (5.104)$$

which is represented in the right panel of Fig. 5.3. Finally, we defined

$$\begin{aligned} S_1 &= \text{sgn}(1-q), & P_1 &= \frac{|1-q|}{\gamma}, \\ S_X &= \text{sgn}(q), & P_X &= \frac{|q|}{\gamma}. \end{aligned} \quad (5.105)$$

Thus, independently from the unravelling of the noise map, i.e. without knowing if the bit-flip noise is applied or not, we apply the map  $\Lambda^{-1}$  in the last line of Eq. (5.103). This can be implemented with the following circuit:



A classical post-processing (CPP) is applied to multiplicate the outcome of the result by the proper sign factor. Eventually, the mitigated result is given by

$$\langle M \rangle = \gamma (S_{\mathbb{1}} P_{\mathbb{1}} M_{\mathbb{1}} + S_X P_X M_X). \quad (5.107)$$

This is an unbiased estimator. The cost of the mitigation procedure goes in the variance, which grows by a factor  $\gamma^2$  compared to the unmitigated one.

Consider a more general case of the noise map  $\Lambda$  acting on a single qubit, which reads

$$\Lambda(\hat{\rho}) = \lambda_0 \hat{\rho} + \lambda_1 \hat{\sigma}_x \hat{\rho} \hat{\sigma}_x + \lambda_2 \hat{\sigma}_y \hat{\rho} \hat{\sigma}_y + \lambda_3 \hat{\sigma}_z \hat{\rho} \hat{\sigma}_z, \quad (5.108)$$

where

$$\lambda_\alpha \geq 0, \quad \text{and} \quad \sum_{\alpha=0}^3 \lambda_\alpha = 1. \quad (5.109)$$

Such a map is a CPTP map. Similarly as done above, we construct the inverse map  $\Lambda^{-1}$  as

$$\Lambda^{-1}(\hat{\rho}) = q_0 \hat{\rho} + q_1 \hat{\sigma}_x \hat{\rho} \hat{\sigma}_x + q_2 \hat{\sigma}_y \hat{\rho} \hat{\sigma}_y + q_3 \hat{\sigma}_z \hat{\rho} \hat{\sigma}_z, \quad (5.110)$$

where we require that

$$\sum_{\alpha=0}^3 q_\alpha = 1, \quad (5.111)$$

but we do not add any restriction on the sign of  $q_\alpha$ . Then, in terms of unravellings, we have 4 possible evolutions provided by  $\Lambda$  and 4 by  $\Lambda^{-1}$  for a total of 16 possible mappings. Explicitly they give

$\Lambda$	$ \Lambda^{-1} $	$\hat{\rho} \rightarrow \hat{\rho}'$	probability $P_{\alpha\beta}$
$\hat{\mathbb{1}}$	$\hat{\mathbb{1}}$	$\hat{\rho}$	$\lambda_0 q_0$
$\hat{\mathbb{1}}$	$\hat{\sigma}_x$	$\hat{\sigma}_x \hat{\rho} \hat{\sigma}_x$	$\lambda_0 q_1$
$\hat{\mathbb{1}}$	$\hat{\sigma}_y$	$\hat{\sigma}_y \hat{\rho} \hat{\sigma}_y$	$\lambda_0 q_2$
$\hat{\mathbb{1}}$	$\hat{\sigma}_z$	$\hat{\sigma}_z \hat{\rho} \hat{\sigma}_z$	$\lambda_0 q_3$
$\hat{\sigma}_x$	$\hat{\mathbb{1}}$	$\hat{\sigma}_x \hat{\rho} \hat{\sigma}_x$	$\lambda_1 q_0$
$\hat{\sigma}_x$	$\hat{\sigma}_x$	$\hat{\sigma}_x^2 \hat{\rho} \hat{\sigma}_x^2$	$\lambda_1 q_1$
$\hat{\sigma}_x$	$\hat{\sigma}_y$	$\hat{\sigma}_x \hat{\sigma}_y \hat{\rho} \hat{\sigma}_y \hat{\sigma}_x$	$\lambda_1 q_2$
$\hat{\sigma}_x$	$\hat{\sigma}_z$	$\hat{\sigma}_x \hat{\sigma}_z \hat{\rho} \hat{\sigma}_z \hat{\sigma}_x$	$\lambda_1 q_3$
$\hat{\sigma}_y$	$\hat{\mathbb{1}}$	$\hat{\sigma}_y \hat{\rho} \hat{\sigma}_y$	$\lambda_2 q_0$
$\hat{\sigma}_y$	$\hat{\sigma}_x$	$\hat{\sigma}_y \hat{\sigma}_x \hat{\rho} \hat{\sigma}_x \hat{\sigma}_y$	$\lambda_2 q_1$
$\hat{\sigma}_y$	$\hat{\sigma}_y$	$\hat{\sigma}_y^2 \hat{\rho} \hat{\sigma}_y^2$	$\lambda_2 q_2$
$\hat{\sigma}_y$	$\hat{\sigma}_z$	$\hat{\sigma}_y \hat{\sigma}_z \hat{\rho} \hat{\sigma}_z \hat{\sigma}_y$	$\lambda_2 q_3$
$\hat{\sigma}_z$	$\hat{\mathbb{1}}$	$\hat{\sigma}_z \hat{\rho} \hat{\sigma}_z$	$\lambda_3 q_0$
$\hat{\sigma}_z$	$\hat{\sigma}_x$	$\hat{\sigma}_z \hat{\sigma}_x \hat{\rho} \hat{\sigma}_x \hat{\sigma}_z$	$\lambda_3 q_1$
$\hat{\sigma}_z$	$\hat{\sigma}_y$	$\hat{\sigma}_z \hat{\sigma}_y \hat{\rho} \hat{\sigma}_y \hat{\sigma}_z$	$\lambda_3 q_2$
$\hat{\sigma}_z$	$\hat{\sigma}_z$	$\hat{\sigma}_z^2 \hat{\rho} \hat{\sigma}_z^2$	$\lambda_3 q_3$

However, we can exploit that  $\hat{\sigma}_\alpha^2 = \hat{\mathbb{1}}$  and that  $\hat{\sigma}_i \hat{\sigma}_j = i \epsilon_{ijk} \hat{\sigma}_k$ . Thus, the above table becomes

$\Lambda^{-1} \hat{\rho} \rightarrow \hat{\rho}' $ probability $P_{\alpha\beta}$			
$\hat{1}$	$\hat{1}$	$\hat{\rho}$	$\lambda_0 q_0$
$\hat{1}$	$\hat{\sigma}_x$	$\hat{\sigma}_x \hat{\rho} \hat{\sigma}_x$	$\lambda_0 q_1$
$\hat{1}$	$\hat{\sigma}_y$	$\hat{\sigma}_y \hat{\rho} \hat{\sigma}_y$	$\lambda_0 q_2$
$\hat{1}$	$\hat{\sigma}_z$	$\hat{\sigma}_z \hat{\rho} \hat{\sigma}_z$	$\lambda_0 q_3$
$\hat{\sigma}_x$	$\hat{1}$	$\hat{\sigma}_x \hat{\rho} \hat{\sigma}_x$	$\lambda_1 q_0$
$\hat{\sigma}_x$	$\hat{\sigma}_x$	$\hat{\rho}$	$\lambda_1 q_1$
$\hat{\sigma}_x$	$\hat{\sigma}_y$	$\hat{\sigma}_z \hat{\rho} \hat{\sigma}_z$	$\lambda_1 q_2$
$\hat{\sigma}_x$	$\hat{\sigma}_z$	$\hat{\sigma}_y \hat{\rho} \hat{\sigma}_y$	$\lambda_1 q_3$
$\hat{\sigma}_y$	$\hat{1}$	$\hat{\sigma}_y \hat{\rho} \hat{\sigma}_y$	$\lambda_2 q_0$
$\hat{\sigma}_y$	$\hat{\sigma}_x$	$\hat{\sigma}_z \hat{\rho} \hat{\sigma}_z$	$\lambda_2 q_1$
$\hat{\sigma}_y$	$\hat{\sigma}_y$	$\hat{\rho}$	$\lambda_2 q_2$
$\hat{\sigma}_y$	$\hat{\sigma}_z$	$\hat{\sigma}_x \hat{\rho} \hat{\sigma}_x$	$\lambda_2 q_3$
$\hat{\sigma}_z$	$\hat{1}$	$\hat{\sigma}_z \hat{\rho} \hat{\sigma}_z$	$\lambda_3 q_0$
$\hat{\sigma}_z$	$\hat{\sigma}_x$	$\hat{\sigma}_y \hat{\rho} \hat{\sigma}_y$	$\lambda_3 q_1$
$\hat{\sigma}_z$	$\hat{\sigma}_y$	$\hat{\sigma}_x \hat{\rho} \hat{\sigma}_x$	$\lambda_3 q_2$
$\hat{\sigma}_z$	$\hat{\sigma}_z$	$\hat{\rho}$	$\lambda_3 q_3$

(5.113)

Finally, we impose that the sum of the probabilities of getting  $\hat{\rho}' = \hat{\rho}$  should be 1, and those such  $\hat{\rho}' \neq \hat{\rho}$  should be 0. Namely

$$\begin{aligned} P_{00} + P_{11} + P_{22} + P_{33} &= \lambda_0 q_0 + \lambda_1 q_1 + \lambda_2 q_2 + \lambda_3 q_3 = 1, \\ P_{01} + P_{10} + P_{23} + P_{32} &= \lambda_0 q_1 + \lambda_1 q_0 + \lambda_2 q_3 + \lambda_3 q_2 = 0, \\ P_{02} + P_{20} + P_{13} + P_{31} &= \lambda_0 q_2 + \lambda_2 q_0 + \lambda_1 q_3 + \lambda_3 q_1 = 0, \\ P_{03} + P_{30} + P_{12} + P_{21} &= \lambda_0 q_3 + \lambda_3 q_0 + \lambda_1 q_2 + \lambda_2 q_1 = 0. \end{aligned} \quad (5.114)$$

The solution to this system of linear equations gives

$$\begin{aligned} q_0 &= \frac{1}{4} \left( 1 + \frac{1}{1 - 2\lambda_1 - 2\lambda_2} + \frac{1}{1 - 2\lambda_1 - 2\lambda_3} + \frac{1}{1 - 2\lambda_2 - 2\lambda_1} \right), \\ q_1 &= \frac{1}{4} \left( 1 - \frac{1}{1 - 2\lambda_1 - 2\lambda_2} - \frac{1}{1 - 2\lambda_1 - 2\lambda_3} + \frac{1}{1 - 2\lambda_2 - 2\lambda_1} \right), \\ q_2 &= \frac{1}{4} \left( 1 - \frac{1}{1 - 2\lambda_1 - 2\lambda_2} + \frac{1}{1 - 2\lambda_1 - 2\lambda_3} - \frac{1}{1 - 2\lambda_2 - 2\lambda_1} \right), \\ q_3 &= \frac{1}{4} \left( 1 + \frac{1}{1 - 2\lambda_1 - 2\lambda_2} - \frac{1}{1 - 2\lambda_1 - 2\lambda_3} - \frac{1}{1 - 2\lambda_2 - 2\lambda_1} \right). \end{aligned} \quad (5.115)$$

The inverse map can be rewritten as

$$\begin{aligned} \Lambda^{-1}(\hat{\rho}) &= \sum_{\alpha=0}^3 q_\alpha \hat{\sigma}_\alpha \hat{\rho} \hat{\sigma}_\alpha, \\ &= \sum_{\alpha=0}^3 \text{sgn}(q_\alpha) |q_\alpha| \hat{\sigma}_\alpha \hat{\rho} \hat{\sigma}_\alpha, \\ &= \gamma \sum_{\alpha=0}^3 S_\alpha P_\alpha \hat{\sigma}_\alpha \hat{\rho} \hat{\sigma}_\alpha, \end{aligned} \quad (5.116)$$

where

$$\gamma = \sum_{\alpha=0}^3 |q_\alpha|, \quad S_\alpha = \text{sgn}(q_\alpha), \quad \text{and} \quad P_\alpha = \frac{|q_\alpha|}{\gamma}. \quad (5.117)$$

Then, the mitigated result is given by

$$\langle M \rangle = \gamma \sum_{\alpha=0}^3 S_\alpha P_\alpha M_\alpha, \quad (5.118)$$

where  $M_\alpha$  is the outcome obtained from the measurement at the end of the circuit at whose beginning we applied  $\hat{\sigma}_\alpha$ .

The application of PEC mitigation works if one has an almost perfect knowledge of the noise. However, for such a characterisation for  $N$  qubits, one needs to quantify  $4^N - 1$  parameters, where 4 is the dimensions of the single-qubit algebra and 1 degree of freedom is fixed as it corresponds to the map given by  $\hat{1}^{\otimes N}$  whose associated probability is given by the unity minus the sum of all the other probabilities. To be quantitative, for 2 qubits one needs 15 parameters, for 10 qubits these become  $\sim 10^6$ , and for 50 qubits we have  $\sim 10^{30}$  parameters. Therefore, it is an approach that requires too many classical processing to be used for a large number of qubits.

## Appendix A

### Solutions of the exercises

#### A.1 Solution to Exercise 1.1

To express the Hadamard gate  $H$  as a rotation, we proceed as follows. We consider the general rotation

$$\hat{R}^{\mathbf{n}}(\theta) = \cos(\theta/2)\hat{\mathbb{1}} - i \sin(\theta/2)\mathbf{n} \cdot \hat{\boldsymbol{\sigma}}, \quad (\text{A.1})$$

of an angle  $\theta$  around  $\mathbf{n}$ , where the Pauli matrices are

$$X = \begin{pmatrix} 0 & 1 \\ 1 & 0 \end{pmatrix}, \quad Y = \begin{pmatrix} 0 & -i \\ i & 0 \end{pmatrix}, \quad Z = \begin{pmatrix} 1 & 0 \\ 0 & -1 \end{pmatrix}. \quad (\text{A.2})$$

From such a rotation, we want to obtain

$$H = \frac{1}{\sqrt{2}} \begin{pmatrix} 1 & 1 \\ 1 & -1 \end{pmatrix}. \quad (\text{A.3})$$

First thing, we highlight that the sum  $X + Z$  gives

$$X + Z = \begin{pmatrix} 1 & 1 \\ 1 & -1 \end{pmatrix}, \quad (\text{A.4})$$

then it follows that

$$H = \frac{X + Z}{\sqrt{2}} = \left\{ \frac{1}{\sqrt{2}}, 0, \frac{1}{\sqrt{2}} \right\} \cdot \hat{\boldsymbol{\sigma}}. \quad (\text{A.5})$$

Such an expression recalls the last term in Eq. (A.1). Finally, we need to set the angle  $\theta$  so that the first term in Eq. (A.1) vanishes. This is  $\theta = \pi$ . Then

$$H = i\hat{R}^{\mathbf{n}}(\pi), \quad \text{where } \mathbf{n} = \left\{ \frac{1}{\sqrt{2}}, 0, \frac{1}{\sqrt{2}} \right\}, \quad (\text{A.6})$$

gives the solution.

#### A.2 Solution to Exercise 1.2

To prove that, given two fixed non-parallel normalised vectors  $\mathbf{n}$  and  $\mathbf{m}$ , any unitary  $\hat{U}$  can be expressed as

$$\hat{U} = e^{i\alpha}\hat{R}^{\mathbf{n}}(\beta)\hat{R}^{\mathbf{m}}(\gamma)\hat{R}^{\mathbf{n}}(\delta), \quad (\text{A.7})$$

with  $\alpha, \beta, \gamma, \delta \in \mathbb{R}$ , then one needs to recast  $\hat{U}$  in the form

$$\hat{U} = e^{i\alpha} \hat{R}^{\mathbf{t}}(\omega), \quad (\text{A.8})$$

with  $\alpha \in \mathbb{R}$  and  $\mathbf{t} \in \mathbb{R}^3$  suitably chosen.

The first step of the proof is to write  $(\mathbf{m} \cdot \hat{\boldsymbol{\sigma}})(\mathbf{n} \cdot \hat{\boldsymbol{\sigma}})$  in terms of a single Pauli matrix vector  $\hat{\boldsymbol{\sigma}}$ . We have

$$\begin{aligned} (\mathbf{m} \cdot \hat{\boldsymbol{\sigma}})(\mathbf{n} \cdot \hat{\boldsymbol{\sigma}}) &= (m_1 \hat{\sigma}_x + m_2 \hat{\sigma}_y + m_3 \hat{\sigma}_z)(n_1 \hat{\sigma}_x + n_2 \hat{\sigma}_y + n_3 \hat{\sigma}_z), \\ &= \mathbf{m} \cdot \mathbf{n} + m_1 n_2 \hat{\sigma}_x \hat{\sigma}_y + m_1 n_3 \hat{\sigma}_x \hat{\sigma}_z + m_2 n_1 \hat{\sigma}_y \hat{\sigma}_x + m_2 n_3 \hat{\sigma}_y \hat{\sigma}_z + m_3 n_1 \hat{\sigma}_z \hat{\sigma}_x + m_3 n_2 \hat{\sigma}_z \hat{\sigma}_y. \end{aligned} \quad (\text{A.9})$$

By applying

$$\hat{\sigma}_i \hat{\sigma}_j = \delta_{ij} \hat{1} + i \epsilon_{ijk} \hat{\sigma}_k, \quad (\text{A.10})$$

we have that Eq. (A.9) becomes

$$(\mathbf{m} \cdot \hat{\boldsymbol{\sigma}})(\mathbf{n} \cdot \hat{\boldsymbol{\sigma}}) = (\mathbf{m} \cdot \mathbf{n}) \hat{1} + i(\mathbf{m} \times \mathbf{n}) \cdot \hat{\boldsymbol{\sigma}}. \quad (\text{A.11})$$

The second step is to consider the composition of two rotations:

$$\begin{aligned} \hat{R}^{\mathbf{m}}(\gamma) \hat{R}^{\mathbf{n}}(\delta) &= (\cos(\gamma/2) \hat{1} - i \sin(\gamma/2) \mathbf{m} \cdot \hat{\boldsymbol{\sigma}}) (\cos(\delta/2) \hat{1} - i \sin(\delta/2) \mathbf{n} \cdot \hat{\boldsymbol{\sigma}}), \\ &= \cos(\gamma/2) \cos(\delta/2) \hat{1} - i \cos(\gamma/2) \sin(\delta/2) \mathbf{n} \cdot \hat{\boldsymbol{\sigma}} - i \cos(\delta/2) \sin(\gamma/2) \mathbf{m} \cdot \hat{\boldsymbol{\sigma}} \\ &\quad - \sin(\gamma/2) \sin(\delta/2) (\mathbf{m} \cdot \hat{\boldsymbol{\sigma}})(\mathbf{n} \cdot \hat{\boldsymbol{\sigma}}). \end{aligned} \quad (\text{A.12})$$

Substituting Eq. (A.11) in the last expression, we find that

$$\hat{R}^{\mathbf{m}}(\gamma) \hat{R}^{\mathbf{n}}(\delta) = \hat{R}^{\mathbf{h}}(\epsilon) = \cos(\epsilon/2) \hat{1} - i \sin(\epsilon/2) \mathbf{h} \cdot \hat{\boldsymbol{\sigma}}, \quad (\text{A.13})$$

where  $\epsilon$  and  $\mathbf{h}$  are taken such that

$$\begin{aligned} \cos(\epsilon/2) &= \cos(\gamma/2) \cos(\delta/2) - \sin(\gamma/2) \sin(\delta/2) \mathbf{m} \cdot \mathbf{n}, \\ \sin(\epsilon/2) \mathbf{h} &= \cos(\gamma/2) \sin(\delta/2) \mathbf{n} + \cos(\delta/2) \sin(\gamma/2) \mathbf{m} + \sin(\gamma/2) \sin(\delta/2) (\mathbf{m} \times \mathbf{n}). \end{aligned} \quad (\text{A.14})$$

Then, we have

$$\hat{R}^{\mathbf{n}}(\beta) \hat{R}^{\mathbf{m}}(\gamma) \hat{R}^{\mathbf{n}}(\delta) = \hat{R}^{\mathbf{n}}(\beta) \hat{R}^{\mathbf{h}}(\epsilon) = \hat{R}^{\mathbf{t}}(\omega), \quad (\text{A.15})$$

where we applied again the composition of two rotations, which ends the proof.

### A.3 Solution to Exercise 1.3

Consider two qubits, where the first is prepared in the superposition

$$|\psi_1\rangle = \frac{|0\rangle + |1\rangle}{\sqrt{2}}, \quad (\text{A.16})$$

while the second is initialised in the ground state  $|\psi_2\rangle = |0\rangle$ . The total state is

$$|\psi_{12}\rangle = \frac{|0\rangle + |1\rangle}{\sqrt{2}} |0\rangle = \frac{|00\rangle + |10\rangle}{\sqrt{2}}. \quad (\text{A.17})$$

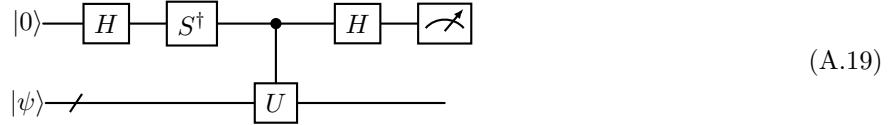
From the first expression, one clearly sees that the state is separable. By applying the CNOT gate, we find that the state becomes

$$|\psi_{12}\rangle = \frac{|00\rangle + |11\rangle}{\sqrt{2}}, \quad (\text{A.18})$$

which is a fully entangled state.

### A.4 Solution to Exercise 1.4

Consider the circuit



Its action is the following

$$\begin{aligned}
 |0\rangle |\psi\rangle &\xrightarrow{\hat{H} \otimes \hat{\mathbb{1}}} \frac{1}{\sqrt{2}}(|0\rangle + |1\rangle) |\psi\rangle \\
 &\xrightarrow{\hat{S}^\dagger \otimes \hat{\mathbb{1}}} \frac{1}{\sqrt{2}}(|0\rangle - i|1\rangle) |\psi\rangle \\
 &\xrightarrow{C(U)} \frac{1}{\sqrt{2}}(|0\rangle |\psi\rangle - i|1\rangle \hat{U} |\psi\rangle) \\
 &\xrightarrow{\hat{H} \otimes \hat{\mathbb{1}}} \frac{1}{2} \left[ (|0\rangle + |1\rangle) |\psi\rangle - i(|0\rangle - |1\rangle) \hat{U} |\psi\rangle \right] \\
 &= \frac{1}{2} \left[ |0\rangle (\hat{\mathbb{1}} - i\hat{U}) |\psi\rangle + |1\rangle (\hat{\mathbb{1}} + i\hat{U}) |\psi\rangle \right].
 \end{aligned} \tag{A.20}$$

Finally, one measures qubit 0, and the probability of finding the qubit in  $|0\rangle$  is

$$P(|0\rangle) = \frac{1}{4} \langle \psi | (\hat{\mathbb{1}} + i\hat{U}^\dagger) (\hat{\mathbb{1}} - i\hat{U}) |\psi\rangle = \frac{1}{2} \left( 1 + \Im \langle \psi | \hat{U} | \psi \rangle \right), \tag{A.21}$$

which ends the exercise.